REPORT NO.
UCB/EERC-77/16
DECEMBER 1977

EARTHQUAKE ENGINEERING RESEARCH CENTER

COMPUTER-AIDED OPTIMUM SEISMIC DESIGN OF DUCTILE REINFORCED CONCRETE MOMENT-RESISTING FRAMES

by

STAN W. ZAGAJESKI
VITELMO V. BERTERO

Report to Sponsor:
National Science Foundation

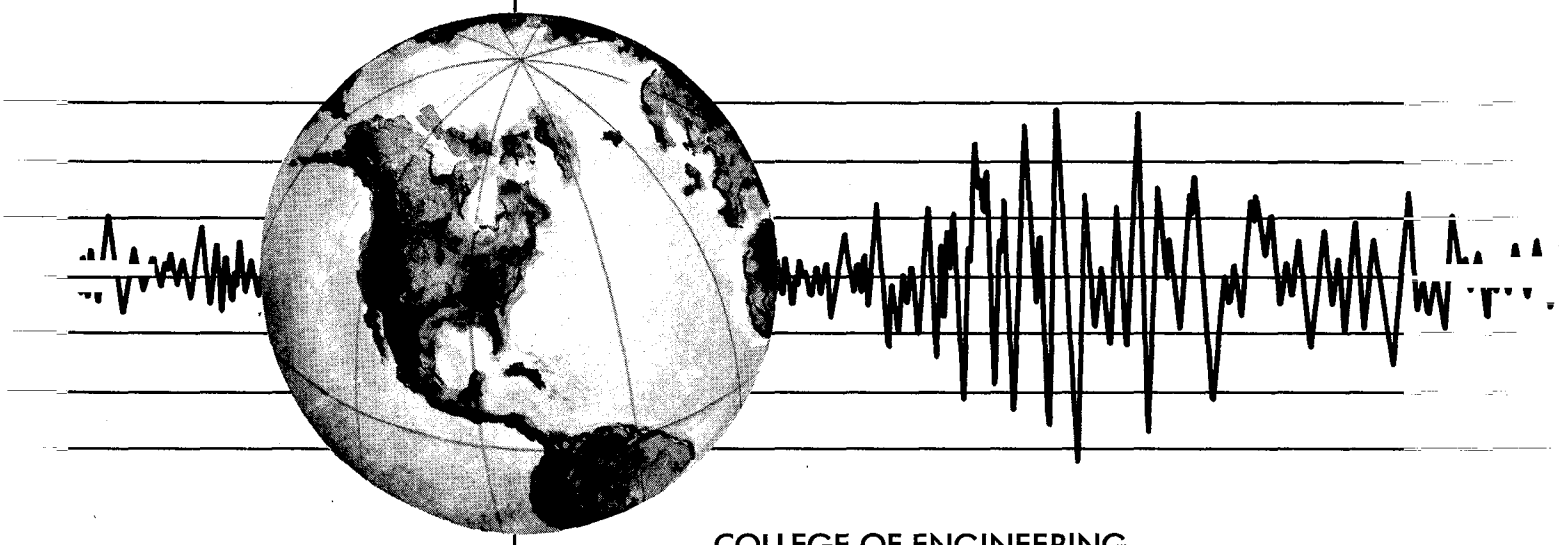

COLLEGE OF ENGINEERING

UNIVERSITY OF CALIFORNIA · Berkeley, California

BIBLIOGRAPHIC DATA SHEET	1. Report No. UCB/EERC-77/16	2.	3. Recipient's Accession No. PB 280197
4. Title and Subtitle Computer-Aided Optimum Seismic Design of Ductile Reinforced Concrete Moment-Resisting Frames			5. Report Date December 1977 6.
7. Author(s) Stan W. Zagajeski and Vitelmo V. Bertero			8. Performing Organization Rept. No. 77/16
9. Performing Organization Name and Address Earthquake Engineering Research Center University of California, Berkeley 47th Street and Hoffman Blvd. Richmond, California 94804			10. Project/Task/Work Unit No. 11. Contract/Grant No. ENV76-01419
12. Sponsoring Organization Name and Address National Science Foundation 1800 G Street, N.W. Washington, D.C. 20550			13. Type of Report & Period Covered 14.
15. Supplementary Notes			

16. Abstracts

A computer-aided design procedure based on limit state design concepts is proposed for multistory reinforced concrete frames of buildings which are expected to experience severe earthquake ground shaking during their service life. In this procedure a structure is designed to meet (1) various serviceability criteria under service loading conditions, (2) damage limitations for abnormal environmental conditions, and (3) safety requirements for extreme earthquake excitations. The design procedure, which makes use of computer optimization methods as well as static and dynamic elastic and nonlinear analysis procedures, consists in five basic steps which are grouped into a preliminary design phase and a final design phase.

The objective of the preliminary design phase is to obtain a preliminary design which is as close as possible to the desired final design. It entails three steps, preliminary analysis, preliminary design, and analysis of the preliminary design.

In the first step, serviceability, damageability, and safety criteria, gravity and wind loading conditions, and the "design earthquakes" are established according to the site, type, and function of the building. Seismic design shears are obtained from an inelastic design response spectrum constructed for appropriate values of damping, and acceptable values of displacement ductility and average story drift using an iterative preliminary analysis procedure based on modal analysis.

In the second step, a preliminary design of structural members is obtained employing a simplified storywise optimization procedure. The optimization objective was to minimize the volume of flexural reinforcement. A weak girder - strong column design philosophy is followed in the formulation of the design problem. Design constraints are imposed to satisfy equilibrium and to arrive at a serviceable and practical design. The solution of the optimum design problem yields beam design moments which are used in conjunction with the weak girder - strong column design philosophy to obtain member sizes and reinforcement.

Once the preliminary design is completed, structural response to various loading conditions is computed (step 3). Both elastic and nonlinear behavior is considered under static and dynamic loading. The results of these analyses are evaluated with respect to the assumptions made and design criteria established in step 1 to determine whether the design is acceptable. Steps 1 through 3 are repeated until satisfactory agreement is reached and the final seismic design story shears can be obtained.

17c. COSATI Field/Group (continued on page 2)

18. Availability Statement	19. Security Class (This Report)	21.
Release Unlimited	UNCLASSIFIED	
	20. Security Class (This Page) UNCLASSIFIED	22. Price PCA07 MFA01

BIBLIOGRAPHIC DATA SHEET	1. Report No. UCB/EERC-77/16 page 2	2.	3. Recipient's Accession No.
4. Title and Subtitle Computer-Aided Optimum Seismic Deisgn of Ductile Reinforced Concrete Moment-Resisting Frames			5. Report Date 6.
7. Author(s)			8. Performing Organization Rept. No.
9. Performing Organization Name and Address			10. Project/Task/Work Unit No. 11. Contract/Grant No.
12. Sponsoring Organization Name and Address			13. Type of Report & Period Covered 14.
15. Supplementary Notes			

16. Abstracts (continued from page 1)

The objective of the final design phase is to obtain an optimum final design. This phase consists in two steps, final design and an analysis of the reliability of the final design. The final design is found by solving an optimization problem based on a more sophisticated and realistic design subassemblage than that used in the preliminary design and using the final seismic design shears obtained in the preliminary design. In the second step, the reliability of the final design is checked under service and ultimate loading conditions. Information needed for detailing critical regions in the structure where yielding and significant inelastic deformations may take place is obtained by determining its nonlinear time history response to severe earthquake ground motions.

The design procedure is illustrated on a ten-story, three-bay reinforced concrete frame. The influence of the different limit states considered is indicated by the example.

This computer-aided design procedure is shown to be very versatile. The use of computers allows alternate designs to be rapidly and economically formulated and evaluated, and it allows realistic consideration of complex environmental actions. The nonlinear dynamic response of the designed structure indicates that the procedure is capable of achieving acceptable designs if the response spectrum used in the definition of the design forces adequately represents the characteristics of the ground motion which excites the structure.

17b. Identifiers/Open-Ended Terms

17c. COSATI Field/Group

18. Availability Statement	19. Security Class (This Report) UNCLASSIFIED	21. No. of Pages
	20. Security Class (This Page UNCLASSIFIED	22. Price

COMPUTER-AIDED OPTIMUM SEISMIC DESIGN OF DUCTILE REINFORCED CONCRETE MOMENT-RESISTING FRAMES

by

Stan W. Zagajeski
Research Assistant
University of California, Berkeley

and

Vitelmo V. Bertero
Professor of Civil Engineering
University of California, Berkeley

A report on research sponsored by
the National Science Foundation

Report No. UCB/EERC-77/16
Earthquake Engineering Research Center
College of Engineering
Univeristy of California
Berkeley, California

December 1977

ABSTRACT

A computer-aided design procedure based on limit state design concepts is proposed for multistory reinforced concrete frames of buildings which are expected to experience severe earthquake ground shaking during their service life. In this procedure a structure is designed to meet (1) various serviceability criteria under service loading conditions, (2) damage limitations for abnormal environmental conditions, and (3) safety requirements for extreme earthquake excitations. The design procedure, which makes use of computer optimization methods as well as static and dynamic elastic and nonlinear analysis procedures, consists in five basic steps which are grouped into a preliminary design phase and a final design phase.

The objective of the preliminary design phase is to obtain a preliminary design which is as close as possible to the desired final design. It entails three steps, preliminary analysis, preliminary design, and analysis of the preliminary design.

In the first step, serviceability, damageability, and safety criteria, gravity and wind loading conditions, and the "design earthquakes" are established according to the site, type, and function of the building. Seismic design shears are obtained from an inelastic design response spectrum constructed for appropriate values of damping, and acceptable values of displacement ductility and average story drift using an iterative preliminary analysis procedure based on modal analysis.

In the second step, a preliminary design of structural members is obtained employing a simplified storywise optimization procedure. The optimization objective was to minimize the volume of flexural reinforcement. A weak girder - strong column design philosophy is followed in the formulation of the design problem. Design constraints are imposed to satisfy equilibrium and to arrive at a serviceable and practical design. The solution of the optimum design problem

yields beam design moments which are used in conjunction with the weak girder - strong column design philosophy to obtain member sizes and reinforcement.

Once the preliminary design is completed, structural response to various loading conditions is computed (step 3). Both elastic and nonlinear behavior is considered under static and dynamic loading. The results of these analyses are evaluated with respect to the assumptions made and design criteria established in step 1 to determine whether the design is acceptable. Steps 1 through 3 are repeated until satisfactory agreement is reached and the final seismic design story shears can be obtained.

The objective of the final design phase is to obtain an optimum final design. This phase consists in two steps, final design and an analysis of the reliability of the final design. The final design is found by solving an optimization problem based on a more sophisticated and realistic design subassemblage than that used in the preliminary design and using the final seismic design shears obtained in the preliminary design. In the second step, the reliability of the final design is checked under service and ultimate loading conditions. Information needed for detailing critical regions in the structure where yielding and significant inelastic deformations may take place is obtained by determining its nonlinear time history response to severe earthquake ground motions.

The design procedure is illustrated on a ten-story, three-bay reinforced concrete frame. The influence of the different limit states considered is indicated by the example.

This computer-aided design procedure is shown to be very versatile. The use of computers allows alternate designs to be rapidly and economically formulated and evaluated, and it allows realistic consideration of complex environmental actions. The nonlinear dynamic response of the designed structure indicates that the procedure is capable of achieving acceptable designs if the

response spectrum used in the definition of the design forces adequately represents the characteristics of the ground motion which excites the structure.

ACKNOWLEDGMENTS

Financial support for this study was provided by the National Science Foundation under NSF/RANN Grant No. ENV76-01419, "Structural Design Implications of Recent Seismic Research Results," Professor V. V. Bertero, Principal Investigator. The facilities of the University of California Computer Center were used during the course of this research.

The authors would like to thank Professor S. Mahin for his assistance and advice regarding analysis procedures employed in this investigation.

In addition, the authors would like to acknowledge the editorial assistance of L. Tsai and the technical illustrations by L. Hashizume.

TABLE OF CONTENTS

LIST OF TABLES

LIST OF FIGURES

NOTATIONS

A_b = area of steel bar

A_{s_i} = steel area corresponding to design moment i

b = width of cross section

$[C_T]$ = damping matrix

C_y = yielding seismic coefficient

d = distance from extreme compressive fiber to centroid of tensile reinforcement

d_b = nominal bar diameter

$d\underline{p}$ = increment load vector

$d\underline{r}$ = incremental displacement vector

$d\dot{\underline{r}}$ = incremental velocity vector

$d\ddot{\underline{r}}$ = incremental acceleration vector

DL = dead load

DPD = Derived Pacoima Dam ground motion

E = earthquake load

EC = N-S component of the El Centro ground motion

f'_c = nominal concrete compressive strength

f_y = nominal steel yield stress

F = 'safety' factor to ensure weak girder - strong column design

FAC = ratio of the value of the ultimate load elastic moment envelope at section j for a given story with the corresponding value for the story above the given one ($M_j^{UE}/M_{j_{above}}^{UE}$)

F_i = lateral shear force applied at story level i

h_b = beam depth

h_c = column depth

h_j = story height at level j

H = total height of structure

$\underline{I}$ = unit vector

jd = distance between the centroids of the resultant compressive and tensile forces

K_B = proportional to the ratio of the column stiffness below a given beam-column joint and the total member stiffness at the joint

K_T = proportional to the ratio of the column stiffness above a given beam-column joint and the total member stiffness at the joint

$[K_T]$ = tangential stiffness matrix

K_{TOTAL} = proportional to the total member stiffness at a given beam-column joint

ℓ = story height

ℓ_c = clear column height

ℓ_d^B = development length for a bottom bar

ℓ_d^T = development length for a top bar

ℓ_α = beam clear spans (α = A,B)

LL = live load

$\underline{M}$, $[M]$ = mass matrix

M_b^D = beam moment capacities corresponding to reinforcement actually supplied

M_H = external work corresonding to lateral shear forces

M_j = beam design moment at section j

$M_{j_{above}}$ = the jth design moment obtained in the solution of the optimization problem for the story above the story being considered

M_j^{SE} = ordinate of elastic moment envelope under service load conditions at section j

M_j^{UE} = ordinate of elastic moment envelope under ultimate load conditions at section j

P = axial load

PF = factor to account for the effect of axial load on column moment capacity in the merit function

$(PSa_{inelastic})_i$ = inelastic spectral acceleration corresponding to T_i

R = service level drift index

R_{ult} = ultimate load drift index

$(Sd_{inelastic})_i$ = inelastic spectral displacement corresponding to T_i

$S_{H_{i-1}}$ = story shear at level i-1

$S_{j_{max}}$ = maximum probable story shear

$S'_{j_{max}}$ = design story shears

T_i = period of vibration in the ith mode

V_c = column shear force

V_b = beam shear force

V_i = base shear corresponding to ith mode

Vol = function proportional to volume of flexural reinforcement

W = wind load

W_b = beam uniform gravity load

W_{DL} = uniform dead load

W_G = ultimate uniform gravity load

W_L = ultimate uniform gravity load used in combination with lateral load

W_{LL} = uniform live load

Y_i = modal displacement corresponding to ith mode

α_F = moment amplification factor corresponding to column slenderness effects

α_{ji} = coefficient of jth design moment in ith equilibrium constraint

β = elastic moment distribution factor used in column design

γ_i = effective length of reinforcement corresponding to M_i

γ_i^* = beam contribution to γ_i

γ_i^{**} = column contribution to γ_i

δ_j = relative story displacement at level j

Δ = relative story displacement

Δ_{roof} = square root of the sum of the squares of the modal maximum displacement at the roof

$(\Delta S_{P-\Delta})_j$ = estimate of additional story shear due to P-Δ effect at level j

θ_P = plastic hinge rotation

$\theta_{P_{ACC}}$ = accumulated plastic hinge rotation

$\theta_{P_{max}}$ = maximum plastic hinge rotation

λ_i^v = base shear participation factor for ith mode

λ_i^y = displacement participation factor for ith mode

λ_0 = factor selected to ensure a serviceable design

μ = displacement ductility factor

$\mu_{\phi_{CYCLIC}}$ = cyclic curvature ductility factor

ξ = damping ratio

ρ = percentage of steel reinforcement

ρ_b = percentage of steel reinforcement corresponding to balanced failure condition

ϕ = curvature

ϕ_b = beam capacity reduction factor

ϕ_c = column capacity reduction factor

$\underline{\phi}_i$ = i<u>th</u> mode shape

ω_i = external work term in i<u>th</u> equilibrium constraint

1. INTRODUCTION

1.1 General Goals and Current Practice of Earthquake-Resistant Design

The general philosophy of earthquake-resistant design for buildings other than essential facilities has been well established and proposes to (1) prevent nonstructural damage in frequent minor ground shakings, (2) prevent structural damage and minimize nonstructural damage in occasional moderate ground shakings, and (3) avoid collapse or serious damage in rare major ground shakings. This philosophy is in complete accord with the concept of comprehensive design [1], but current design methodologies fall short of realizing its objectives.

Application of the comprehensive design approach to seismic-resistant design is, however, complex because of difficulties involved in assessing the relationship between loss and seismic excitation. According to the concept of comprehensive design, the ideal design is that which results in the minimum total cost, including possible losses, for all limit states. However, this ideal is not an immediate practical possibility in actual design. No practical design method has yet been developed that satisfies simultaneously all the requirements imposed by the different limit states. In practice the simplest approach would be to estimate the most critical limit state and to use this state as the basis for proportioning members in the preliminary design; all other main limit states should then be checked through a comprehensive analysis. To facilitate the application of this approach, the different limit states have been grouped as either serviceability or ultimate limit states.

For buildings which may experience a severe earthquake ground shaking during their service life, the most critical limit states are the ultimate. However, most current seismic design procedures are based on (1) the use of equivalent (or effective) static seismic lateral forces defined at service or at first significant yielding

level, (2) the determination of internal design forces by linear-elatic analyses, and (3) the proportioning of members using either working (service) stress methods or by considering the ultimate strength of their critical sections. Only recently has design practice in regions of high seismic risk begun using procedures based on ultimate limit states, focussing on safety against collapse of the main structure as the controlling ultimate limit state. The desirability of introducing into seismic-resistant design practice a new group of limit states based on damageability to bridge the serviceability and collapse limit states is discussed in reference 1.

The authors believe that structural design should be based on the limit state that actually controls it. If an ultimate limit state (damageability or collapse) controls the design and a fictitious linear-elastic limit state is adopted for preliminary design, the resulting design should be checked at ultimate states using realistic models.

The advantages of developing a design method based on two failure stages have been discussed by Sawyer [2]. For simple structures subjected to standard loading, a design method based on two behavioral criteria (collapse and loss of serviceability) and on four optimizing criteria has been developed by Cohn [3]. Application of the latter method to the seismic-resistant design of ductile moment-resisting steel frames seems feasible and practical [4].

The ultimate objective of the designer is to have an economical, serviceable and safe building. To achieve this aim, an efficient preliminary design is necessary. Sophisticated and efficient computer programs recently developed for the analysis of complex structures do not necessariliy guarantee an efficient design, particularly for the case of seismic-resistant design. Regardless of how sophisticated the computer programs are, repeated analyses of a poor preliminary design will usually only lead to an improved "poor final design."

Recognizing the importance of the overall design concept and the need for a sound preliminary design, the authors have developed the seismic-resistant design procedure described herein. It should be emphasized that the proposed procedure has been developed for and applied to the design of reinforced concrete framed structures of buildings located in regions near active faults where there is the possibility that very severe earthquake ground shaking might occur during the service life of these buildings. Therefore, the resulting seismic design forces as well as the resulting values for the response parameters (i.e. displacements, story drifts, etc.) apply only to buildings which will be subjected to these very severe ground motions.

1.2 Main Objectives of Proposed Design Procedure

The principal objective of this procedure is to develop the most economical and practical design which is consistent with serviceability requirements under all possible service excitations and which will be able to control damage and minimize the danger of collapse under a possible, but highly unlikely, severe earthquake ground shaking.

The procedure should be versatile to permit the inclusion of new and more reliable data as they become available as well as new design requirements and/or practical design constraints. In addition, the procedure should be automated as much as possible to produce a preliminary design in a relatively short time.

1.3 Scope

The proposed seismic design procedure was developed specifically for reinforced concrete ductile moment-resisting frames. It represents an extension of the procedure developed by Bertero and Kamil for steel frames [4]. To achieve the above objectives, the procedure developed employs a computer-aided iterative technique in five basic steps which are grouped into a preliminary design phase and a final design phase. In this report emphasis is placed on the

preliminary design phase.

2. GENERAL DESCRIPTION OF DESIGN PROCEDURE

2.1 Preliminary Design Phase

The objective of this phase is to obtain efficiently a preliminary design which is as close as possible to the final "optimum" design. This is deemed essential in obtaining a true optimum design. The preliminary design phase consists in three basic steps, which form an iterative loop to be repeated until an acceptable design is obtained. These steps are preliminary analysis, preliminary design, and analysis of the preliminary design.

2.1.1 Preliminary Analysis

The final objective of this first step is to obtain the design story shear forces. To this end the given data regarding the function of the building and the building site are studied in order to establish serviceability, damageability and safety requirements and to select a realistic design earthquake. At present, a convenient, practical, and satisfactory way of specifying the design earthquake is by a smooth ground spectrum [5]. A smooth linear-elastic response spectrum is constructed from the selected ground spectrum by establishing an appropriate damping ratio. To include the beneficial effect of energy dissipation associated with acceptable inelastic deformations, an inelastic design spectrum is constructed from the linear-elastic spectrum by selecting an appropriate displacement ductility factor. The damping ratio and particularly the ductility factors should be selected on the basis of economic considerations and the serviceability and damageability design limit states. Finally, the design story shear forces are obtained from the inelastic spectrum by a modal superposition analysis based on estimated values of periods of vibration and mode shapes. Expected P-Δ effects are estimated and included in the design story shears.

Inherent in the use of the modal analysis technique is the assumption that a sufficient number of plastic hinges form simultaneously

to transform the frame into a mechanism. In other words, the frame is assumed to behave as an elastic, perfectly plastic, single degree-of-freedom system (Fig. 1). The likelihood of this happening, especially in response to an earthquake excitation, is very small. First, it should be recognized that the proportioning of members is based on envelopes of internal forces that include all possible load combinations. Thus, design of the different critical regions are governed not only by different load combinations, but also by forces that do not occur simultaneously. In addition, during the response to an earthquake ground motion plastic hinges typically migrate from the lower to the upper stories. Plastic hinges which formed in the lower stories during the initial stages will in many cases close before a sufficient number of hinges can form in the upper stories to transform the structure into a mechanism. Because the plastic hinges form gradually, the change in stiffness at "yield" is more gradual than in the idealized case, and a more realistic generalized force displacement relationship would be that indicated by the dashed curve in Fig. 1. As indicated in this figure, overstrength would be expected not only because of the gradual hinge formation, but also due to the fact that actual member yielding strength available (available strength) will differ (typically greater) from the computed required design capacity (demand strength) because of the finite number of combinations of member sizes and reinforcement arrangements, and the fact that strain hardening of the reinforcement will result in an increase in moment capacity after yielding occurs.

In spite of this assumption it is believed that the above method is a considerable improvement over current seismic code procedures for establishing the design forces [6].

2.1.2 Preliminary Design

The preliminary design consists of a storywise weak girder - strong column limit state design using an optimization procedure. Linear programming techniques are employed to find the beam design moments which minimize an objective function proportional to the required

volume of flexural reinforcement. The beam design moments must satisfy equilibrium constraints derived from the kinematic theorem of simple plastic theory. Additional constraints are imposed to include serviceability requirements and practical design considerations. The merit function combined with the equilibrium, serviceability, and practical constraints comprise a standard linear programming problem. A solution for the beam design moments is obtained using a Simplex algorithm. The beams are then proportioned to provide these design moment capacities, and the columns are subsequently designed to satisfy the weak girder - strong column design criterion. The member sizes and reinforcement are determined by a computer program which is based on the 1973 ultimate strength requirements for reinforced concrete members [7].

An iterative loop exists within the preliminary design step. Elastic analyses at service and ultimate load conditions are required to define the serviceability and several practical design constraints, as well as to construct the merit function. Consequently, member sizes (starting) are required to formulate the design problem. The subsequent design based on the optimum design moments will, in general, result in member sizes different than those used in the formulation of the design problem. As a result, the formulation and solution of the optimization problem are repeated, with the member sizes obtained in the previous solution being used in the formulation of the new problem, until the new and starting member sizes are the same. This loop is shown schematically in Fig. 2.

2.1.3 Analysis of Preliminary Design

In this final step, the preliminary design is analyzed to determine its acceptability. The dynamic characteristics of the designed structure are determined using standard procedures and are compared with those selected in the preliminary analysis. The behavior under service load conditions is determined to check serviceability requirements.

An inelastic static analysis of the designed frame subjected

to the lateral force pattern corresponding to the seismic design story shears is carried out to determine displacement ductility factors and static overstrength factors and to locate any apparent weaknesses in the design.

Finally, if the results of the static analyses are satisfactory, the response of the designed frame to different earthquake ground motions is obtained using a nonlinear dynamic analysis program. In this program all members are represented by a two-component element which effects an elasto-plastic moment curvature relationship with linear strain hardening. The P-Δ effect, the influence of axial force on the column yielding strength, and the influence of the floor slab on the frame stiffness are included in the analysis.

Unfortunately, both the static and dynamic nonlinear analyses programs used in the current study are limited to the analysis of the planar behavior of frames. Consequently, a three-dimensional structural analysis of the entire structural system, which would include torsional effects, cannot be carried out with these programs.

Maximum values as well as time histories of the main dynamic response parameters (such as story shears and story displacements, story drift indices, beam and column curvature ductilities, and plactic hinge rotations) are examined to determine whether they are acceptable with respect to: (1) the established design criteria for damageability and safety, (2) the known member deformation capacities, and (3) the assumptions made in the first step (preliminary analysis).

If these analyses prove that the designed structure meets the established design criteria (i.e., that the design characteristics are similar to those assumed in the preliminary analysis, and that the required inelasitc deformations are compatible, that is, can be developed by the members), then the preliminary design process is complete, and a final optimum design is attempted. If any characteristic of the designed structure is unacceptable, the design is modified, either by starting at the first step or by making the necessary

adjustments to eliminate the observed shortcomings.

2.2 Final Design Phase

The final design phase consists of two steps. In the first step a final optimum design is obtained. The design procedure is similar to that employed in the preliminary design phase, with the exception that a more sophisticated subassemblage is used in the formulation of the optimization problem. The seismic design forces are determined from the inelastic design specturm utilizing the dynamic characteristics of the accepted preliminary design. As in the preliminary phase, a weak girder - strong column design criterion is established. In the second step, the optimum design is analyzed to evaluate its overall reliability under service and ultimate loading conditions.

2.3 Summary of Design Procedure

A flow chart of the design procedure is shown in Fig. 3. The steps in the preliminary design phase are repeated until an acceptable preliminary design is obtained, at which point the final optimization is attempted.

The proposed design procedure will be illustrated by presenting a detailed discussion of the design of a ten-story three-bay frame (Fig. 4). Throughout the presentation emphasis is placed on the methodology of the design procedure rather than on detailed computations. The preliminary design phase is discussed in Chapter 3 and the final design phase in Chapter 4. Conclusions and recommendations for future research are presented in Chapter 5.

3. PRELIMINARY DESIGN PHASE

3.1 General Design Criteria

As already noted, the objective of the preliminary design phase is to obtain efficiently a design which is as close as possible to the final desired design. In seismic-resistant design the following general design characteristics are considered desirable.

1. A weak girder - strong column design should result. In other words, it is desired to force inelastic deformations to occur in the girders in order to limit as much as possible the inelastic deformational demands in the columns and to minimize the possibility of soft stories (partial sway mechanisms). Typically, because of the effect of axial load and high shear forces,* the inelastic deformational capacity of columns is less than that of girders. In addition, failure (collapse) of a column is in general of a more serious consequence with respect to progressive collapse and therefore with respect to the safety of the structure as a whole than failure of a girder.

2. Abrupt transitions in mass, stiffness, strength, and ductility should be avoided throughout the total height as well as the plan area of each story of the structure. If a change in stiffness is necessary, for example when the beam or column size is changed, a corresponding change in strength should be included in the members in this area. This is required to prevent early yielding in a particular region which might result in large localized inelastic deformations and lead to a possible failure, as defined by the damageability or collapse limit states. The importance of a smooth transition in stiffness and strength cannot be overemphasized.

The above characteristics have been established as design criteria in both the preliminary and final phases of the design procedure.

The methodology of the preliminary design procedure will now

---

*Columns typically have shorter shear spans than beams.

be illustrated by applying it to the example frame shown in Fig. 4.

3.2 Preliminary Analysis

The objective of this step is to obtain the lateral story shears corresponding to a given or selected design earthquake. It involves the following.

3.2.1 Analysis of Given Data

The frame geometry, standard design loads (dead, live and wind), and story masses (obtained from the dead loads and any live load attached mechanically or by high friction to the permanent mass) are given in Fig. 4(a). The most difficult task in the first step is the selection of the proper design earthquake(s). For the present application it is described quantitatively by the inelastic response spectrum shown in Fig. 5. This spectrum is constructed from given values of effective peak ground acceleration, 0.4g, ground velocity, 486 mm/sec (19.2 in./sec), and ground displacement, 366 mm (14.4 in.), that are expected to occur at the building site, following the method suggested by Newmark [8]. It should be noted that the ground motion spectrum in Fig. 5 represents a severe ground shaking which might occur only at regions near active faults. For a detailed discussion of the importance of the selection of the proper design earthquake, see reference 5.

3.2.2 Selection of Main Seismic Design Parameters

The seismic design parameters are the "yielding" seismic coefficient (C_y) acceptable drift indices (at service R, and at ultimate, R_{ult}), period ratios (T_1/T_i) where T_1 is the first mode period, and T_i is the ith mode period, and mode shapes (ϕ_i).

The acceptable limit values for C_y should be assigned according to present design and construction experience and economic considerations involved in the design criteria selected. Acceptable values for R should be selected on the basis of acceptable damage at the service load limit state, and for R_{ult} on the basis of damageability and safety against collapse at the ultimate limit state.

As discussed in detail in reference 1, the acceptable damage levels should result from functional and economic implications of this damage. However, reliable quantification of damageability limit states is still unavailable.

For the example, it was decided that C_y should be less than 0.2 and that R should be less than 0.002 at service load conditions, and R_{ult}, which quantified in a very simplistic way the damageability limit state, should be less than 0.015.

The frequency ratios and mode shapes can be found from available tables [9], from previous experience, or from a frequency analysis of a similar design. The latter method is used for this example and the results are summarized below.

$$\frac{T_1}{T_2} = 2.75 \qquad \frac{T_1}{T_3} = 4.75 \qquad \frac{T_1}{T_4} = 7.1 \qquad \frac{T_1}{T_5} = 9.45$$

ϕ_1 = [1.000 .943 .859 .757 .663 .555 .435 .322 .204 .090]

ϕ_2 = [1.000 .646 .179 -.282 -.562 -.734 -.767 -.675 -.482 -.228]

ϕ_3 = [1.000 .115 -.706 -1.002 -.702 -.062 .593 .908 .850 .460]

ϕ_4 = [1.000 -.618 -1.152 -.228 .700 .951 .313 -.489 -.893 -.608]

ϕ_5 = [1.000 -1.355 -.661 1.292 .881 -.781 -1.291 -.141 1.144 1.080]

3.2.3 Selection of Values of T_1, μ, and ξ

Initially, it is necessary to assume a value for each of the following parameters: the first mode period, T_1, the displacement ductility factor, μ, and the damping ratio, ξ. Based on an analysis of the frequencies of similar structures, T_1 was assumed equal to 1.0 sec. From previous experience with similar structures, μ was assumed equal to 6, and ξ, 5%. It should be noted that the value of ξ is generally found to vary little with the natural frequency and seems to depend almost exclusively on the structural material, structural system, and nonstructural components and their interaction with

the structure, and on the degree of damage expected which in turn is a function of μ. The final selection of the proper values for these three factors usually requires an iterative procedure which includes a series of computations described in the next step. In each step of this procedure the value of C_y and R_{ult} resulting from computations based on the set of values assumed for T_1, μ, and ξ are compared with the values that were originally selected as desirable, i.e. $C_y = 0.2$ and $R_{ult} = 0.015$. This procedure is repeated, modifying the values of T_1, μ, and ξ until close agreement between the computed and desired values of C_y and R_{ult} are obtained.

3.2.4 Estimation of First Mode Maximum Response

The inelastic design spectrum for a single degree-of-freedom system (SDOFS) is obtained from the selected ground motion spectrum in two steps. The elastic response spectrum is first constructed by multiplying the ground motion spectrum by the amplification factors suggested by Newmark for the assumed value of the damping ratio, ξ [8]. The inelastic spectrum is then constructed by dividing the elastic spectrum by appropriate functions of the assumed displacement ductility [8]. The elastic and inelastic response spectra for $\xi = 5\%$ and $\mu = 6$ are shown in Fig. 5. It should be noted that there are actually two inelastic design spectra. The inelastic spectrum indicated in Fig. 5 defines the inelastic acceleration response, $PS_{a_{inelastic}}$. The inelastic displacement response is defined by a second spectrum which is found by multiplying the displacement associated with the inelastic acceleration response spectrum, $S_{d_{inelastic}}$, by the assumed value of μ. Maximum response parameters and the range of periods over which the established limitations on C_y and R_{ult} can be satisfied may be obtained from the first period mode shape and the assumed value of T_1, as indicated below.

The maximum lateral displacement:

$$Y_1 = \frac{\underline{M}\,\underline{I}\,\underline{\phi}_1}{\underline{\phi}_1^T\,\underline{M}\,\underline{\phi}_1} \cdot \mu\, S_{d_{inelastic}} = \frac{L_1^*}{M_1^*} \cdot \mu\, S_{d_{inelastic}} \qquad (1)$$

where

$\underline{M}$ = structure mass matrix

$\underline{\phi}_1$ = first period mode shape vector

$\underline{I}$ = unit vector

$S_{d_{inelastic}}$ = inelastic spectral displacement corresponding to T_1

The computed Y_1 or $S_{d_{inelastic}}$ can be used to obtain an idea of the expected story drift:

$$R_1 = \frac{Y_1}{H} = \frac{L_1^*}{M_1^* H} \cdot \mu S_{d_{inelastic}} = 0.00092 \cdot \mu S_{d_{inelastic}} \quad (2)$$

where H is the total structure height.

The base shear:

$$V_1 = \frac{(L_1^*)^2}{M_1^*} \cdot PS_{a_{inelastic}} = C_1 \cdot W_{1_{effective}} \quad (3)$$

where

$PS_{a_{inelastic}}$ = inelastic spectral acceleration corresponding to T_1

$$W_{1_{effective}} = \frac{(L_1^*)^2}{M_1^*} \cdot g$$

can be used to give an idea of the expected seismic coefficient:

$$C_1 = \frac{V_1}{W_{1_{effective}}} = \frac{PS_{a_{inelastic}}}{g} \quad (4)$$

From Fig. 5 it can be seen that the design requirements of $C_1 \leq 0.2$ and $R_1 \leq 0.015$ can be satisfied for the following range of T_1:

$$.67 \text{ sec} \leq T_1 \leq 2.6 \text{ sec}$$

A similar check could have been performed for the serviceability limit state if a design spectrum had been established for this limit state.

For the assumed value of $T_1 = 1.0$ sec, the spectrum of Fig. 5 gives $C_1 = 0.12$ and $R_{1_{ult}} = 0.0063$. Although the value of C_1 is considerably lower than the acceptable limit of 0.20, the effect of higher modes will increase the response, and the current value of T_1, μ, and ξ can be accepted for carrying out the preliminary design.

3.2.5 Estimation of Lateral Story Shears

The displacement and base shear modal participation factors, λ_i^y and λ_i^v, respectively, can be estimated from the selected mode shapes by the expressions:

$$\lambda_i^y = \frac{L_i^*}{M_i^*} \tag{5}$$

and

$$\lambda_i^v = \frac{(L_i^*)^2}{M_i^*} \tag{6}$$

where

$L_i^* = \underline{M}\,\underline{I}\,\underline{\phi}_i$

$M_i^* = \underline{\phi}_i^T\,\underline{M}\,\underline{\phi}_i$

$\underline{\phi}_i$ = ith mode shape vector

Using the selected values of T_1/T_i and T_1, the contribution of each mode to the maximum displacement and base shear is then found from the expressions:

$$Y_i = \lambda_i^y \cdot \mu(S_{d_{inelastic}})_i \tag{7}$$

and

$$V_i = \lambda_i^V \cdot (PS_{a_{inelastic}})_i \qquad (8)$$

By examining these modal contributions, the number of modes which can have a significant effect on the response may be determined. For the design example, only the first three modes were significant.

Once the story shears for each of the significant modes are computed, the maximum probable story shear, $S_{j_{max}}$, is estimated by computing the square root of the sum of the squares of the modal maxima (SRSSMM).

Although in this example it was assumed that the story ductility, μ_j, was constant throughout the height of the building, it would generally be more rational to use different ductility values through the height. This is because the state of stress in the girders at the upper stories usually permits the development of large ductility, and the consequences of large story drifts are less detrimental, as far as structural behavior is concerned, in the upper than in the lower stories.

The P-Δ effect has been included in the design forces by estimating additional story shears:

$$(\Delta S_{P-\Delta})_j = P_j \cdot \frac{\delta_j}{h_j} \qquad (9)$$

where

P_j = the total dead load plus the reduced live load of levels above level j

δ_j = the maximum relative story deflection at level j (this value should be estimated considering the expected inelastic response which depends on the value of μ_j at that story)

h_j = the story height of level j

For the design example, δ_j/h_j was assumed constant through the

height of the frame and equal to:

$$\frac{\delta_j}{h_j} = \frac{\Delta_{roof}}{H} \tag{10}$$

where

Δ_{roof} = the square root of the sum of the squares of the modal maximum displacements at the roof

H = the total height of the frame

The final design story shears are obtained from the expression:

$$S'_{j_{max}} = S_{j_{max}} + (\Delta S_{P-\Delta})_j \tag{11}$$

The design forces for the design example are compared to the UBC (1973) seismic design forces in Fig. 6. The UBC forces shown in Fig. 6 are for ultimate strength design; i.e., they are the forces at working stress level actually defined by the code multiplied by a factor of 1.4. Figure 6 indicates that for a given severe earthquake ground shaking, a structure designed according to UBC design forces is generally expected to experience significantly larger inelastic deformations than one designed according to spectral design forces because it is usually weaker and more flexible.

3.3 Preliminary Design

The basic problem in this step of the procedure may be stated as follows:

Given:

1. Gravity and wind loads.
2. Seismic lateral story shears obtained in the preliminary analysis (Fig. 6).
3. Critical load combinations. Those considered were:

   0.75 (1.4 DL + 1.7 LL + 1.7 W)
   1.4 DL + 1.7 LL

   } from UBC Sect. 2609 (d)

$$\left.\begin{array}{l} 1.2\ DL + 1.0\ LL \pm 1.0\ E \\ 0.8\ DL \pm 1.0\ E \end{array}\right\} *$$

4. Mechanical characteristics of the construction materials. The nominal compressive strength of concrete was taken as 27.6 MPa (4,000 psi), and the nominal yield strength of the reinforcement was taken as 413.7 MPa (60,000 psi).

Find:

The sizes of beams and columns as well as the distribution of beam flexural reinforcement and column longitudinal reinforcement.

This problem is solved by a simplified storywise weak girder - strong column optimum limit state design.

3.3.1 Design Subassemblage

The single story subassemblage used in the preliminary design is shown in Fig. 7. Use of this subassemblage and the weak girder - strong column design criterion simplifies the design problem because it reduces the number of design variables to the selected girder moments in a given story. In a typical intermediate story the use of this subassemblage is justified by the presence of large seismic shear forces which force the column inflection points to be very close to mid-height. In the design procedure, both the negative and positive design moments at a given section are considered independent design variables. If the design moments are assumed to be symmetric about midspan of the center bay, 8 independent design moments may be identified in the example frame (Fig. 7). Determining the optimum value of these design moments is the objective of the optimization procedure presented below.

3.3.2 Design Procedure

Linear programming techniques are used to obtain an optimum

---

*Because the earthquake design forces are obtained considering the inertial forces to be developed under the most severe ground motion, the load factors adopted differ from those of UBC Section 2626(d).

inelastic design. The optimization process attempts to minimize the volume of flexural reinforcement. Equilibrium constraints obtained from the kinematic theorem of simple plastic theory form a physical bases for the optimization, with additional constraints imposed to satisfy serviceability as well as practical requirements.

More realistic objective functions than the volume of flexural reinforcement (such as the total cost of construction which would include the cost of concrete, steel reinforcement, and formwork [10]) might be formulated as part of the optimization procedure. However, it is generally difficult to formulate realistic linear relationships between cost variables and design variables (the beam moment capacities), and since an approximate linear relationship between the area of steel and the design moment capacity exists, the volume of flexural reinforcement was chosen as the objective (merit) function. The possibility of considering a nonlinear total cost function by employing a different mathematical programming technique, such as the method of feasible directions used by Walker and Pister [11], should be studied.

3.3.3 Starting Design

Elastic analyses for the service and ultimate load states must be carried out before starting the above design procedure because: (1) the merit function and several practical constraints are based on ultimate load elastic moment envelopes; and (2) the serviceability constraints are based on the service load envelopes. To carry out these analyses a starting preliminary design (starting relative sizes of members) is required. This presents a problem of how to obtain a good starting design in the first iteration of the design process. Although upper and lower bound approaches can be used, the following procedure is suggested.

1. Assume that the moment capacity in a given span is constant.

2. Formulate an optimization problem based only on the

equilibrium constraints at collapse, thus eliminating the need for elastic analyses.

3. Use the computed moment capacities to size the beams.

4. Use beam capacities found in item 3 to size the columns to ensure a weak girder - strong column design.

The sizes of beams and columns in all stages of the design process were based on the permissible percentage of reinforcement, ρ, bounded as follows.

In the beam design:

$$\frac{200}{f_y} \leq \rho \leq 0.025 \quad \text{or} \quad \leq 0.75\,\rho_b \quad \text{whichever is smaller}$$

The lower bound is a code requirement for the minimum amount of flexural reinforcement. The upper limit of 0.025 is that recommended by the UBC (2626) for ductile moment-resisting reinforced concrete space frames. The upper limit of $0.75\,\rho_b$ is that recommended by the UBC (2610) for the design of flexural members. In this design example the upper bound, $\rho \leq 0.75\,\rho_b$, controlled the design.

In the column design:

$$0.01 \leq \rho \leq 0.04$$

The upper limit is chosen in improve the column's inelastic behavior and also to relieve congestion of reinforcement at beam-column joints. The lower bound is a code requirement.

Details of the design relationships used and the relationship between beam moment capacities and column design moments as well as the results of the suggested starting design procedure will be presented after a discussion of the optimization procedure.

3.3.4 Formulation of Design Problem

In order to use a linear programming technique to obtain the stated optimization objective, it is necessary to formulate a linear function in the desired moment capacities which is proportional to the

volume of flexural reinforcement (Vol). Such a function is obtained from the following relationship between the moment capacity, M_i, and area of steel, A_{s_i}:

$$M_i = A_{s_i} \cdot f_y \cdot jd \tag{12}$$

where

f_y = steel yield stress

jd = distance between the centroids of the resultant compressive and tensile forces

Consequently, the merit or objective function may be expressed as:

$$Vol \sim \sum M_i \gamma_i \tag{13}$$

where γ_i is the effective length over which area A_{s_i} is required.

The quantity γ_i is an effective length because it includes required development lengths at columns and the effect of bar cutoffs. As a consequence it is dependent on the bar size used in design. Typically larger bars will result in larger values of γ_i. In order to arrive at the smallest volume of reinforcement and also to minimize the possibility of significant bond deterioration, use of the smallest possible bar size is recommended.

The contribution of the column reinforcement to the volume of flexural reinforcement should be considered in construction of the merit function. Since a weak girder - strong column design criterion is imposed, the sum of the column moment capacities at a given joint can be expressed in terms of the beam moment capacities at that joint. This expression can be multiplied by an appropriate length factor and added to the merit function. This factor should include the effect of axial load on the column moment capacity and any slenderness effects which may be considered in the actual member design, as well as the extra length of the reinforcing bars needed in case lap splices are used.

The equilibrium constraints used in this design example are given by the following equations which correspond to the mechanisms given in Fig. 8.* Details of the derivation of the equilibrium constraints are presented in Appendix A.

$$\text{(a)} \quad M_1^- + 2M_2^+ + M_3^- \geq \frac{W_{A_G} \ell_A^2}{4}$$

$$\text{(b)} \quad 2M_4^- + 2M_5^+ \geq \frac{W_{B_G} \ell_B^2}{4}$$

where

$W_G = 1.4\, W_{DL} + 1.7\, W_{LL}$

ℓ_A, ℓ_B = clear spans

$$\text{(c)} \quad M_1^- + M_1^+ + M_3^- + M_3^+ + M_4^- + M_4^+ \geq M_H$$

where

$$M_H = F_i \cdot \frac{h_i}{2} + S_{H_{i-1}} \left(\frac{h_{i-1}}{2} + \frac{h_i}{2} \right)$$

$$\text{(d)} \quad M_1^- + 2M_2^+ + 2M_3^- + M_3^+ + M_4^+ + M_4^- \geq M_H + \frac{W_{A_L} \ell_A^2}{4}$$

---

*It should be noted that the equilibrium inequalities, which include the sway mechanism, are not rigorous since the effect of the rigid zone associated with the column width on the virtual plastic rotation is not considered. To include this effect, the coefficient, α_{ji}, associated with the moments in a given span, would be multiplied by XL/L where XL is the length between the column centerlines and L is the clear span. The external work associated with gravity load in the combined mechanism inequalities (e-h) would also be multiplied by XL/L and the external work associated with the sway mechanism (c) would be modified to include work done by gravity loads during the sway vertical displacement. The latter external work correction is required only if the rigid zones at the beam ends are not equal. For this particular design, XL/L varied from a minimum of 1.09 at the roof to a maximum of 1.13 at the second floor level.

where

$$W_L = 1.2\, W_{DL} + 1.0\, W_{LL}$$

$$\text{(e)}\quad 2M_1^- + M_1^+ + 2M_2^+ + M_3^- + M_4^- + M_4^+ \geq M_H + \frac{W_{A_L} \ell_A^2}{4}$$

$$\text{(f)}\quad M_1^- + 2M_2^+ + 2M_3^- + M_3^+ + 2M_4^- + 2M_5^+ \geq M_H + \frac{W_{B_L} \ell_B^2}{4} + \frac{W_{A_L} \ell_A^2}{4}$$

$$\text{(g)}\quad 2M_1^- + M_1^+ + 2M_2^+ + M_3^- + 2M_4^- + 2M_5^+ \geq M_H + \frac{W_{B_L} \ell_B^2}{4} + \frac{W_{A_L} \ell_A^2}{4}$$

$$\text{(h)}\quad 2M_1^- + 4M_2^+ + 2M_3^- + 2M_4^- + 2M_5^+ \geq M_H + \frac{W_{B_L} \ell_B^2}{4} + \frac{W_{A_L} \ell_A^2}{2}$$

$$\text{(i)}\quad M_1^- + M_1^+ + M_3^- + M_3^+ + 2M_4^- + 2M_5^+ \geq M_H + \frac{W_{B_L} \ell_B^2}{4}$$

$$\text{(j)}\quad 2M_1^- + 4M_2^+ + 2M_3^- + M_4^- + M_4^+ \geq M_H + \frac{W_{A_L} \ell_A^2}{2} \qquad (14)$$

The above equilibrium constraints may be represented by the expression:

$$\alpha_{ji}\, M_j \geq \omega_i$$

where

j = 1, number of design moments (N)

i = 1, number of equilibrium constraints (NEQ)

α_{ji} = the coefficient of the jth design moment, M_j, in the ith equilibrium constraint

ω_i = the work done by the external forces in the ith equilibrium constraint

and the repeated indices on the left-hand-side imply summation.

The serviceability constraints place a lower bound on the design moment capacities. The lower bound used in this design procedure is one suggested by Cohn, and it is imposed to prevent yielding, wide cracking, and large deflection under service load conditions [3]. Thus:

$$M_j \geq \lambda_0 M_j^{SE} \tag{15}$$

where

M_j = the jth design moment

M_j^{SE} = the ordinate of the elastic moment envelope under service load conditions

λ_0 = a factor that depends on the serviceability requirements (a value of 1.2 was used)

The remaining constraints are imposed to (1) meet code requirements; (2) achieve a desired inelastic redistribution of moments; and (3) obtain a practical design.

The adopted optimization procedure has the advantage of providing an experienced designer opportunity to use additional constraints based on his or her many years of design experience. The following constraints were used in the design example.

At the beam ends:

$$0.5\,|M_j^-| \leq |M_j^+| \leq |M_j^-| \tag{16}$$

This constraint bounds the positive moment capacity at a given support section with respect to the negative moment capacity at that section. The lower bound is based on code requirements (UBC 2626). It not only recognizes the severity and cyclic (with reversal) characteristics of the seismic excitation, but also represents an attempt to include in member design the beneficial effect of compressive reinforcement on the inelastic deformation characteristics of the

member. The upper bound is based on practical considerations. As will be indicated shortly, the negative support moment capacity is bounded from above by the ordinate of the ultimate load elastic moment envelope at the support. The positive value of this envelope is always less than the corresponding negative value that would be obtained under a 'symmetric' reversal of seismic moments because of gravity load effects. As a result, it was decided to impose the same upper bound constraint on the positive moment capacity as was imposed on the negative moment capacity.

At beam midspan:

$$M_{span} \geq 0.25\, M_{support} \tag{17}$$

This constraint is based on code requirements that at least one-quarter of the larger amount of support reinforcement be continued through the girder. For the design example this constraint results in the following inequalities:

$$M_2 \geq 0.25\, M_1^+$$

$$M_2 \geq 0.25\, M_3^+$$

$$M_5 \geq 0.25\, M_4^+$$

At the beam ends:

$$M_j \leq M_j^{UE} \tag{18}$$

where M_j^{UE} is the ordinate of the elastic moment envelope for the ultimate load condition at section j. This constraint represents an upper bound on the design moment capacity and was imposed only on the negative support moment capacities. It was imposed to relieve steel congestion at the beam column joint. The final practical constraint imposed was:

$$|M_j^-| \geq FAC \cdot |M_{j_{above}}^-| \tag{19}$$

where

$$FAC = \frac{M_j^{-UE}}{M_{j_{above}}^{-UE}}$$

$M_{j_{above}}^-$ = the design moment at section j obtained in the solution of the optimization problem for the story above the current story j

This constraint is an attempt to incorporate the general design criterion of a smooth transition in member strength and stiffness through the height of the structure in the optimization problem.

A last practical constraint is imposed in conjunction with the serviceability constraint. If the product $\lambda_0 M_j^{SE}$ is less than the moment capacity corresponding to the minimum allowable percentage of reinforcement ($M_{\rho_{min}}$), then the latter value was used as a lower bound constraint.

Before continuing the presentation of the preliminary design procedure the construction of a typical merit function is briefly discussed.

3.3.5 Merit Function

The merit function consists of the sum of two components: the beam contribution, γ_i^*, and the column contribution, γ_i^{**}.

$$\gamma_i = \gamma_i^* + \gamma_i^{**} \tag{20}$$

In the design example the beam contribution to the merit function was determined from ultimate load elastic moment envelopes constructed for typical stories through the height of the frame.

One such envelope is shown in Fig. 9. The first step in constructing the merit function is to choose the bar size to be used in design in order to estimate development lengths and bar cutoffs. For

the design example a #8 bar was selected, and the development lengths are given by the UBC equations [2612(f)1 and 2612(g)]:

$$\ell_d^B \geq 0.040\, A_b \frac{f_y}{\sqrt{f'_c}} \quad \text{or} \quad \geq 0.0004\, d_b f_y \geq 304 \text{ mm (12 in.)} \tag{21}$$

where

ℓ_d^B = development length for a bottom bar (in.)

A_b = bar area (in^2)

f_y = steel yield stress (psi)

f'_c = nominal concrete compressive strength (psi)

d_b = bar diameter (in.)

For the design example the first inequality controls, and for a #8 bar, f_y = 413.7 MPa (60,000 psi), and f'_c = 27.6 MPa (4,000 psi):

$$\ell_d^B = 760 \text{ mm (30 in.)}$$

The development length for a top bar, ℓ_d^T, is:

$$\ell_d^T = 1.4\, \ell_d^B = 1.06 \text{ m (42 in.)}$$

The evaluation of a typical γ_i^* is based on the UBC requirement for reinforcement development (UBC Section 2612). In the following it is assumed that the transverse reinforcement is detailed to permit bar curtailment in tension zones [UBC (2612(b)6]. In addition, because of the relatively small bar diameter assumed, and since at least one-third of the negative moment reinforcement was continued through each span, limitations at inflection points do not affect bar curtailment [UBC 2612(c), 2612(d)]. The following example, based on the moment envelope in Fig. 9, illustrates the evaluation of γ_i^{-*}.

If bars are to be cut off in pairs, the steel required to resist M_1^- must be continued to at least point A. However, in order

to develop the full yield stress of all bars at the column face (Fig. 9), these bars must be continued beyond the column face a distance equal to the required development length, ℓ_d^T (point B in Fig. 9). In addition, the reinforcement must extend beyond the point it is no longer required to resist flexure (point A in Fig. 9), a distance ℓ^* equal to the effective depth of the member or 12 bar diameters, whichever is greater [UBC 2612(b)4]. This requirement accounts for the fact that, because of possible shifts in the location of maximum moment and because of inclined cracking, the tensile stress at a given section may be greater than that indicated by the moment envelope. In this example ℓ^* is equal to the effective depth and the bars must be extended to point C. The curtailment schedule for a given moment capacity is determined by satisfying the above requirements for each possible bar cutoff, and γ_1^{-*} becomes (Fig. 9):

$$\gamma_1^{-*} = \ell_{11}^- + \frac{5}{6}\ell_{21}^- + \frac{2}{3}\ell_{31}^- + \frac{1}{2}\ell_{41}^- + \frac{1}{3}(\frac{1}{2}\ell^-) + [\ell_d^+] \qquad (22)$$

where the term in brackets accounts for bar anchorage into the column and $(1/2\ \ell^-)$ is used because the other half is added to γ_3^{-+}. The remaining values of γ_i^* are evaluated in a similar way.

To include bar anchorage at interior beam-column joints, one-half the calculated development length was added to the γ_i^* term of both moment capacities at the joint. In practice, beam reinforcement is typically continued through the column and only bars which are cut because of a difference in moment capacity across the joint require anchorage. In view of this, one-half the column depth (h_c) should be added to γ_i^* corresponding to the smaller moment at the joint and $1/2\ h_c$ plus the development length of bars to be curtailed in the joint should be added to γ_i^* corresponding to the larger moment. However, the larger moment capacity as well as the difference in moment capacity was not known beforehand, and an approximation was required. This approximation should depend on the size of the bar considered

in design. In this example, it was felt that one-half the computed development length would adequately reflect the contribution of bar anchorage to a typical γ_i^* (1/2 ℓ_d^T contributes between 10% and 15% to a typical γ_i^*, while 1/2 h_c, which is a lower bound on the correct value, would contribute between 8% and 10%). In this development bar splices have been excluded to simplify the construction of the merit function.

From the UBC definition of development length it is evident that ℓ_d increases as the bar size increases. As a result, smaller volumes of reinforcement are required to supply a given steel area when smaller diameter bars are employed. In addition, smaller bars will allow more curtailment of reinforcement, further reducing the volume. Consequently, in terms of material used and expected seismic behavior, in particular with respect to bond deterioration, it is advantageous to use smaller bars if these bars are adequately restrained laterally by closely spaced ties.

A brief study in the effect of bar size on the optimization solution indicated that the results in the intermediate and lower stories were sensitive to the bar size assumed in the construction of the merit function. Further study of the construction of the merit function, in particular with respect to the definition of development lengths and bar cutoffs is necessary.

The column contribution to the merit function, γ_i^{**}, is found on the basis of the weak girder - strong column design criterion. The objective of this criterion is to limit as much as possible the inelastic column behavior which requires that the sum of the design column moment capacities at a given beam-column joint exceed a function of the beam design moments at that joint. This function is derived from joint equilibrium considering the critical combination of possible beam hinging. Once derived the function is simplified and multiplied by appropriate lengths, and is then added to the beam contribution, γ_i^*, discussed previously, to yield the merit function. In the design example different relationships for exterior and

interior columns were required.

For an exterior column:

$$C(M_j) = \frac{h_b}{h_c} \cdot \ell_c \cdot F \cdot \frac{1}{\phi_c} \left[|M_1^-| + \frac{h_c}{2\ell_A} \left(|M_1^-| + |M_3^+| \right) \right] \cdot PF \tag{23a}$$

For an interior column:

$$\begin{aligned} C(M_j) = \frac{h_b}{h_c} \cdot \ell_c \cdot F \cdot \frac{1}{\phi_c} \Bigg[& \frac{1}{2} \left(|M_3^-| + |M_4^+| + |M_3^+| + |M_4^-| \right) \\ & + \frac{h_c}{4\ell_A} \left(|M_1^-| + |M_1^+| + |M_3^+| + |M_3^-| \right) \\ & + \frac{h_c}{2\ell_B} \left(|M_4^-| + |M_4^+| \right) \Bigg] \cdot PF \end{aligned} \tag{23b}$$

where h_b, h_c, ℓ_A, ℓ_B, and M_j are defined in Fig. 10,

F = safety factor used in the design of columns for a weak girder - strong column design

ℓ_c = clear column height (see Appendix A, Section A2.2)

PF = factor accounting for the effect of axial load on moment capacity

ϕ_c = code capacity reduction factor for columns

The derivation of these expressions and the simplifying assumptions made are given in Appendix A.

The ratio h_b/h_c accounts for the effect of different beam and column depths on the moment capacity. From eq. (12) it can be seen that a linear relationship exists between the moment capacity and member depth.

The choice of the factor F will vary according to the expected ductility, the stress-strain characteristics of the steel, and how the beam moment capacities are evaluated. A value of 1.2 was used in

the design example. A detailed discussion of the factors which should be considered in the choice of an appropriate column overstrength factor to ensure a weak girder - strong column design is presented by Park in reference 12.

The PF factors were determined from the geometric and strength characteristics of the columns found in the starting preliminary design. The moment amplification due to column slenderness effects has not been considered in the PF factor since UBC 2610(1)7 required that it also be included in the beam design.

The factor $1/\phi_c$ is included to account for the increase in column design moments caused by the code capacity reduction factor.

In an attempt to average the effect of the four design moments at a typical interior joint, the first bracket in eq. (23) was multiplied by 1/2. The actual column design moment would depend on $(|M_3^-| + |M_4^+|)$ or $(|M_4^-| + |M_3^+|)$, whichever is greater. An average value is used in the merit function to prevent any bias in the optimization procedure.*

The terms multiplied by the factor h_c/ℓ_α (α = A or B) account for the effect of beam shear forces on joint equilibrium. The equilibrium equation also has a gravity term, but it can be ignored in the merit function because it is independent of the design variables. These shear terms represent an average of the possible beam shear forces due to lateral loads. It should be noted that the shear terms are small and could be neglected. They are included here for completeness. The construction of a typical merit function is illustrated by a numerical example in Appendix A.

*An average value was not used in the expression for the exterior column because of the design constraint that $M_1^- \geq M_1^+$. In accord with accepted practice a symmetric distribution of column steel is assumed in column design. The amount of steel required for the exterior column is determined on the basis of the critical combination of beam design moments, which, because of the above constraint, always depends on M_1^-. Consequently, all the exterior column steel is assigned for M_1^-. The effect of this characteristic of the merit function on the solution of the optimization problem is now being investigated.

3.3.6 Summary of Optimization Problem

The optimization problem may be summarized as follows.

Find $M_j \geq 0$ $\quad j=1,N$

which satisfies:

(a) equilibrium constraints

$$\alpha_{ji} M_j \geq \omega_i \qquad j=1,N \qquad i=1,NEQ$$

(b) serviceability constraints:

$$|M_j| \geq m_j \qquad j=1,N$$

where m_j is the greater of $|\lambda_0 M_i^{SE}|$ or $|M_{\rho_{min}}|$

(c) practical constraints:

$$0.5\,|M_j^-| \leq |M_j^+| \leq |M_j^-|$$

$$|M_{span}| \geq 0.25\,|M_{support}|$$

$$|M_j^-| \leq |M_j^{-UE}|$$

$$|M_j^-| \geq FAC \cdot |M_{j_{above}}^-|$$

and minimizes the linear function:

$$\gamma_j M_j \geq 0 \qquad j=1,N$$

An optimization problem is formulated for each story and then solved with the aid of a standard Simplex algorithm. The optimum girder moment capacities, M_j, obtained are then used to design the frame members.

3.3.7 Member Design

The beams and columns were designed using available computer programs based on the following design relationships.

(a) Beam design

The beams were designed according to the equation:

$$\frac{M_u}{\phi} = bd^2 \left\{ \rho f_y \left[1 - \frac{f_y}{f'_c}\ 0.59\ \rho \right] \right\} \tag{24}$$

where

ϕ = 0.9, the UBC capacity reduction factor for flexural members

d = effective depth

b = section width (assumed = t/2, where t = section depth)

ρ = percentage of flexural reinforcement (A_s/bd)

The term M_u is the optimized beam design moment multiplied by an amplification factor, α_F, to account for the column slenderness effects. The value of α_F is determined from the column moment amplification factors corresponding to the member sizes of the starting design.

After the girders have been designed, their moment capacities are evaluated and used as the basis of the column design.

(b) Column design

The columns are designed to ensure that the weak girder - strong column criterion is satisfied. The following expression, derived from equilibrium of a typical beam-column joint, is used to relate the column design moments to beam moment capacities (Fig. 10):

$$M_c^T \cdot f(\ell_c^T, h_b) + M_c^B \cdot f(\ell_c^B, h_b) \geq F \cdot \left[f(M_b^D) + f\left(\frac{M_b^D}{\ell_b}, h_c\right) + f(W_b \ell_b, h_c) \right] \quad (25)$$

where

M_c^T, M_c^B = top and bottom column design moments

$f(\ell_c^T, h_b)$, $f(\ell_c^B, h_b)$ = functions of column height and beam depth which account for the effect of V_c^T and V_c^B on joint equilibrium

F = column overstrength factor (a value of 1.2 is used)

$f(M_b^D)$ = a function of beam moment capacities computed on the basis of the provided reinforcement which accounts for the beam moments in joint equilibrium

$f\left(\frac{M_b^D}{\ell_b}, h_c\right)$ = a function of beam design moments, span lengths (ℓ_b), and column width (h_c) which accounts for the part of the beam shear due to lateral shear forces

$f(W_b\ell_b, h_c)$ = a function of beam gravity loads (W_b), span lengths, and column width which accounts for different gravity load shears in the joint equilibrium equation

The three functions on the right-hand side of the above inequality should be chosen to yield the maximum possible column design moments. That is, all possible combinations should be considered, and the one which results in the largest value for the right-hand side should be selected. It should be noted that column slenderness effects are included in the above expression since the beams were designed to supply moment capacities amplified to account for column slenderness. The above functions are defined for various cases in Appendix A.2.2.

In the column design it is assumed that the reinforcement which defines the column moment capacity is the same above and below a joint. That is, all column splices occur near mid-column height. If boundary conditions of the columns above (top) and below (bottom) a given joint are assumed to be the same, the distribution of $\sum M_c^D$ to the top and bottom column can be based on the following equation:

$$M_c^T = \beta M_c^B \tag{26}$$

where β is a moment distribution factor obtained from the distribution of elastic stiffness at the beam-column joint. For a typical joint:

$$\beta = \frac{K_T}{K_B}$$

where

$$K_T \sim \frac{\frac{E\, I_c^T}{\ell_c^{T^2}}}{K_{total}} \qquad K_B \sim \frac{\frac{E\, I_c^B}{\ell_c^{B^2}}}{K_{total}}$$

$$K_{total} \sim \sum_{beams} \frac{EI_b}{\ell_b^2} + \sum_{columns} \frac{EI_c}{\ell_c^2}$$

and the subindices c and b refer to columns and beams, respectively.

When a change in column section occurs through a joint, each section is designed to resist its own design forces, and the larger amount of reinforcement obtained is used for both columns. This procedure is followed because it is assumed that column reinforcement is continuous through the joint.

In order to consider all critical column load combinations, a bound on the axial force due to overturning effects (tension and compression) must be obtained. For an exterior column such a bound is easily established. The maximum possible beam shear, which corresponds to a condition of hinging at both ends of the exterior beam, can be expressed in terms of:

$$V_{tension} = \frac{|M_1^+| + |M_3^-|}{\ell_A}$$

$$V_{compression} = \frac{|M_1^-| + |M_3^+|}{\ell_A} \qquad (27)$$

A bound on the column overturning axial force at a given story is obtained by summing the maximum possible beam shear for the beams

of all the floors above the given story.

Such bounds cannot be so easily obtained for an interior column, however, and the overturning moment axial forces obtained in the ultimate load elastic analysis used to formulate the preliminary design problem were considered in the interior column design. Once known, the tensile and compressive overturning axial forces for a given member are added to the respective gravity load axial forces to yield and lower and upper bound design axial force.

In the column design, the most critical combination of axial load and bending moment was considered. The moment corresponding to the code minimum eccentricity* was also checked to see whether it controlled the design. The computer program used to design the columns was based on the ACI ultimate strength design code [13]. A standard capacity reduction factor of 0.7 was used. This value was increased for small axial loads, as allowed in UBC 2609(c)2D. The column size was selected such that the column axial load would be kept below the balance point of the axial force - moment interaction relationship, in order to have some ductility available in case the column should yield.

3.3.8 Final Remarks

Preliminary design involves two iterative loops. The first loop was discussed in Section 2.1.2 and is illustrated in Fig. 2. Iteration is required because member sizes are needed to formulate the optimization problem, the solution of which will generally result in different member sizes.

A second iterative loop exists in the actual design. The column design moments are based on the beam moment capacities which depend on the moment slenderness amplification factors which are in turn dependent on the column sizes. Since the sizes of the most

---

*UBC 2610(d)6 specified $e_{min} \geq 1$ in. (2.54 cm) or, for a tied column, $e_{min} \geq 0.1\ h$, where h is the larger column dimension.

recently designed members will generally differ from those used in evaluating the initial slenderness effects, iteration is used to arrive at a design in which the initial and final moment amplification factors are in close agreement. The following steps are involved.

1. The moment amplification factors corresponding to the design employed to formulate the optimization problem are used to find the beam design moments.

2. The beams are designed and the beam moment capacities are evaluated.

3. The columns are designed.

4. New moment amplification factors corresponding to the new column sizes are determined and compared to the previous values. If there is close agreement, the member design is complete. If not, the member design is repeated with beam design moments corresponding to the new moment amplification factors.

3.4 Design Results

3.4.1 Starting Preliminary Design

As discussed previously, member sizes are required to initiate the optimization process because various design constraints depend on the results of elastic analyses and the construction of the merit function herein is based on the envelope of elastic moments. In the present application, the initial design was obtained by following the procedure suggested in Section 3.3.3. An optimization problem was formulated on the basis of the equilibrium constraints which result when the moment capacity in a given span is assumed constant. For the design example this assumption results in two unknown design moments (the symmetry assumed in Section 3.3.1 is also assumed here), and the equilibrium constraints defined by eq. (14) reduce to:

$$\text{(a)} \quad M_A \geq \frac{W_{A_G} \ell_A^2}{16}$$

$$(b) \quad M_B \geq \frac{W_{B_G} \ell_B^2}{16}$$

$$(c) \quad 4M_A + 2M_B \geq M_H$$

$$(d) \quad 6M_A + 2M_B \geq M_H + \frac{W_{A_L} \ell_A^2}{4}$$

$$(e) \quad 6M_A + 4M_B \geq M_H + \frac{W_{B_L} \ell_B^2}{4} + \frac{W_{A_L} \ell_A^2}{4}$$

$$(f) \quad 8M_A + 4M_B \geq M_H + \frac{W_{B_L} \ell_B^2}{4} + \frac{W_{A_L} \ell_A^2}{2}$$

$$(g) \quad 4M_A + 4M_B \geq M_H + \frac{W_{B_L} \ell_B^2}{4}$$

$$(h) \quad 8M_A + 2M_B \geq M_H + \frac{W_{A_L} \ell_A^2}{2} \qquad (28)$$

where

M_A = moment capacity in span A (also span C)

M_B = moment capacity in span B

A merit function proportional to the volume of flexural reinforcement was constructed. The beam contribution was taken as the beam clear span plus required development lengths into columns. The column contribution was taken as:

$$C(M_\alpha) = F \cdot \ell \cdot f(M_\alpha) \qquad (29)$$

where

F = factor which ensures a weak girder - strong column design

ℓ = column height

$f(M_\alpha)$ = M_A for an exterior column and
= $M_A + M_B$ for an interior column

The effect of the finite joint dimensions on joint equilibrium have been neglected in the above expression for simplicity. In eq. (29) it is assumed that the column reinforcement required to provide a given design moment is twice the beam reinforcement required to provide the same moment (Appendix A.2.3).

The beam design moments were found by solving the optimization problem.

Find:

$$M_\alpha \geq 0 \qquad \alpha = A, B$$

which minimizes:

$$\gamma_\alpha M_\alpha \geq 0$$

and satisfies the equilibrium constraints:

$$\alpha_{j\alpha} M_\alpha \geq \omega_j \qquad j=1,NEQ \qquad \alpha = A, B$$

The results for the design example are shown in Fig. 11. The frame members were designed on the basis of these design moments following the procedure discussed in Section 3.3.7. The resulting member sizes are shown in Fig. 12.

3.4.2 Results of Preliminary Design

The preliminary design, obtained after two iterations of the optimization procedure (Fig. 2), is summarized in Figs. 13-16. The optimization beam design moments are shown in Fig. 13, and the resulting member sizes are shown in Fig. 14. Selection of member sizes was based on the design criterion of a smooth transition in stiffness through the height of the structure with consideration of

the economics involved in formwork changes. For the design example the member sizes were constrained to be constant for two stories. Although for economic reasons the practice in the U. S. is to keep member sizes, particularly the beams, constant for a larger number of stories, indiscrimate use of this practice can lead to sudden changes in strength and/or stiffness and thus result in a design which is in conflict with the basic principle of achieving toughness in the whole structure.

The final beam moment capacities* are shown in Fig. 15, and the variation of column reinforcement is shown in Fig. 16.

The significant difference between the preliminary optimized design moments (Fig. 13) and the final beam moment capacities (Fig. 15)--ranging from from 1.3 to 1.7--is due to three factors. First, a code capacity reduction factor for flexural members of 0.9 was used in the member design. Secondly, the beam moments shown in Fig. 13 were amplified to account for the column slenderness effects. Amplification ranged from 1.06 in the upper stories to 1.25 in the lower stories. (Details are given in Appendix A.4.) Finally, the use of practical formwork sizes and a limited number of available bar sizes caused the selected beam size and reinforcement arrangement to provide moment capacities greater than actually required.

3.5 Analyses of Preliminary Design

3.5.1 Results of Elastic Analyses

An elastic frequency analysis of the designed structure resulted in a first mode period of 1.21 sec. This value is somewhat higher than the value of 1 sec assumed in determining the seismic design forces. However, in view of the shape of the design spectrum used (Fig. 5), the design forces of a new preliminary design should be smaller, but not significantly, than those used.

---

*T-beam effect of the slab on the beam moment capacity was not considered in the design.

The period ratios (T_1/T_i) and the mode shapes (ϕ_i) obtained in this analysis were also similar to those chosen initially. In this frequency analysis and subsequent elastic and nonlinear static and dynamic analyses, the effect of the floor slab on the frame's stiffness was included by using a method proposed by Malik and Bertero [14].

The results of an elastic analysis for service load conditions (DL + LL + WL) yielded a maximum story drift index of 0.00026, well under the established design criteria of 0.002. This clearly indicates that the design for a severe earthquake ground motion leads to an improvement in serviceability under other types of hazards (wind in this case). This is a factor that is not usually recognized when the extra cost for earthquake design is discussed or evaluated.

3.5.2 Results of Nonlinear Static Analyses

The nonlinear static behavior of the designed frame was evaluated using a modified version of the program ULARC [15]. In this analysis, member yielding was modeled by the formation of localized plastic hinges at the member ends. The moment curvature relationship is assumed to be elastic, perfectly plastic. The effect of axial load on the column yield moment, the P-Δ effect, and rigid beam-column joints were included in the modified version of the program. The frame was subjected to design gravity loads and a monotonically increasing seismic base shear which was distributed through the height of the frame according to the lateral force pattern obtained from the spectral modal analysis.

Results of the nonlinear static analysis are summarized in Fig. 17. Variations of roof and first story lateral displacements with the increasing value of the base shear are shown in this figure. Two analyses were carried out in order to investigate the P-Δ effect. A comparison of the two roof displacement responses demonstrates the 'negative stiffness' contribution of the P-Δ effect. This is particularly evident at large displacements [250-380 mm (10-15 in.)] where the applied lateral force decreases with increasing displacements.

A significant overstrength is observed whether or not the P-Δ effect is considered, the maximum base shear was greater than the design base shear by 55%. Two factors contribute to this overstrength. First, the final beam strengths were, as discussed previously, significantly larger than required. Secondly, the design forces were based on the assumption that the entire frame would be transformed into a mechanism simultaneously. An examination of the sequence of hinge formation indicated that this did not occur. The first plastic hinge formed at stage A-A', which corresponds to a base shear of approximately one-half the design value. Subsequent hinge formation was gradual and is depicted in Fig. 17.

The changes in the deformation pattern through the height of the frame with increasing roof displacement level and the associated plastic hinge patterns are of interest. From Fig. 17 it is evident that the first story displacement response remained essentially elastic throughout the analysis. This is consistent with the observed hinge formation sequence (Figs. 18 and 19). Plastic hinges formed initially in the upper stories and gradually progressed downward. Consequently, the stiffness of the lower stories is affected by yielding at a much later stage than that in the upper stories. In this particular example the sequence of hinge formation is such that the stiffness of the first story remains essentially unchanged.

The above observation is supported by the deformation patterns in Fig. 20. The first pattern is the elastic pattern and corresponds to point A-A; in Fig. 17. In going from A-A' to C-C' the deformation pattern becomes slightly irregular but does not deviate significantly from the elastic pattern, particularly in the lower stories. The plastic hinge pattern at stages C-C' (Fig. 18) indicates that there are critical regions at essentially every story which remain elastic and prevent a significant change in deformation pattern. At stages E-E', however, plastic hinges have formed at both ends of all beams from story 5 to the roof, and the flexural stiffness of the individual columns provides the only resistance to lateral deformation (Fig. 19).

As a result, the incremental deformation pattern of the upper region of the frame is similar to that of a cantilever column. As the displacement level is increased, this cantilever behavior continues in the upper stories and extends downward as additional plastic hinges form (stages M-M' in Fig. 20).

In the static analysis, yielding was limited to the beams until stages M-M' wherein the columns of the fifth story yielded (Fig. 21). Subsequent increases in displacement resulted in a partial sway mechanism of the part of the frame above this story at a roof displacement of 680 mm (27 in.). Column yielding is due to a change in the distribution of the beam moments between the columns above and below a typical beam-column joint. This change, caused by beam yielding, was such that almost the entire joint moment was resisted by one column.

The column yielding demonstrates the difficulty in ensuring an efficient weak girder - strong column design. Overdesigning the columns by a factor of 1.7 with respect to the beams failed to prevent column yielding prior to complete beam yielding. As is discussed in subsequent sections, this problem becomes even more prominent in the dynamic response.

3.5.3 Results of Nonlinear Dynamic Analyses

The nonlinear dynamic response of the designed structure to the El Centro N-S component and the Derived Pacoima Dam ground motions was assessed using SERF, a program developed by Mahin and Bertero [16]. The accelerations of both ground motions were scaled to have peak values of 0.4g and 0.5g. Although the frame design was based on an effective peak ground acceleration of 0.4g, because of the uncertainties involved in estimating the peak acceleration at a given building site, a peak acceleration of 0.5g was also considered in order to evaluate the consequence of a more severe ground motion occurring. It should be noted that while the El Centro ground motion had dynamic characteristics represented by the ground spectrum selected as the design earthquake, the Derived Pacoima Dam motion

did not [5]. In the analyses the following assumptions are introduced:

1. Rayleigh-type damping with a 5% damping ratio in the first two modes.

2. Both the beams and columns have a bilinear M-ϕ relationship with linear strain hardening. A strain hardening value of 5% was assumed.* The effect of this parameter on the dynamic response was investigated in the final design and is discussed in Chapter 4.

3. Column yielding is determined from the corresponding axial force-bending moment interaction.

4. P-Δ effect is included.

5. Beam-column joints are rigid.

Based on the results of the dynamic analyses, the following observations are made.

1. There was a significant difference in response for the two ground motions considered. Although the maximum ground accelerations of the two input motions were the same, the maximum displacements during the response to the Derived Pacoima ground motion were approximately three times those recorded during the El Centro motion (Fig. 22). This demonstrates the need to consider all possible ground motions at a given site and also all characteristics (acceleration, velocity, and displacement) of these ground motions (not just the peak ground acceleration) when selecting a design earthquake [5]. The long-duration pulses in the initial portion of the Derived Pacoima ground motion caused severe inelastic behavior in one direction (Fig. 23) which, as will be discussed later, raises questions as to the reliability of the design. The displacement time histories at various floor levels are shown in Figs. 23 and 24.

---

*In reference 16, Mahin and Bertero evaluated the strain hardening ratio on the basis of analytical moment-curvature behavior of the frame members. They obtained average values of 2% and 3%. Based on this work, a value of 5% may be considered an upper bound.

Results of the nonlinear static analysis may be used to obtain an estimate of the dynamic floor displacement ductilities. The static base shear - roof displacement relationship is reproduced in Fig. 25. If the first significant lateral yield displacement of the frame is defined by the $\Delta_{y_{roof}}$ indicated in Fig. 25, and the displacement pattern corresponding to this roof displacement is assumed as the yield displacement pattern, the floor displacement ductilities given in Table 1 may be computed. From these ductility data it is evident that the Derived Pacoima ground motion causes significantly larger (three times) inelastic deformations than the El Centro ground motion. In addition, it appears that the displacement ductility assumed in determining the seismic design forces is exceeded during the response to the Derived Pacoima ground motion. It should be noted, however, that the displacement ductilities given in Table 1 are just estimates because of the different nature of the responses during which the yield and maximum displacements were determined, and these ductility demands should be used as guideline values only.

2. Comparison of the envelopes of actual and design story shears (Fig. 26) indicates that the dynamic story shears are greater than the design forces. This is due to a number of factors.

(a) The members had been overdesigned; an increase in shear capacity has already been revealed by the static analysis (Fig. 17).

(b) Strain hardening increased the moment capacity of the members, particularly that of the beams.

(c) The story shear forces given for the dynamic response are absolute maximum values at each story, and did not occur at the same time during the response. The story shear distribution occurring at any given time is generally quite different from the distribution indicated by the envelope. This is illustrated in Fig. 29, which compares the story shear distribution occurring at the time that the maximum base shear is reached with the envelope of story shear for the Pacoima ground motion at 0.5g.

(d) The design shear forces were determined assuming that the entire frame was transformed into a mechanism simultaneously. As in the static analysis, this did not occur in the dynamic response either. Examination of plastic hinge formation during the dynamic response to ground motion indicates that there is a migration of plastic hinges from the base to the top of the building and that as plastic hinges form in the upper stories, the hinges in the lower stories close. For example, consider Fig. 28 in which recorded plastic hinge patterns during the response to the El Centro ground motion are presented. It is evident that a complete or even partial mechanism does not occur because the lower story hinges close before those in the upper stories form. It should be noted that this is the principal objective and advantage of imposing a weak girder - strong column design criterion, i.e. to avoid formation of partial sway mechanisms and thus reduce the possibility of large concentrated inelastic deformations in the columns of one or more stories.

3. Comparison of the story shear envelopes for the two ground motions (Fig. 26) indicates that the Pacoima ground motion resulted in larger story shears, particularly in the lower stories. This difference is attributed to the different characteristics of the two ground motions and the fact that strain hardening was considered in the assumed member $M-\phi$ relationships. Strain hardening increased the beam moment capacities beyond those computed on the basis of yielding of the reinforcement. Since the columns were overdesigned with respect to the beams (by a factor of about 1.7), story shears greater than those corresponding to the designed beam capacities could result. The increase in beam moment capacity associated with strain hardening is directly proportional to the magnitude of inelastic deformation. Since the inelastic deformations recorded during the Pacoima response were larger than those of the El Centro response, the increase in beam moment capacity was greater during the former. For example, strain hardening increased the beam moment capacity by as much as 54% during the Pacoima response, while the increase during

the El Centro response was less than 24%. Since the story shears are proportional to the beam moment capacities, greater story shears are expected during the Pacoima response.

4. Envelopes of the story drift index (Fig. 29) indicate that the design criteria for R_{ult} is violated during the response to the Pacoima ground motion with a maximum acceleration of 0.5g. The large story drifts at the intermediate stories demanded by the Pacoima ground motion indicates a high probability of severe nonstructural damage.

5. Examination of the required column ductilities (Figs. 30 and 31) indicates that the weak girder - strong column design criterion is satisfied during the El Centro response. Column yielding, however, does occur at various locations during response to the Pacoima ground motion and is attributed in part to the increase in beam moment capacities caused by strain hardening. In addition, the distribution of beam moments between the column sections above and below a given joint was typically different from that assumed in design. In design the beam moments at a given joint were distributed to the columns at the joint on the basis of an elastic stiffness distribution factor (Section 3.3.7). However, higher mode response and, as indicated by the nonlinear static analysis, formation of beam plastic hinges can alter the moment distribution at that joint to the extent that the sum of the beam moment capacities is resisted by only one of the columns at the joint. This is illustrated in Figs. 32 and 33 which depict the variation of column bending moments through the height of the frame at two instances during the response to the 0.5g Pacoima ground motion. Figure 32 gives the distribution for an exterior column and Fig. 33 for an interior column. The corresponding plastic hinge patterns are indicated in Fig. 34. Both moment variations indicate the difference between the actual distribution of beam moments to the columns at a joint and the distribution assumed in design. The difference is greatest in the upper and intermediate stories, which is as expected since higher mode

effects are more significant in these stories. As an example, consider the exterior beam-column joint at the eighth floor in Fig. 32. The column below the joint yielded just prior to 1.0 sec (t = 0.985 sec). This yielding is primarily a consequence of the large portion of the joint moment which this column had to resist. At 1.0 sec the exterior column below the joint was resisting more than 90% of the joint moment (Fig. 32).

An additional example, which also illustrates the effect of strain hardening on column yielding, is provided by the interior beam-column joint at the sixth floor (Fig. 33). Although the column below the joint resisted more than 80% of the joint moment, column yielding probably would not have occurred except for the fact that, as a result of strain hardening, the moment capacities of the two adjacent beams at this joint increased by 54% and 25%.

Higher mode response during the Pacoima ground motion is illustrated in Fig. 23 and also by the unloading and reloading of the upper story beam plastic hinges depicted in Fig. 34 during the first large acceleration pulse.

Another source of inconsistency between the moment distribution assumed in design and the actual moment distribution is the assumption made in the preliminary design that the end conditions of the upper and lower columns at a given joint are the same. An examination of where column yielding occurred indicates that the effect of different end conditions on the column moment distribution at a given joint may have had an influence on column yielding. Yielding occurred at story levels corresponding to columns with different end conditions and in the column with the stiffer end condition. For example, at the eighth story the upper interior column is restrained at its far end by a 355-mm x 710-mm (14-in. x 28-in.) beam and a 660-mm x 660-mm (26-in. x 26 in.) column, while the lower column is restrained by a 405-mm x 810-mm (16-in. x 32-in.) beam and a 760-mm x 760-mm (30-in. x 30-in.) column. For a given joint rotation the stiffer end restraint in the lower column would cause

it to resist a larger moment than the upper column. In the design of these and other sections which yielded, the beam moments were distributed equally to the upper and lower columns. Therefore the lower column was 'underdesigned'.

An attempt is made in the final design to eliminate the problem of different column end conditions by designing the columns based on a moment distribution found from an elastic analysis. However, the analysis of the final design, which will be discussed in the next chapter, indicates that this factor had a minimal effect on column yielding.

The magnitude of the inelastic column deformation (plastic hinge rotation) in the upper stories was small, being less than 0.003 rad. The accumulated rotation was essentially the same as the maximum value, indicating just one large inelastic excursion. The maximum plastic rotation in the columns at the ground level was approximately 0.01 rad and could be tolerated with proper detailing.

6. The considerable difference in the effects that different ground motions have on the individual members is illustrated by analyzing the inelastic deformation behavior of the beams. For the El Centro ground motion, the maximum cyclic curvature ductility, $\mu_{\phi_{cyclic}}$, is less than 9 (Fig. 35). However, in the response to the Pacoima ground motion, values greater than 17.5 were obtained. This trend is also indicated by the maximum plastic hinge rotation, $\theta_{P_{max}}$, and the accumulated plastic hinge rotations, $\theta_{P_{acc}}$ (Figs. 36 and 37), where:

$$\theta_{P_{acc}} = \sum_{N} |\theta_p|, \text{ N = number of yield excursions}$$

For the El Centro ground motion, $\theta_{P_{max}}$ was 0.0065 rad, and $\theta_{P_{acc}}$ was 0.033 rad, while during the Pacoima ground motion, the values were 0.020 and 0.06 rad, respectively. The large difference in $\theta_{P_{max}}$ between the two ground motions demonstrates the effect that the long acceleration pulses contained in the Pacoima ground motion had on the

structure's response. These pulses caused the structure to deform in one direction for a long period of time (0.56 sec) during which it experienced large inelastic deformations.

The variation of inelastic beam deformation through the height is also different for the two ground motions. For example, consider the variation of maximum plastic hinge rotation (Fig. 36). In the upper stories the variation of rotation is similar for both records. However, at floor 7 the plastic hinge rotation begins to decrease as one proceeds down toward the ground level for the El Centro ground motion, but continues to increase for the Pacoima ground motion. This is again a consequence of the long acceleration pulses contained in the Pacoima ground motion which, when suddenly applied to the foundation, causes it to displace considerably with respect to the upper part.

Comparison of the plastic hinge rotation demands with experimental results obtained by several investigators [17,18] indicates that the frame should be capable of safely resisting the El Centro earthquake. Because of large inelastic deformation requirements, however, the current structure might experience severe structural damage and possible structural failure if it were excited by a ground motion with characteristics similar to the Pacoima record and the reinforcement were not specifically designed and detailed to develop these deformations.

7. Nonlinear and linear-elastic dynamic responses for a ground acceleration of 0.5g are compared in Figs. 38 and 39. The elastic displacements are greater than the corresponding nonlinear values for both the Derived Pacoima Dam and El Centro ground motions (Fig. 38). The relative increase in displacement which occurred when completely elastic behavior was assumed is inversely related to the amount of inelastic deformation experienced during the nonlinear response (Fig. 36). The increase is greater for the El Centro ground motion (30%-60%) during which the frame experienced relatively small inelastic deformations compared to those for the Pacoima

ground motion (5%-30%). In addition, for a given ground motion, the increase was greater at stories where the inelastic deformations were smaller (Figs. 36 and 38).

The maximum elastic base shear was greater than the inelastic response by a factor of approximately two for the El Centro motion and a factor of four for the Pacoima motion (Fig. 39). A comparison of the maximum beam moments obtained in the elastic analyses with the beam moment capacities obtained by the proposed design procedure (Fig. 14) indicates that for the response to remain elastic, member capacities would have to be increased by as much as four times for the El Centro ground motion and by as much as seven times for the Pacoima motion. The magnitude of these increases demonstrates the economic necessity of relying on ductile inelastic deformations in seismic design.

8. Ratios of maximum story displacements, story drift indices, story shears, and maximum beam plastic hinge rotations recorded at peak ground accelerations of 0.5g and 0.4g are compared for the two ground motions in Table 2. An examination of the data in Table 2 indicates that the story shear is increased by approximately 10% for each of the ground motions as the peak acceleration is increased from 0.4g to 0.5g. The increase is attributed to the increase in beam moment capacities caused by an increase in strain hardening at the larger value of peak acceleration.

The effect on the floor displacement response of increasing the ground acceleration differs significantly for the two ground motions (Table 2). The increase in floor displacements varied between 40% and 70% as the ground acceleration was increased from 0.4g to 0.5g for the Pacoima ground motion. During the El Centro ground motion, however, the maximum increase was only 25%. This difference is attributed to the degree of inelastic behavior caused by the Pacoima ground motion, in particular yielding in the lower story columns. These results clearly demonstrate that an error in the estimation of the effective peak ground acceleration which might

occur at a building site can lead to considerable underestimates of deformation, particularly for ground motions with characteristics similar to the Pacoima ground motion.

3.6 Summary

The results of the nonlinear dynamic analysis indicate that the designed structure will be capable of resisting a ground motion with characteristics similar to the El Centro record without suffering extensive structural damage, and that the building will not undergo severe nonstructural damage. However, significant nonstructural and, possibly, structural damage would be expected in the lower and intermediate stories if a ground motion with characteristics similar to the Pacoima record should shake the building.

Long acceleration pulses such as those in the Pacoima ground motion cause large inelastic beam deformations which lead to a number of design problems. First, the large inelastic deformation requirements may lead to beam failures. This is particularly true in the lower stories where the beam shears are high. Secondly, large inelastic deformations result in large story drifts. The drift indices recorded during the Pacoima response exceeded or approached the limiting value of 0.015, indicating the possibility of significant nonstructural damage. Finally, the strain hardening associated with the inelastic beam deformation increases the beam moment capacities and contributes to column yielding. Column yielding is also caused by changes in the beam-column joint moment distribution which are attributed to the sequence of plastic hinge formation and higher mode effects associated with the response to the Pacoima ground motion.

In general, column yielding is undesirable because of the relatively poor inelastic deformational capabilities of columns and particularly because of the possibility of partial sway mechanisms developing. However, the extent of inelastic deformations in the upper story columns is small ($\theta_{P_{max}} < 0.003$ rad) with only one significant excursion and well within the deformational capabilities of

ductile reinforced concrete columns. A problem may arise in the first story columns where plastic rotations of approximately 0.01 rad are required. The detrimental effects of high axial loads and high shear forces on the column inelastic deformation capacity may prevent the development of a plastic rotation of this magnitude and cause structural failure. It is felt, however, that proper detailing of the column could prevent such a failure.

Design modifications should be made to eliminate the above shortcomings in the current design when subjected to ground motions like the Pacoima. The structure should be strengthened in order to decrease the required inelastic deformations; i.e., the design forces should be increased. This poses the problem of how to increase the forces within the context of the proposed design procedure. In reference 5 it is shown that the Pacoima ground motion is not accurately represented by the chosen ground motion spectrum, in particular with respect to the effective peak ground velocity. Redefining the ground motion spectrum with a ground velocity more representative of the characteristics of the Pacoima ground motion will permit a systematic increase in design forces. These new design forces should result in a stronger structure which does not have the shortcomings of the current design.

The acceptable behavior during the El Centro ground motion, whose characteristics are precisely the ones considered in the formulation of the response spectra used in the design, is an indication that the general procedure works and that the current preliminary design can be used to formulate a final design.

The significantly different responses to the El Centro and Pacoima ground motions clearly demonstrate that the problem that remains to be solved is the development of more reliable design earthquakes for ultimate state design. The significant increase in deformation (70%) which occurred with an increase in peak ground acceleration of 25% above that assumed in the evaluation of design forces demonstrates the importance of obtaining an accurate estimate

of the effective peak ground acceleration expected at a building site when design is based on ductility.

4. FINAL DESIGN PHASE

4.1 Introduction

The objective of the final design phase is to arrive at the 'optimal' solution to the seismic design problem. Seismic design forces are determined from characteristics of the structure found in the preliminary design phase. These forces are then used in conjunction with a more sophisticated subassemblage to formulate the optimization problem from which the final design is obtained. Once a design has been obtained, a series of static and dynamic analyses are carried out to check the overall reliability of the design and to provide guidelines for proper detailing to ensure the ductile behavior assumed in the evaluation of the design forces. The final design procedure is illustrated in the following sections by applying it to the example frame.

4.2 Final Design

4.2.1 Design Subassemblage

The subaseemblage selected for the final design is shown in Fig. 40. It has been used by El-Hafez and Powell in a nonlinear static analysis program [19]. They investigated the reliability of this subassemblage in analysis and concluded that good results can be obtained if the structure does not have radical changes in stiffness. Since a smooth variation in stiffness is one of the basic principles of seismic-resistant design, this subassemblage should be applicable to the proposed seismic design procedure.

As in the preliminary design, a weak girder - strong column design criterion is established, and the only design variables are the beam moments. If the design symmetry assumed in the preliminary design is also assumed in the final design, 16 design variables may be identified in a typical subassemblage of the example frame (Fig. 40).

The solution of the optimization problem based on this subassemblage yields one-half the moment capacity of a given section; i.e., it is assumed that one-half of the moment capacity of each beam section goes to the story subassemblage above the beam and the other half to the story subassemblage below it. When the two subassemblages are rejoined, the total moment capacity for that beam is recovered.

There are two advantages in using this subassemblage. First, it involves more design parameters than the subassemblage used in the preliminary design and, consequently, should provide a better distribution of moment capacities throughout a particular story and through the height of the structure. Secondly, the assumption that the points of inflection occur at midheight of the columns, which is inherent in the preliminary design subassemblage, has been eliminated. As a result, this subassemblage should be more realistic than the one used in the preliminary design.

4.2.2 Estimation of Lateral Story Shears

The dynamic characteristics of the structure found in the preliminary design are used in conjunction with the design spectra to evaluate the seismic story shears by the modal analysis procedure discussed in the preliminary design phase. In this particular example the dynamic characteristics of the preliminary design did not differ significantly from those assumed in the evaluation of the preliminary design story shears. Hence, the seismic design forces used in the preliminary design (Fig. 6) are used in the final design process.

4.2.3 Final Optimization

The formulation of the final design optimization problem is identical to the procedure used in the prelimnary design. Briefly, the optimization problem is: find the beam design moments (actually, one-half the beam design moments) which:

1. satisfy a set of design constraints established to ensure equilibrium and a serviceable and practical design, and

2. minimize a linear function of the design moments which is proportional to the volume of flexural reinforcement.

In addition to the serviceability and practical constraints imposed in the preliminary design, the practical constraint defined by the inequality:

$$|M^{support}_{below}| \geq |M^{support}_{above}| \tag{30}$$

is imposed in the final design to ensure a smooth transition in beam support design moments through the height of the structure. For the design example this constraint results in the following six inequalities (Fig. 41):

$$\bar{M}_{6_*} \geq \bar{M}_{1_*} \qquad \bar{M}_{8_*} \geq \bar{M}_{3_*} \qquad \bar{M}_{9_*} \geq \bar{M}_{4_*}$$

$$M^{+}_{6_*} \geq M^{+}_{1_*} \qquad M^{+}_{8_*} \geq M^{+}_{3_*} \qquad M^{+}_{9_*} \geq M^{+}_{4_*}$$

4.2.4 Final Member Design

Final member design follows the same procedure outlined in the preliminary design phase (Section 3.3.7). In the current example, only the amount of reinforcement at the critical region was determined in the final design because the member sizes established in the preliminary design phase were considered acceptable. The relationships used to design the members are the same as those used in the preliminary design with one exception. The distribution of the sum of the beam moments at a given joint to the column sections above and below the joint was based on the results of an elastic analysis. This represents an attempt to eliminate one of the factors thought to be responsible for the column yielding observed in the analyses of the preliminary design.

4.2.5 Results of Final Design

The beam design moments found from the solution of the

optimization problem are shown in Fig. 41. Comparison of these moments with the preliminary design moments (Fig. 13) indicates the following differences:

1. The subassemblage used in the final design results in a smoother variation in exterior span design moments in going from story seven to story four. This is attributed to the additional practical constraint imposed in the final design.

2. Notable differences between the two designs occur in the tenth, third, and second stories. Typically, the left exterior support moments were larger and the interior support moments smaller or the same at these stories in the final design. Differences at these stories would be expected, however, because the assumption inherent in the preliminary design subassemblage, that column inflection points are at mid-story height, is less likely to be true at these story levels.

The as-designed beam moment capacities are given in Fig. 42 and the variation in column reinforcement in Fig. 43. The final column design differed only slightly from that obtained in the preliminary phase (Fig. 16). The most notable differences are in the lower two stories where the exterior column reinforcement increased and the interior column reinforcement decreased due to changes in the beam design moments (Figs. 42 and 15).

To reduce the inelastic column deformation which was recorded during the response of the preliminary design to the Pacoima ground motion, the column reinforcement at the ground level was increased above that required at the first floor to satisfy the weak girder - strong column design criterion. In the preliminary design, the steel at ground level was taken as the same as that required at the first floor. The increase was limited by the established upper bound on the amount of column reinforcement, i.e., $\rho \leq 0.04$. Therefore, the only difference was in the exterior columns.

4.3 Reliability of Final Design

Only a limited series of analyses was carried out for the final structure of the example problem because of the similarities between the final and preliminary designs. In general the same series of nonlinear analyses which was carried out to investigate the acceptability of the preliminary design should be carried out to evaluate the reliability of the final design.

The analytical results indicated that the gross structural behavior of the final design (lateral displacement, story shears, and story displacements) was virtually identical to that of the preliminary design. In the time history analyses there were significant differences in some member inelastic deformation demands, however. In general, the peak demands obtained in the preliminary design were eliminated in the final design. In the discussion that follows only the significant differences in behavior between the two designs are presented.

4.3.1 Nonlinear Static Analysis

The nonlinear static behavior of the preliminary and final designs was the same with the exception of the plastic hinge formation sequence near collapse. In the preliminary design a partial sway mechanism occurred in story five before all the beam hinges had formed. In the final design, however, all beam hinges had formed prior to any column yielding, and the column plastic hinges were scattered through the height of the frame and did not lead to a partial sway mechanism.

4.3.2 Nonlinear Dynamic Analysis

The nonlinear dynamic response of the final structure subjected to the El Centro and Pacoima ground motions was evaluated for a peak acceleration of 0.5g. Strain hardening ratios of 5%, 1%, and 0.5% were considered in order to investigate the influence of this parameter on response. On the basis of the results of the analyses for a 5% strain hardening ratio, the following observations concerning

the difference in behavior between the final and preliminary designs may be made.

1. A comparison of the envelopes of beam cyclic curvature ductility is given in Fig. 44. The difference between the envelopes follows the same pattern for both ground motions. For example, in the exterior span the final design ductilities increased in the upper stories and decreased in the lower stories. In addition, the peaks observed at stories eight and six in the preliminary design have been eliminated in the final design, indicating an improved design. The observed difference in behavior between the two designs is attributed to the changes in beam design moments. For example, the negative interior design moment at story ten decreased from 745 k-ft in the preliminary design to 607 k-ft in the final design, while the curvature ductility increased from 5.2 to 8.2.

The changes in maximum beam plastic rotations follow a pattern similar to the changes in curvature ductility (Fig. 45).

2. As in the preliminary design, column yielding occurred only during the response to the Pacoima ground motion (Figs. 46 and 47). A comparison of the envelopes of column curvature ductilities for the two designs indicates that the effect of using the joint moment distribution found from an elastic analysis in the final column design is minimal, indicating that strain hardening, higher mode effects, and the sequence of beam plastic hinge formation are the significant factors influencing column yielding. In order to minimize the possibility of column yielding, 'dynamic magnification' factors suggested by Paulay [20] may be used to determine column design moments at a typical joint. These factors, which generally depend on the dynamic characteristics of the structure and the characteristics of the input ground motion, allow the inclusion in the design process of the effect of higher mode dynamic response on the column bending moment pattern.

The effect of the strain hardening ratio varied between the two ground motions, being more significant during the response to

the Pacoima ground motion. This is expected, however, since the inelastic deformations during the response to this ground motion were substantially larger than those which occurred during the El Centro ground motion. The results for strain hardening ratios of 1% and 0.5% were essentially the same and the following discussion will be based on comparisons of response for ratios of 5% and 0.5%.

Maximum story shears decreased as the strain hardening ratio decreased from 5% to 0.5% (Fig. 48). The decrease was greatest for the Pacoima ground motion in the intermediate and lower stories, and is attributed to the fact that the increase in beam moment capacity associated with strain hardening was less for the smaller strain hardening ratio. For example, beam moment capacities increased by more than 40% during the Pacoima response and by more than 15% during the El Centro response when a strain hardening ratio of 5% was assumed. The respective increases for a strain hardening ratio of 0.5% were only 4% and 2%.

The maximum story drift index increased in the intermediate stories and decreased in the upper stories during the Pacoima ground motion as the strain hardening ratio was decreased (Fig. 49). During the El Centro ground motion, R_{ult} increased at all story levels except the ground story where it decreased slightly (Fig. 49).

Similar changes are observed in the beam plastic hinge rotation envelopes (Fig. 50). These changes are attributed to the different post-yield dynamic characteristics associated with the different strain hardening ratios. This is discussed in more detail below.

The strain hardening ratio had a significant effect on the story displacement response after the first large acceleration pulse (Fig. 51). Although the second floor response for the two strain hardening ratios is virtually the same, the other floor displacements exhibit a severe residual negative displacement for a strain hardening ratio of 0.5%. For example, the maximum positive roof displacement decreased from 217 mm (8.5 in.) at a strain hardening

ratio of 5% to 25.4 mm (1.0 in.) at a ratio of 0.5%.

It should be noted that the decrease in R_{ult} and $\theta_{P_{max}}$ in the upper stories which occurred as the strain hardening ratio was decreased during the response to the Pacoima ground motion (Figs. 49 and 50) is related to the above difference in displacement response. For a strain hardening ratio of 5% the maximum values of R_{ult} and θ_p in the upper stories occurred after the first large acceleration pulse (t = 1.9 sec in Fig. 51). For a ratio of 0.5% they occurred prior to or during the first pulse.

This difference in response is attributed primarily to the different member post-yield stiffness associated with the different strain hardening ratios. The order of magnitude difference in post-yield stiffness associated with the strain hardening ratios considered here should result in a notable difference in structural stiffness properties when significant yielding has occurred. In some cases the post-yield stiffness associated with a strain hardening ratio of 0.5% when combined with the P-Δ effect may result in a negative resistance function.

Examination of the incremental equilibrium equation:

$$[M]\ d\ddot{\underline{r}} + [C_T]\ d\dot{\underline{r}} + [K_T]\ d\underline{r} = d\underline{p} \qquad (31)$$

where

$[M]$ = mass matrix

$[C_T]$ = damping matrix

$[K_T]$ = tangential stiffness matrix

$d\underline{p}$ = load vector

$d\ddot{\underline{r}}$ = acceleration vector

$d\dot{\underline{r}}$ = velocity vector

dr = displacement vector

indicates that since $d\underline{p}$ and $[M]$ are the same, changes in $[K_T]$, which

will cause changes in the stiffness proportional part of $[C_T]$, will change the response vectors $d\underline{r}$, $d\dot{\underline{r}}$, and $d\ddot{\underline{r}}$. The extent of the changes in the response vectors depend on the characteristics of $d\underline{p}$ and the extent of the changes in $[K_T]$ caused by the different strain hardening ratios.

The effect of varying the strain hardening ratio on column yielding is illustrated in Figs. 52 and 53. In the upper stories and at the bottom of the third story column, yielding has been eliminated during the response for a strain hardening ratio of 0.5%, indicating that the increase in moment capacity associated with strain hardening was a major factor influencing column yielding at these locations. Column yielding does occur at some stories for both strain hardening ratios and in some cases the required column ductility increases for the smaller strain hardening ratio, demonstrating that the effects of higher mode response and the sequence of plastic hinge formation may also result in inelastic column behavior.

4.4 Summary

The results of the final design indicate that a smoother transition in strength may be obtained using a more sophisticated design subassemblage. The use of a more elaborate design subassemblage, for example using a two-story subassemblage, does not seem warranted. From a comparison of the preliminary and final design, it is felt that any improvement in design which might be achieved would not be justified in view of the significant increase in computational effect required to obtain the design. The dynamic response of the final design during the Pacoima ground motion again demonstrates the problems which can be caused in design by this ground motion, particularly when there is uncertainty regarding the actual value of the effective peak ground acceleration.

5. CONCLUSIONS AND RECOMMENDATIONS

The proposed design procedure permits the inclusion of the important factors affecting and/or controlling selection of design criteria which are in accord with the accepted general philosophy of seismic-resistant design. Consequently, it provides an efficient and rational basis for the seismic design of multistory moment-resisting frame structures. The procedure's versatility permits present design constraints to be changed and/or new constraints to be added in order to obtain several preliminary designs in a relatively short time which can be used as guidelines for the final design. The subassemblage suggested for the final design provides smoother transitions in strength than can be obtained in the preliminary design. Consequently, it results in an improvement of the preliminary design.

In the development of this seismic design procedure, a number of problems were identified which warrant further study.

1. The significant differences between the responses to the Derived Pacoima Dam and El Centro ground motions demonstrates the need to establish better design earthquakes for inelastic design, particularly for building sites where ground motions with the dynamic characteristics of the Pacoima Dam motion can occur. For these sites, design earthquakes should take into account the severe long-duration acceleration pulses contained in the Pacoima ground motion.

2. The considerable increase in deformation (up to 70%) which was observed during the response to the Pacoima ground motion when the peak ground acceleration was increased by 25% above that assumed in the evaluation of the seismic design forces, points out the need for more accurate evaluation of the peak ground acceleration expected at a building site when design is based on ductility.

3. The relatively recent concern about a damageability limit state creates problems with regard to its inclusion in the design process. The precise definition of this limit state (the story

drift index was used here) and how to incorporate it rationally in design must still be decided upon.

4. The selection of the displacement ductility factor for a multiple degree-of-freedom system should be examined more closely. In particular, the consequences of varying the ductility factor through the height of the structure should be studied.

5. The use of additional and/or different constraints in the optimization procedure in order to obtain more practical designs should be studied. For example, constraining of the beam moments at both sides (faces) of the column at an interior beam-column joint to be equal should result in a more efficient distribution of beam moment capacities with respect to practicality, economics, and structural performance, because all bars would be continued through the joint, and bar anchorage would not be required.

6. There is a need to improve the expression for the merit function which will require the formulation of more practical rules defining the cutoff point of flexural reinforcement than those which are derived by satisfying present code requirements. The sensitivity of the design solution to the merit function used should be determined. For example, various techniques should be employed to construct the merit function so that the resulting designs can be compared.

7. The significance of the considerable overstrength that is obtained using recommended code equations and values for the different factors (ϕ, α_F) should be investigated. An additional contribution to this overstrength arises from the convention of using unfactored beam capacities in the column design. More rational values than those presently used for the column overstrength factor, F, should also be studied.

8. Participation of the floor system in the strength of the beam critical sections (regions) should be investigated.

9. A better model than the two-component model is needed to

predict member inelastic deformations. In addition, a model to account for beam-column joint deformations, concrete as well as steel slippage, should be developed. Also, the amount of strain hardening which may be expected in real members should be determined and the design parameters controlling this magnitude should be identified and their influence quantified.

10. The current dynamic analysis program should be extended to three dimensions in order to investigate the effect of torsion of the whole structural system (building) on the reliability of the design.

11. A comparison should be made between the proposed seismic design procedure and those used in current practice, as well as those suggested recently in the literature, with respect to the volume and cost of materials required and to the structural response to critical design excitations.

REFERENCES

[1] Bertero, V. V. and Bresler, B., "Failure Criteria (Limit States)," Panel Position Paper on Design and Engineering Decisions, preprint from the Sixth World Conference on Earthquake Engineering (6WCEE), New Delhi, India, January 1977. Also published in Report No. UCB/EERC-77/06, EERC, University of California, Berkeley, February 1977.

[2] Sawyer, H. A., Jr., "Comprehensive Design of Reinforced Concrete Frames by Plasticity Factors," 9th Planning Session of the CED Symposium: Hyperstatique, Ankara, Turkey, September 1964.

[3] Cohn, M. Z., "Optimal Limit Design of R/C Structures," Inelasticity and Non-Linearity in Structural Concrete, University of Waterloo Press, 1972.

[4] Bertero, V. V. and Kamil, H., "Nonlinear Seismic Design of Multistory Frames," Canadian Journal of Civil Engineering, Vol. 2, No. 4, December 1975.

[5] Bertero, V. V., "Establishment of Design Earthquakes - Evaluation of Present Methods," Proceedings, International Symposium on Earthquake Structural Engineering, St. Louis, August 19-21, 1976.

[6] Applied Technology Council, "An Evaluation of a Response Spectrum Approach to Seismic Design of Buildings," A Study Report for the Center for Building Technology, Institute of Applied Technology, National Bureau of Standards, Washington, D. C., September 1974.

[7] Uniform Building Code Standards, 1973 Edition, International Conference of Building Officials, Whittier, 1973.

[8] Newmark, N. M., "Seismic Design Criteria for Structures and Facilities Trans-Alaska Pipeline System," U. S. Conference on Earthquake Engineering, Ann Arbor, 1976.

[9] Skinner, A. J., Handbook for Earthquake-Generated Forces and Moments in Tall Buildings, Dominion Physics Laboratory, New Zealand, 1960.

[10] Anand, Y. N., Rhomberg, E. T., and Miranda, C. F., "Computer-Aided Design: Design of Concrete Structures," Methods of Structural Analysis, Proceedings of the National Structural Engineering Conference, ASCE Specialty Conference, University of Wisconsin, Madison, Wisconsin, August 22-25, 1976.

[11] Walker, N. D. and Pister, K. S., "Study of a Method of Feasible Directions for Optimal Elastic Design of Framed Structures Subjected to Earthquake Loading," Report No. EERC 75-39, EERC, University of California, Berkeley, December 1975.

[12] Park, R., "Accomplishments and Research and Development Needs in New Zealand," preprint of a paper presented at the Workshop on Earthquake-Resistant Reinforced Concrete Building Construction (ERCBC), University of California, Berkeley, July 11-15, 1977.

[13] American Concrete Institute, Design Handbook, SP-17 (73), ACI, Detroit, 1973.

[14] Malik, L. E. and Bertero, V. V., "Contribution of a Floor System to the Dynamic Characteristics of Reinforced Concrete Buildings," Report No. EERC 76-30, EERC, University of California, Berkeley, December 1976.

[15] Sudhakar, A., "Computer Program for Small Displacement Elasto-Plastic Analysis of Plane Steel and R/C Frames," Graduate Student Report No. 561, University of California, Berkeley, 1972.

[16] Mahin, S. A. and Bertero, V. V., "An Evaluation of Some Methods for Predicting Seismic Behavior of Reinforced Concrete Buildings," Report No. EERC 75-5, EERC, University of California, Berkeley, February 1975.

[17] Ma, S. M., Bertero, V. V., and Popov, E. P., "Experimental and Analytical Studies on the Hysteretic Behavior of Reinforced Concrete Rectangular and T-Beams," Report No. EERC 76-2, EERC, University of California, Berkeley, May 1976.

[18] Bertero, V. V., Popov, E. P., and Wang, T.Y., "Hysteretic Behavior of Reinforced Concrete Members with Special Web Reinforcement," Report No. EERC 74-9, EERC, University of California, Berkeley, 1974.

[19] El-Hafez, M. D. and Powell, G. H., "Computer-Aided Ultimate Load Design of Unbraced Multistory Steel Frames," Report No. 73-3, EERC, University of California, Berkeley, April 1973.

[20] Paulay, T., "Capacity Design of Reinforced Concrete Ductile Frames," preprint of paper presented at the ERCBC Workshop, University of California, Berkeley, July 11-15, 1977.

TABLE 1. FLOOR DISPLACEMENT DUCTILITIES
(1 in. = 25.4 mm)

FLOOR	LATERAL DISPL. AT FIRST SIGNIFICANT YIELDING Δ_y (in.)	LATERAL DISPLACEMENT DUCTILITIES, μ, UNDER			
		DERIVED PACOIMA		EL CENTRO	
		0.5g	0.4g	0.5g	0.4g
ROOF	3.79	5.04	3.63	1.64	1.47
10	3.41	5.49	3.92	1.76	1.58
9	3.00	6.24	4.27	1.90	1.67
8	2.58	6.57	4.65	2.00	1.71
7	2.18	7.02	4.95	2.04	1.69
6	1.80	7.30	5.10	2.00	1.62
5	1.43	7.44	5.10	1.90	1.52
4	1.07	7.33	4.86	1.76	1.41
3	.70	7.10	4.50	1.61	1.31
2	.33	7.20	4.24	1.53	1.34

TABLE 2. RATIOS OF MAXIMUM VALUES FOR DIFFERENT RESPONSE PARAMETERS FOR 0.5g AND 0.4g PEAK GROUND ACCELERATIONS.

FLOOR	EL CENTRO				PACOIMA			
	FLOOR DISPL.	DRIFT INDEX	STORY SHEAR	$\theta_{p_{max}}$ BEAM	FLOOR DISPL.	DRIFT INDEX	STORY SHEAR	$\theta_{p_{max}}$ BEAM
ROOF	1.12	1.47	1.12	1.51	1.39	1.34	1.09	1.41
10	1.12	1.22	1.04	1.31	1.40	1.42	1.04	1.37
9	1.14	1.36	1.07	1.47	1.40	1.34	1.08	1.45
8	1.17	1.40	1.10	1.58	1.41	1.38	1.10	1.33
7	1.20	1.14	1.06	1.30	1.42	1.38	1.11	1.52
6	1.22	1.20	1.05	1.30	1.43	1.35	1.10	1.42
5	1.24	1.25	1.06	1.32	1.46	1.35	1.09	1.38
4	1.25	1.26	1.09	1.91	1.54	1.39	1.10	1.40
3	1.23	1.27	1.10	2.38	1.58	1.49	1.11	1.50
2	1.13	1.14	1.04	4.75	1.70	1.70	1.07	1.80

Note: Maxima do not always occur in same directions for the two peak ground accelerations.

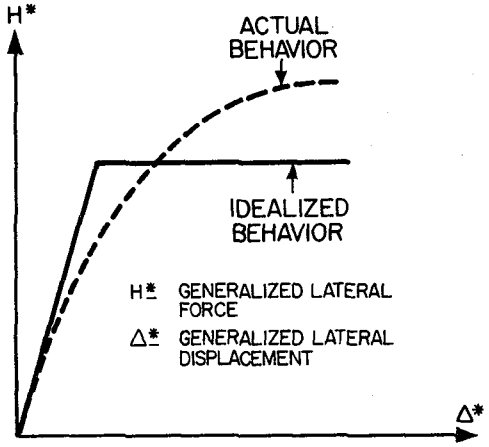

FIG. 1 LATERAL FORCE-DISPLACEMENT BEHAVIOR

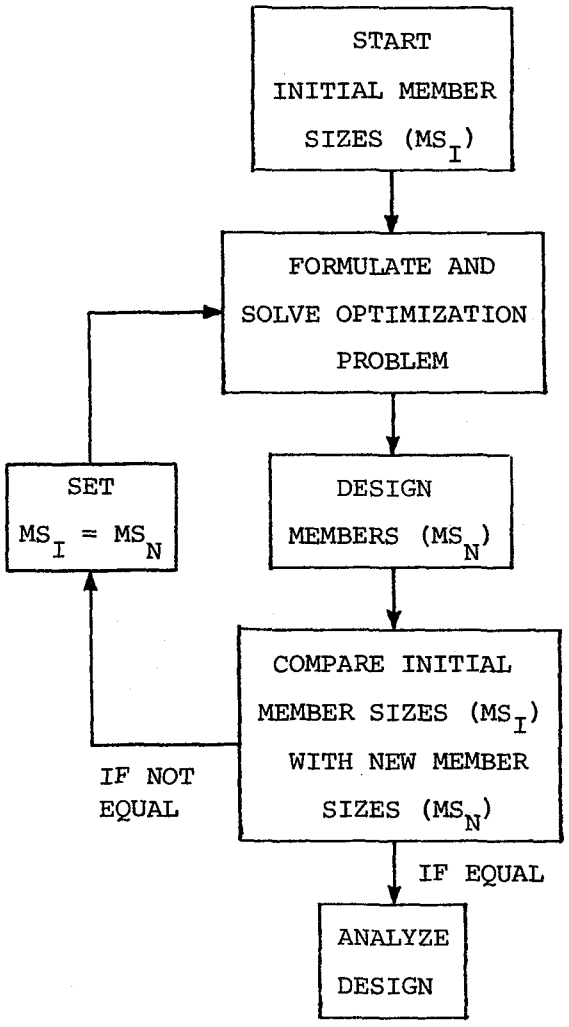

FIG. 2 ITERATIVE LOOP IN PRELIMINARY DESIGN STEP

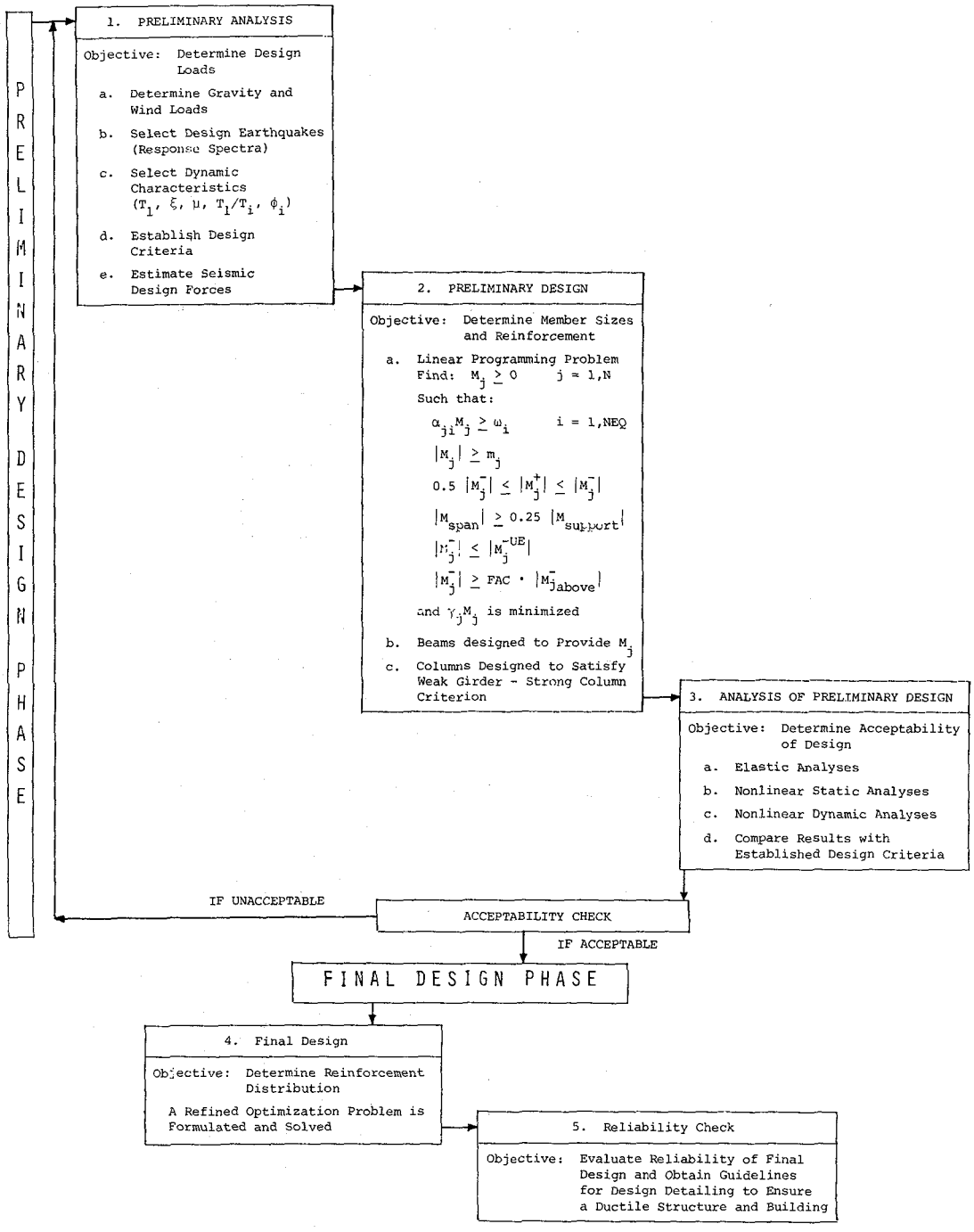

FIG. 3 SUMMARY OF DESIGN PROCEDURE

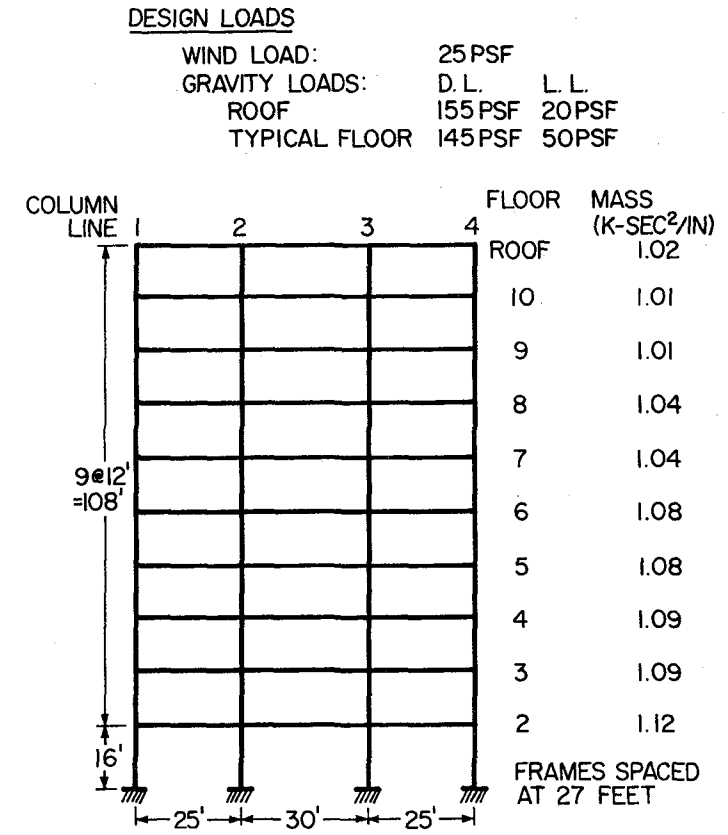

(a) Frame Elevation and Design Data

1 in. = 25.4 mm
1 ft = 0.3048 m
1 kip = 4.448 kN
1 psf = 0.0479 kN/m^2

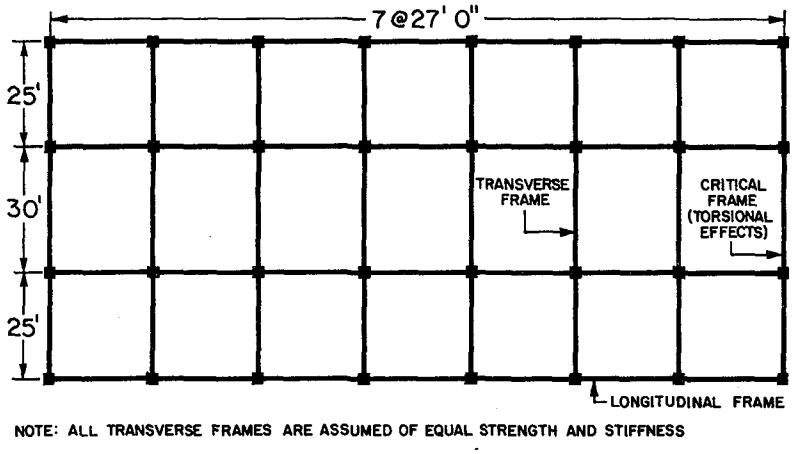

(b) Typical Floor Plan

FIG. 4 TEN-STORY THREE-BAY FRAME

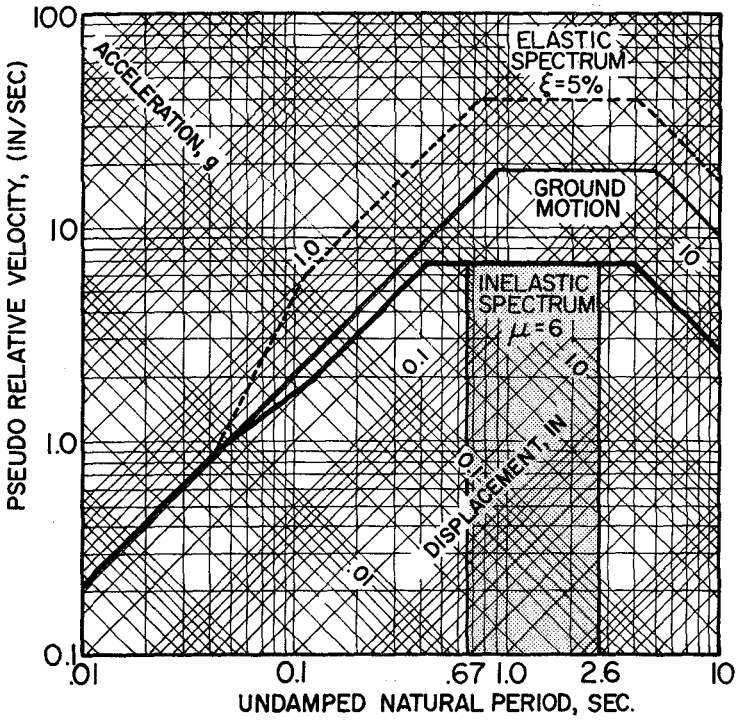

FIG. 5 DESIGN SPECTRA

1 in. = 25.4 mm
1 kip = 4.448 kN

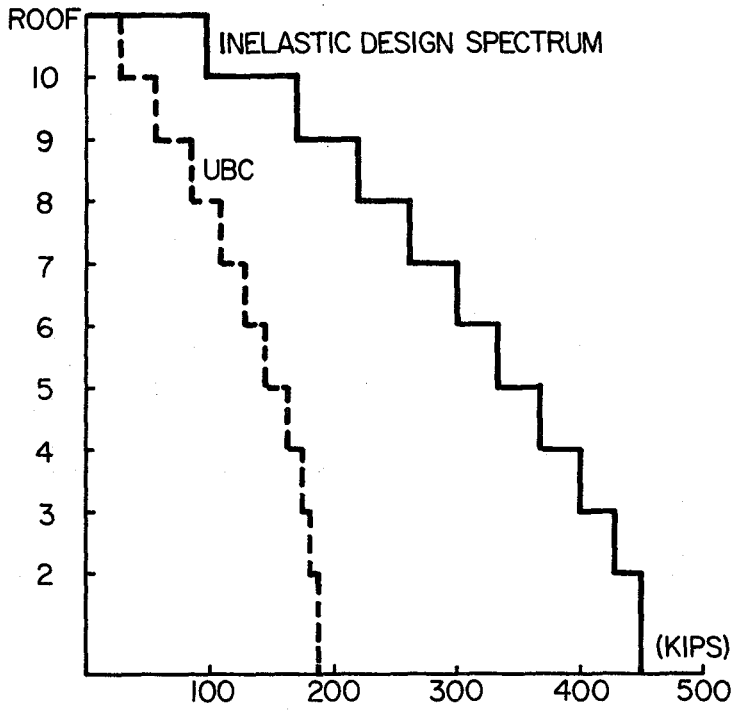

FIG. 6 DESIGN FORCES

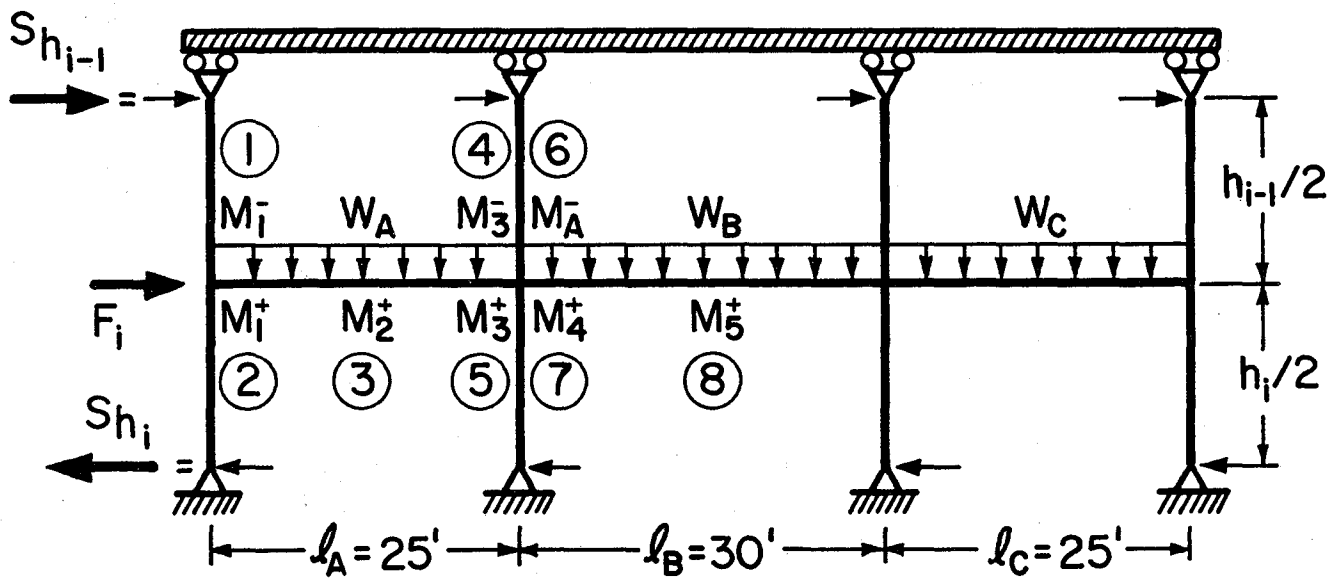

FIG. 7 SUBASSEMBLAGE FOR PRELIMINARY DESIGN 1 ft = 0.3048 m

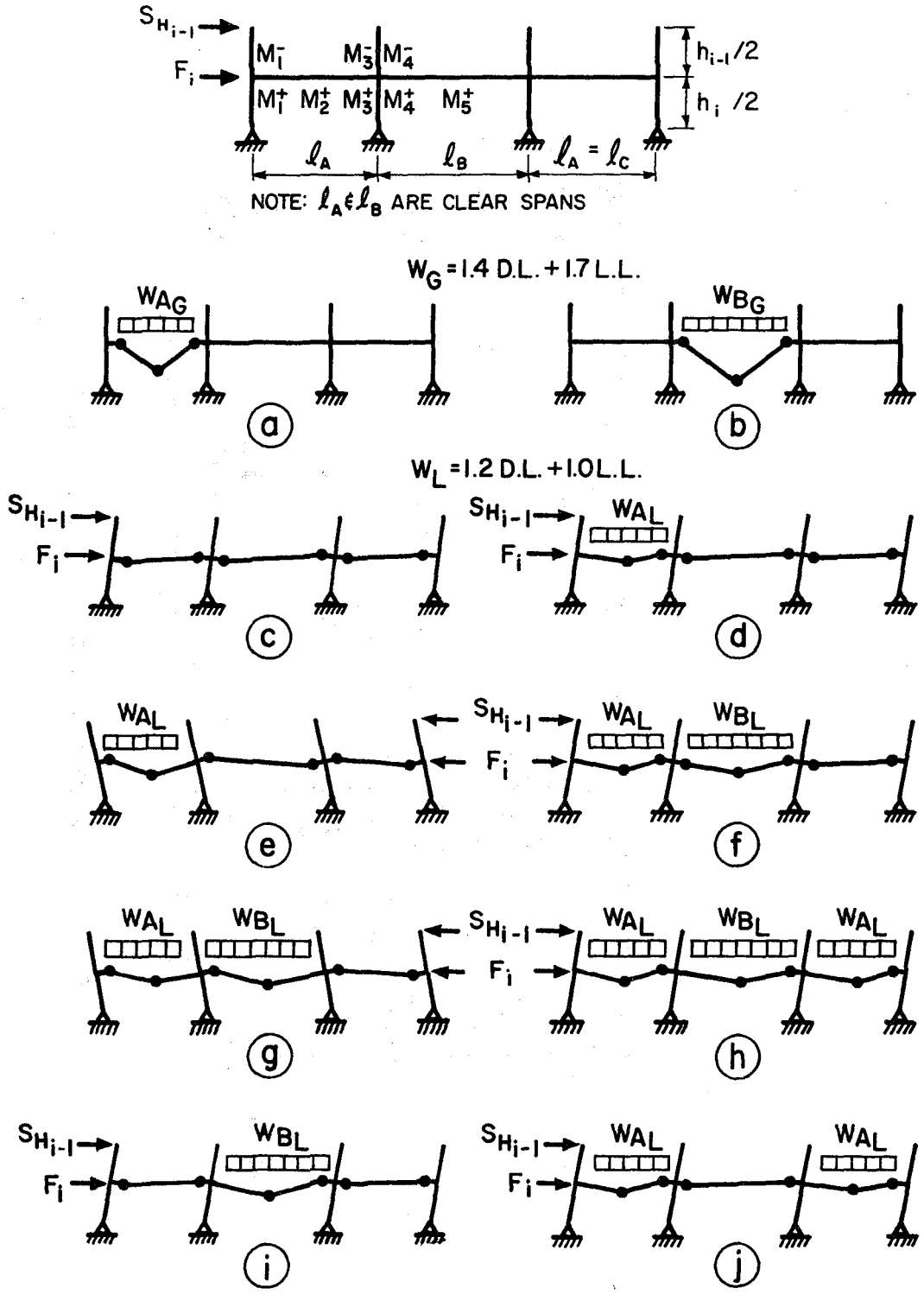

FIG. 8 MECHANISMS CONSIDERED IN FORMULATION OF EQUILIBRIUM CONSTRAINTS

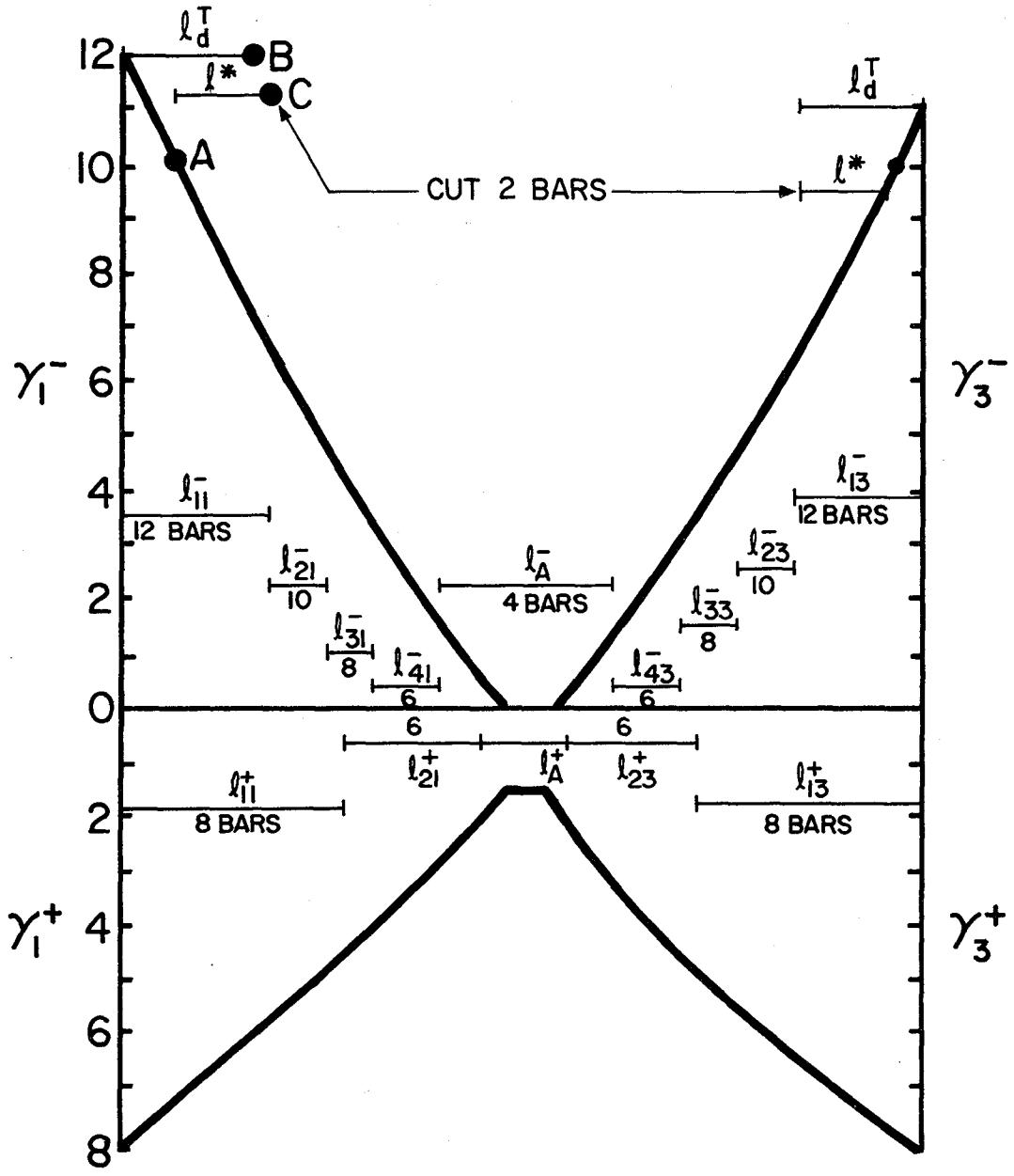

FIG. 9 TYPICAL ELASTIC MOMENT ENVELOPE AND BAR CURTAILMENT

1 in. = 25.4 mm
1 ft = 0.3048 m
1 kip = 4.448 kN

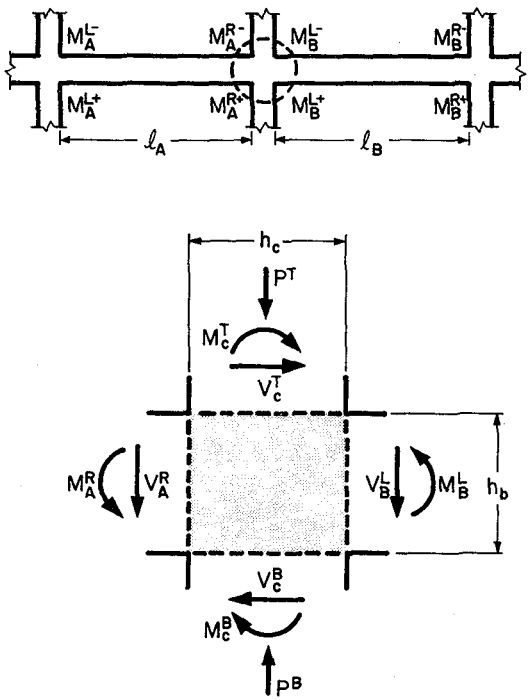

FIG. 10 FORCES AT A TYPICAL BEAM-COLUMN JOINT

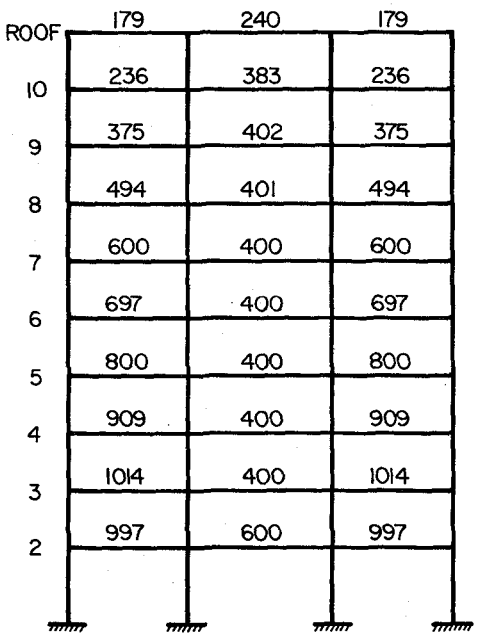

FIG. 11 'OPTIMUM' BEAM DESIGN MOMENTS FOR STARTING PRELIMINARY DESIGN (MOMENTS IN K-FT)

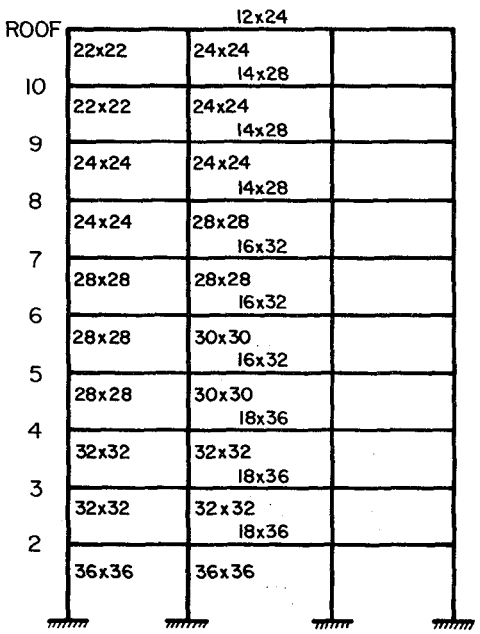

FIG. 12 STARTING PRELIMINARY DESIGN: MEMBER SIZES (IN IN.)

1 in. = 25.4 mm 1 ft = 0.3048 m 1 kip = 4.448 kN

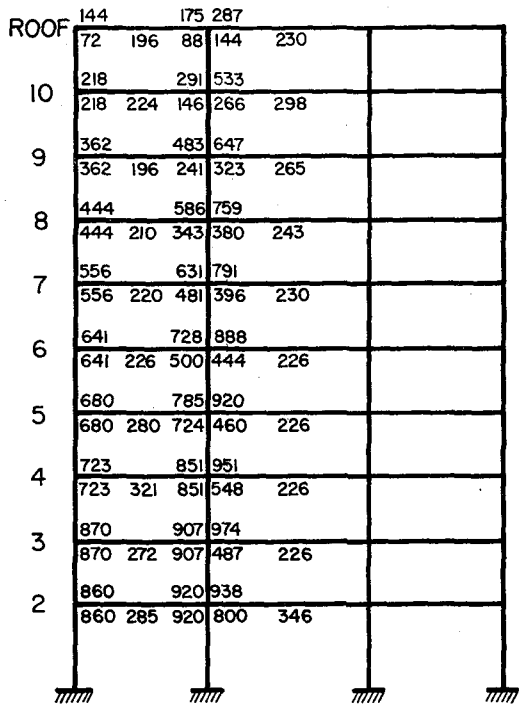

FIG. 13 'OPTIMUM' BEAM DESIGN MOMENTS FOR FINAL PRELIMINARY DESIGN (IN K-FT)

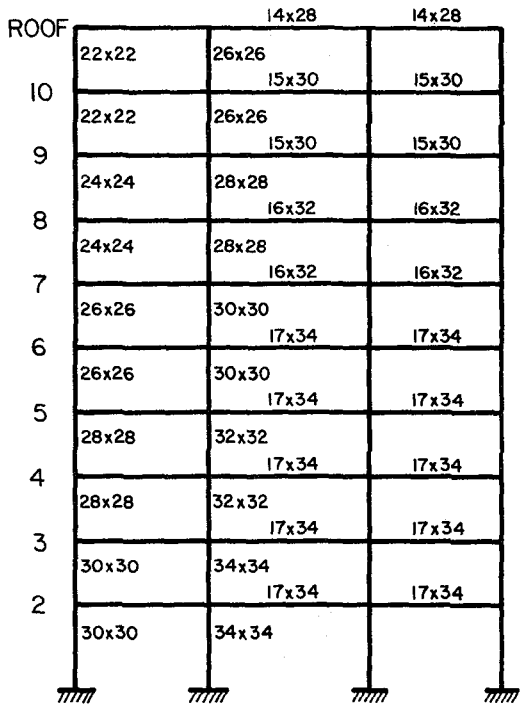

FIG. 14 MEMBER SIZES FOR FINAL PRELIMINARY DESIGN (IN IN.)

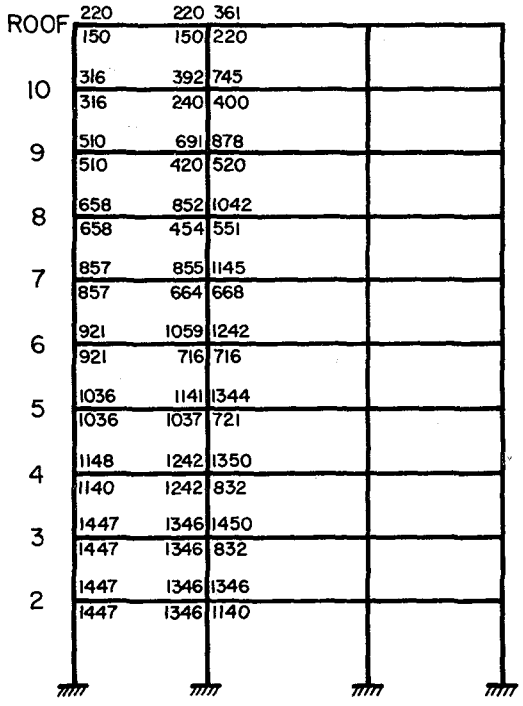

FIG. 15 AS-DESIGNED BEAM MOMENT CAPACITIES FOR FINAL PRELIMINARY DESIGN (IN K-FT)

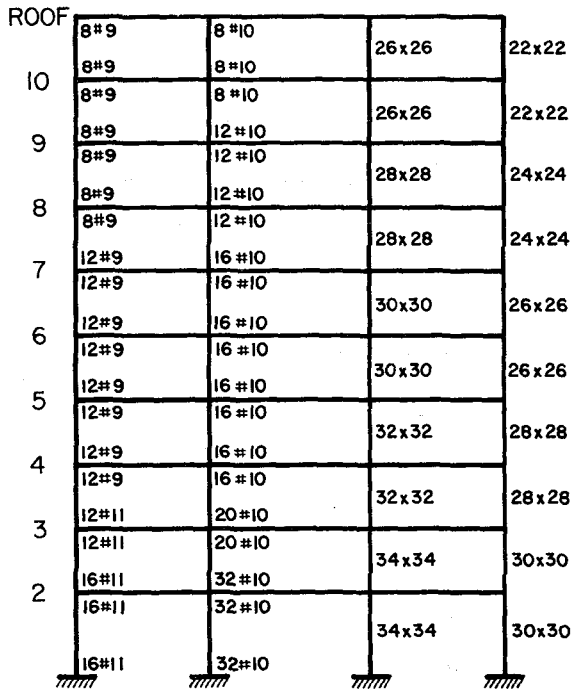

FIG. 16 COLUMN SIZES AND REINFORCEMENT SCHEDULE FOR FINAL PRELIMINARY DESIGN

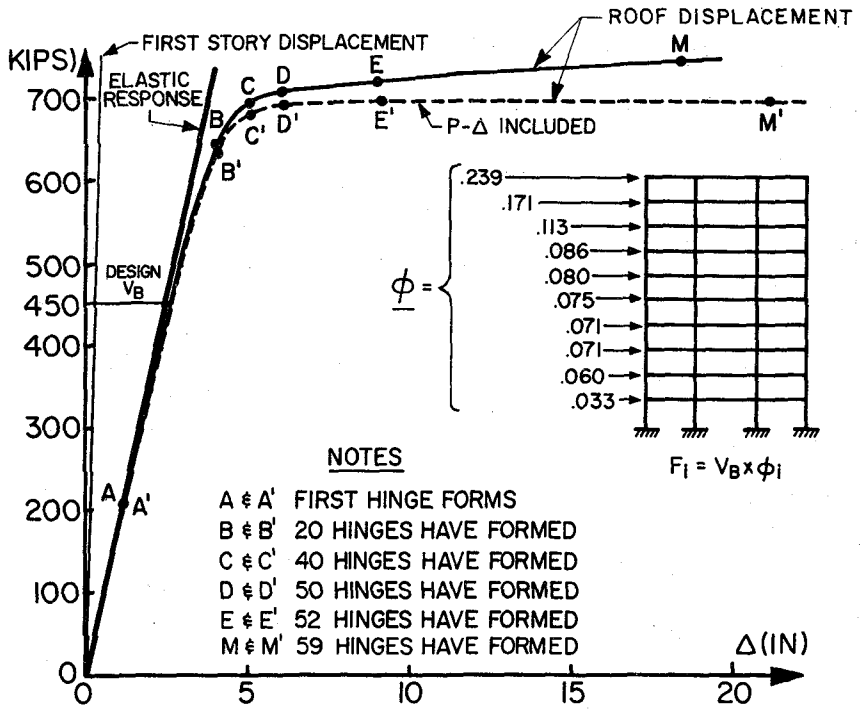

FIG. 17 LATERAL LOAD-DISPLACEMENT RELATIONSHIP FOR PRELIMINARY DESIGNED FRAME

1 in. = 25.4 mm
1 kip = 4.448 kN

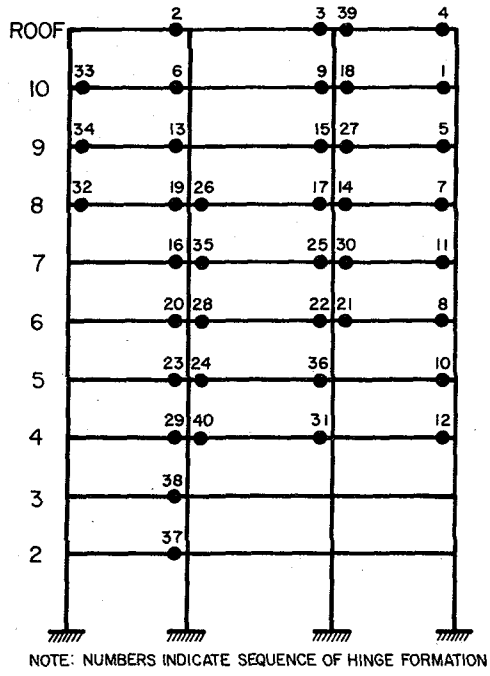

FIG. 18 PLASTIC HINGE PATTERN AT STAGES C AND C' IN FIG. 17

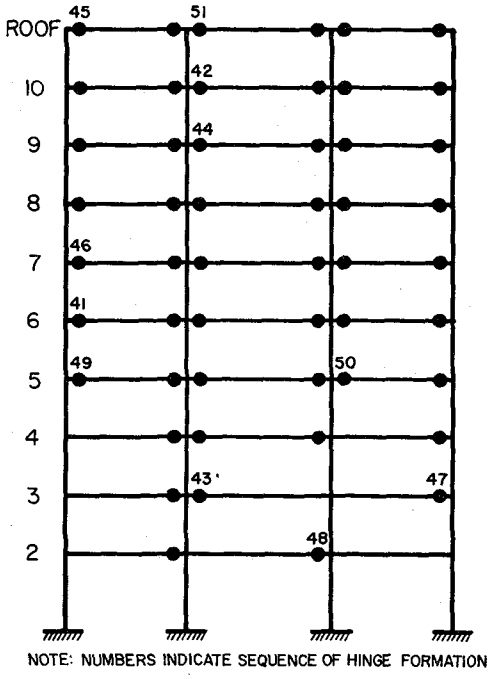

FIG. 19 PLASTIC HINGE PATTERN AT STAGES E AND E' IN FIG. 17

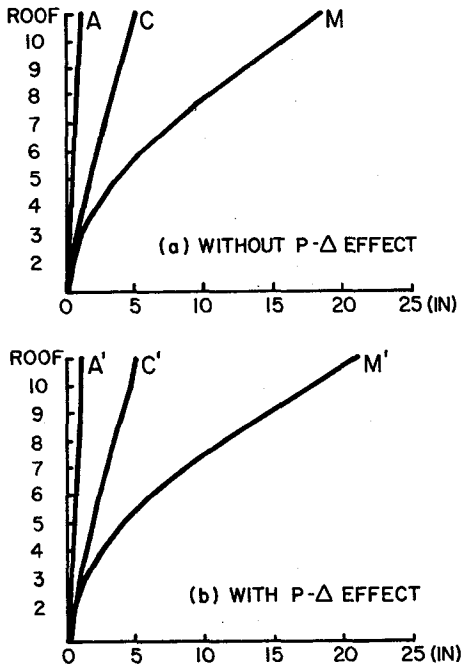

FIG. 20 DISPLACEMENT PATTERNS DURING APPLICATION OF STATIC LATERAL LOADS

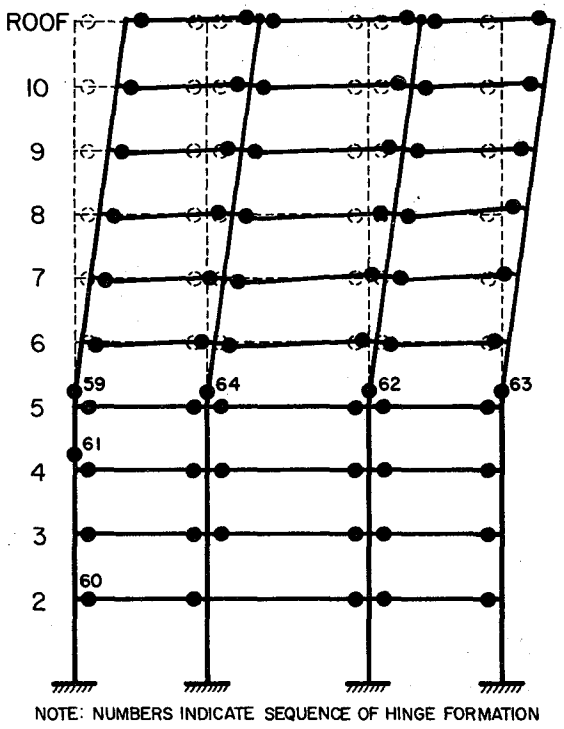

FIG. 21 PARTIAL SWAY MECHANISM

1 in. = 25.4 mm

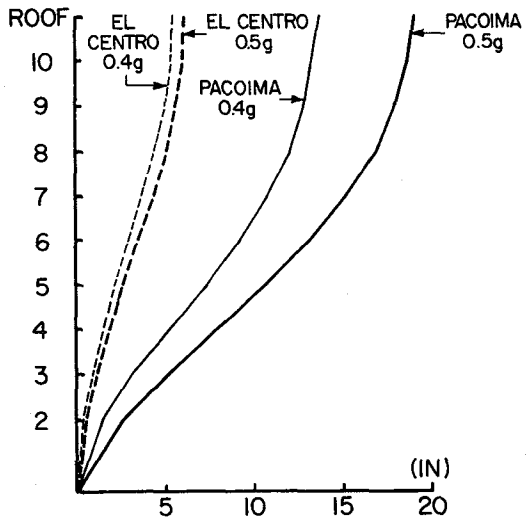

FIG. 22 ENVELOPES OF FLOOR DISPLACEMENTS

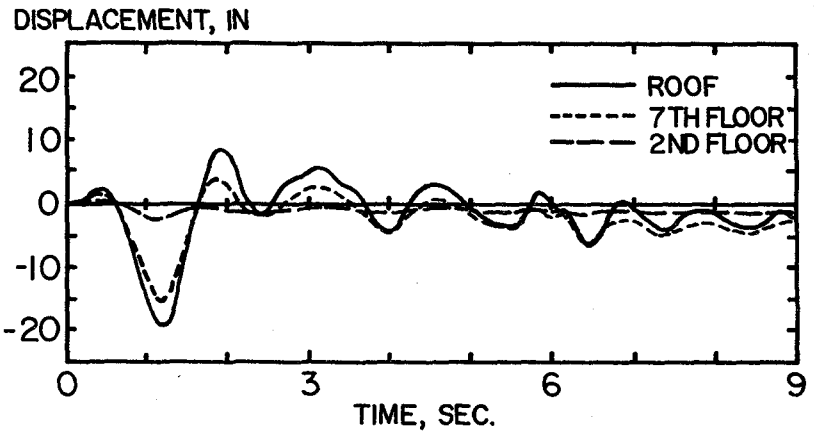

(a) DISPLACEMENT TIME HISTORIES

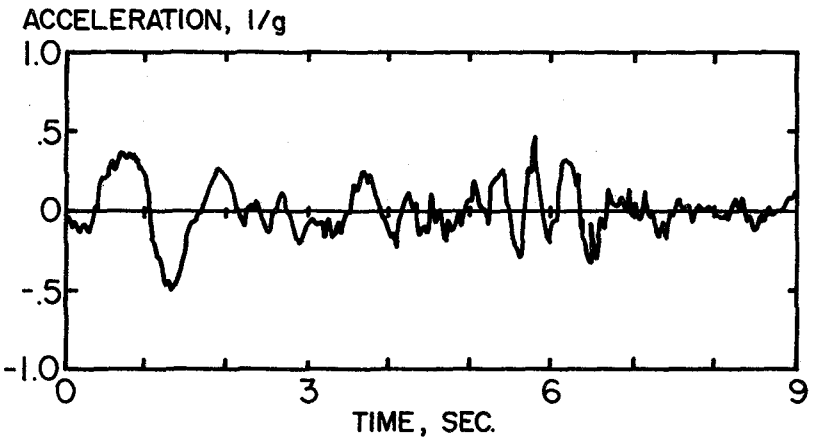

(b) DERIVED PACOIMA DAM ACCELEROGRAM (0.5g)

FIG. 23 STORY DISPLACEMENT TIME HISTORIES FOR DERIVED PACOIMA DAM MOTION

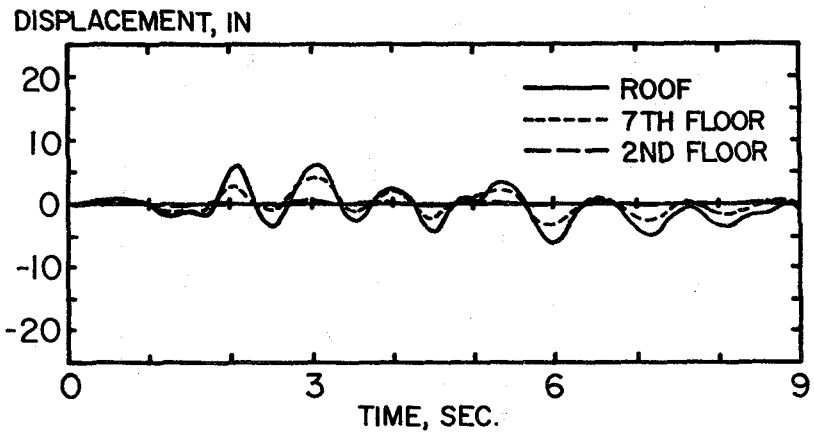

(a) DISPLACEMENT TIME HISTORIES

1 in. = 25.4 mm

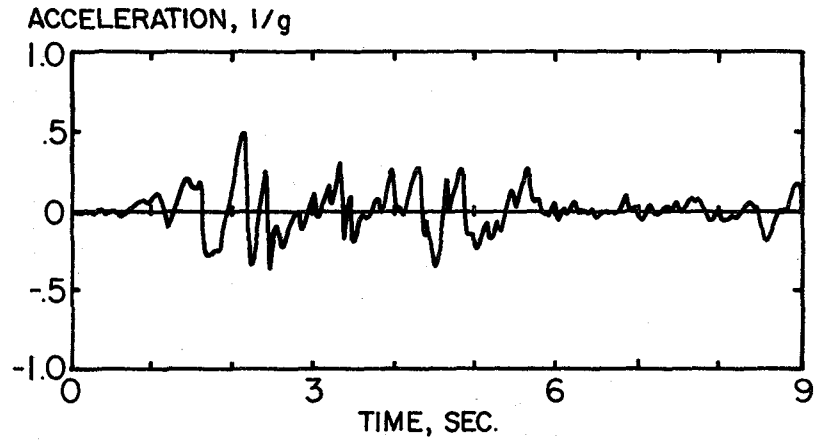

(b) EL CENTRO N-S ACCELEROGRAM (0.5g)

FIG. 24 STORY DISPLACEMENT TIME HISTORIES FOR EL CENTRO N-S MOTION

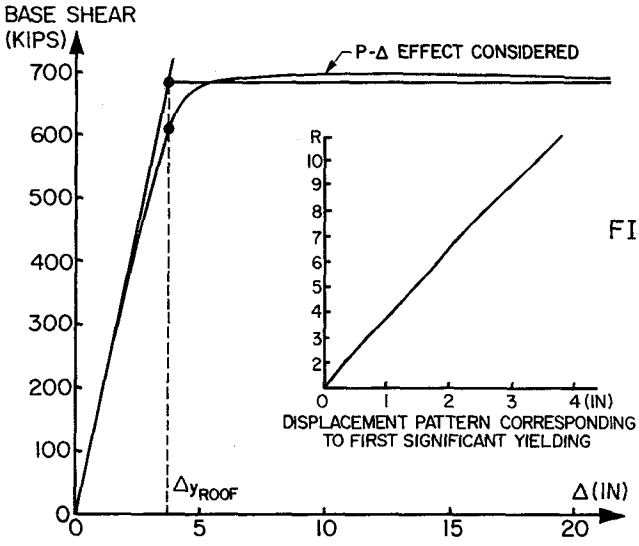

FIG. 25 DEFINITION OF FLOOR YIELD DISPLACEMENT UNDER STATIC LATERAL LOADING

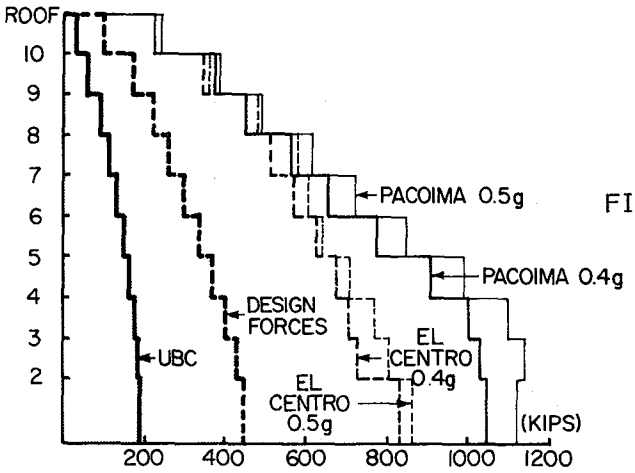

FIG. 26 COMPARISON OF STORY SHEAR ENVELOPES

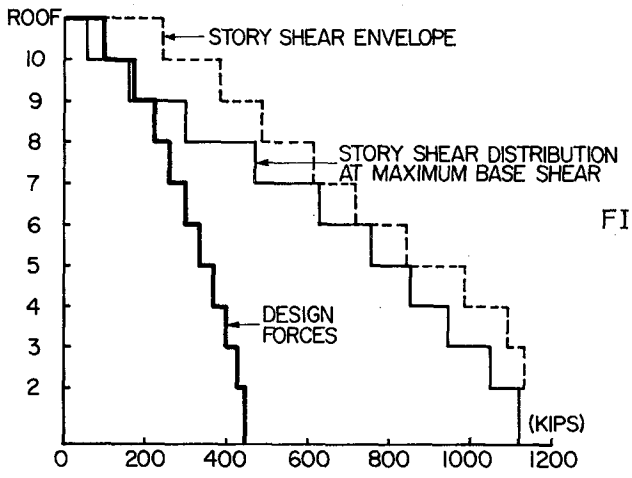

FIG. 27 COMPARISON OF STORY SHEAR ENVELOPE AND STORY SHEAR DISTRIBUTION AT MAXIMUM BASE SHEAR FOR PACOIMA GROUND MOTION AT 0.5g

1 in. = 25.4 mm
1 kip = 4.448 kN

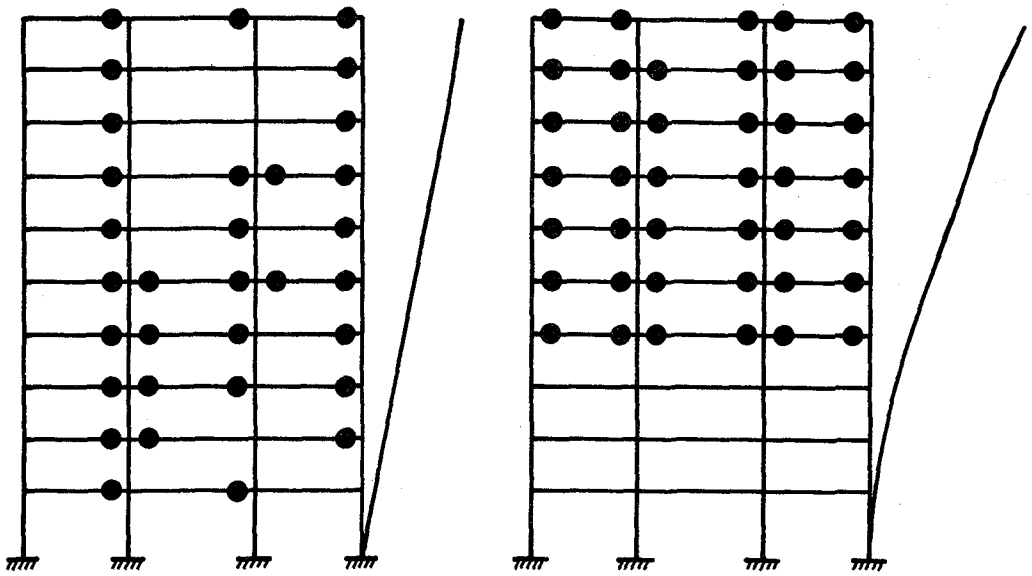

FIG. 28 PLASTIC HINGE PATTERNS DURING RESPONSE TO EL CENTRO GROUND MOTION AT 0.5g

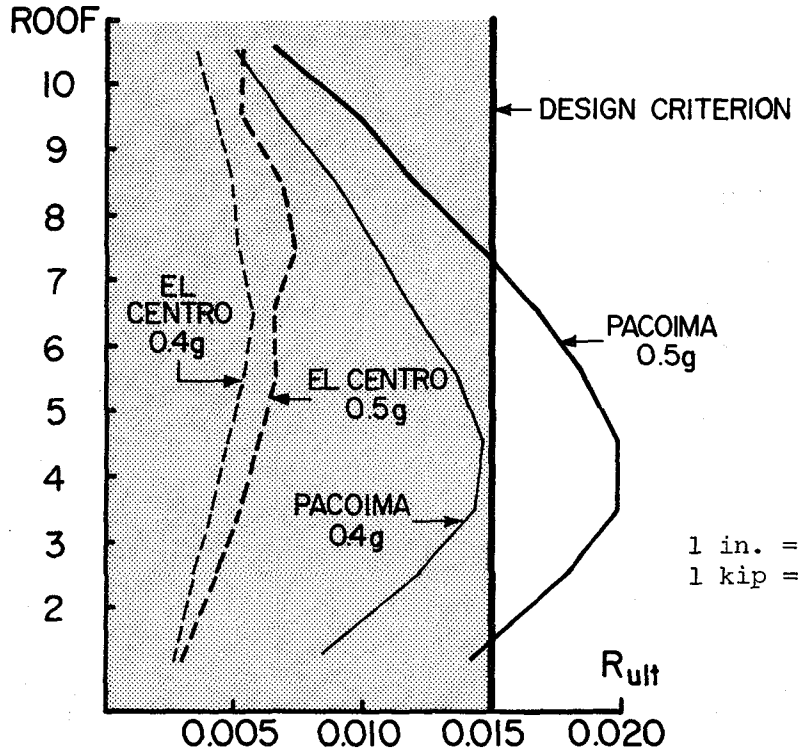

FIG. 29 ENVELOPES OF STORY DRIFT INDEX, R_{ULT}

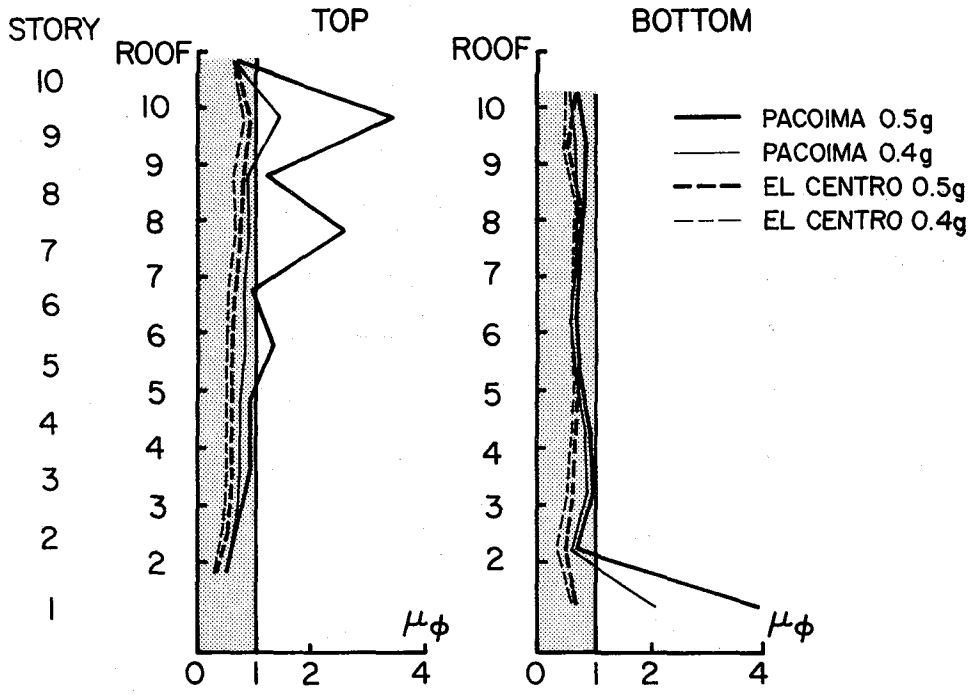

FIG. 30 ENVELOPES OF COLUMN CURVATURE DUCTILITY, μ_ϕ, FOR INTERIOR COLUMNS

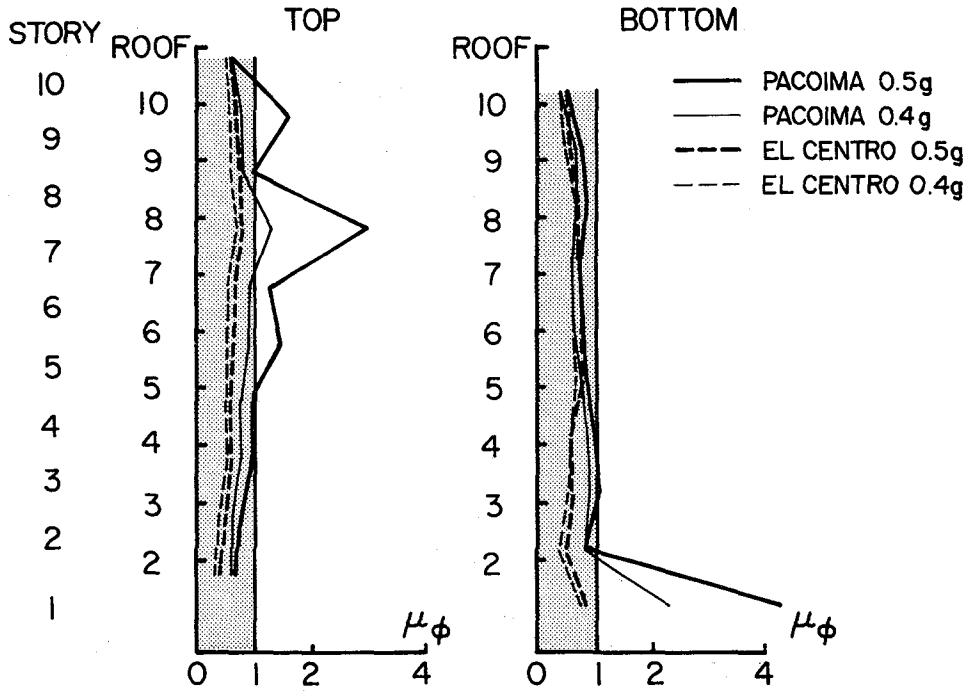

FIG. 31 ENVELOPES OF COLUMN CURVATURE DUCTILITY, μ_ϕ, FOR EXTERIOR COLUMNS

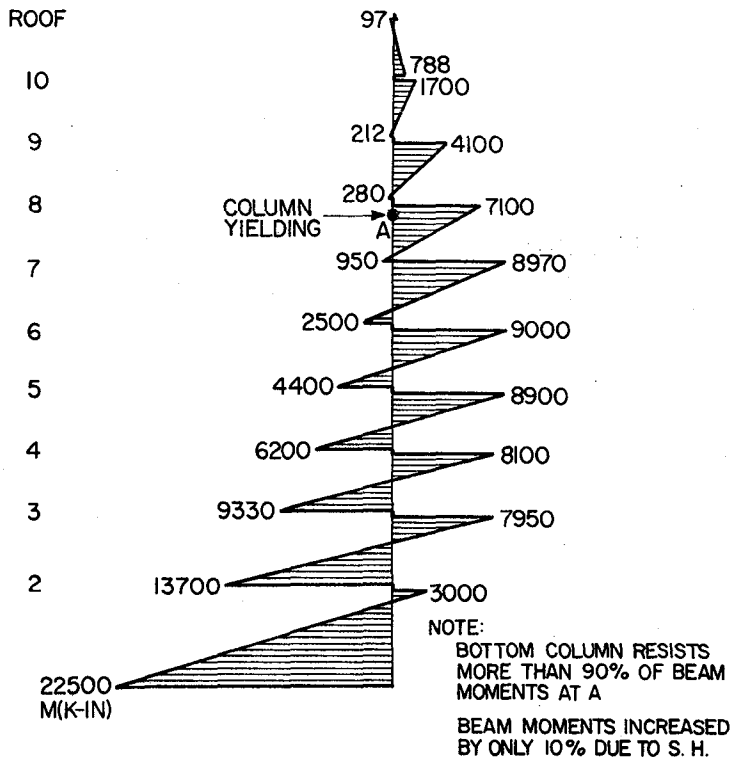

FIG. 32 EXTERIOR COLUMN MOMENTS (K-IN.) - DISTRIBUTION TIME = 1 SEC

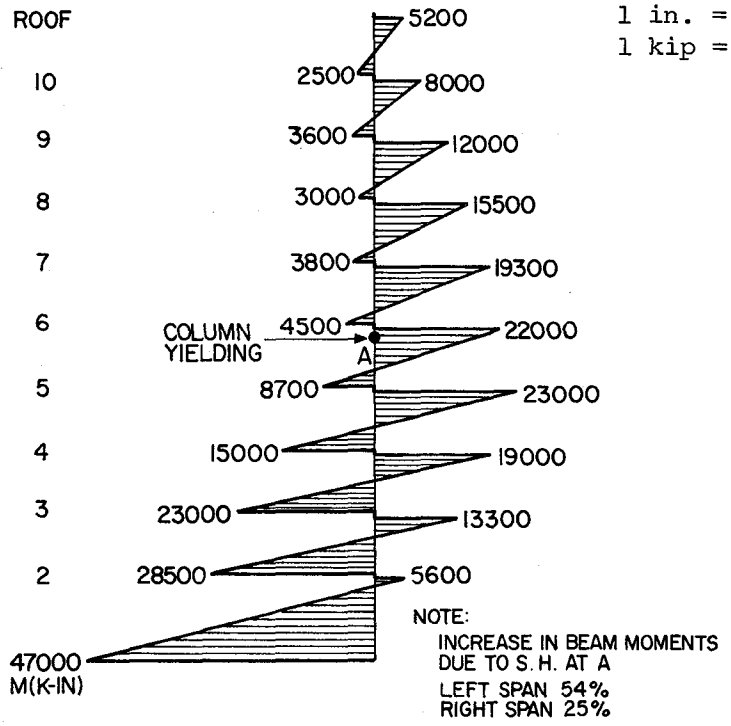

1 in. = 25.4 mm
1 kip = 4.448 kN

FIG. 33 INTERIOR COLUMN MOMENTS (K-IN.) - DISTRIBUTION TIME = 1.14 SEC

1 in. = 25.4 mm
1 kip = 4.448 kN

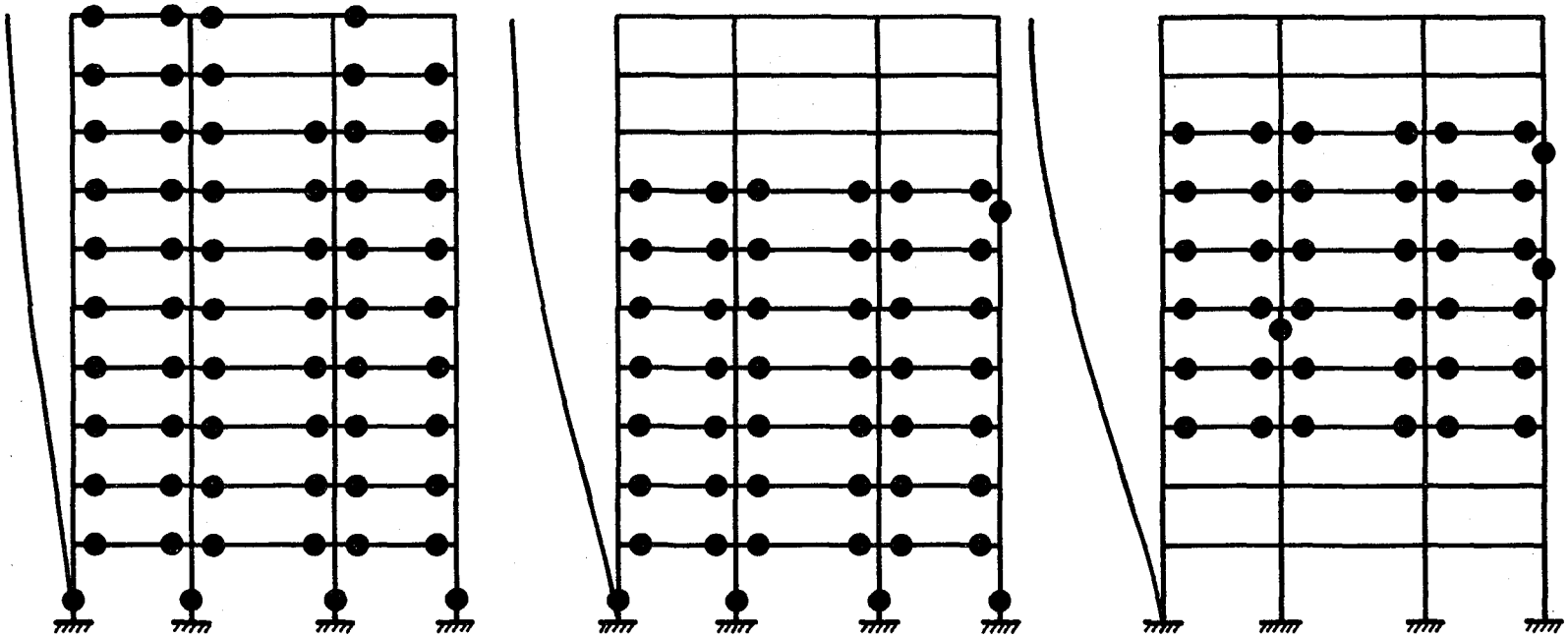

FIG. 34 PLASTIC HINGE PATTERNS DURING RESPONSE TO PACOIMA GROUND MOTION AT 0.5g

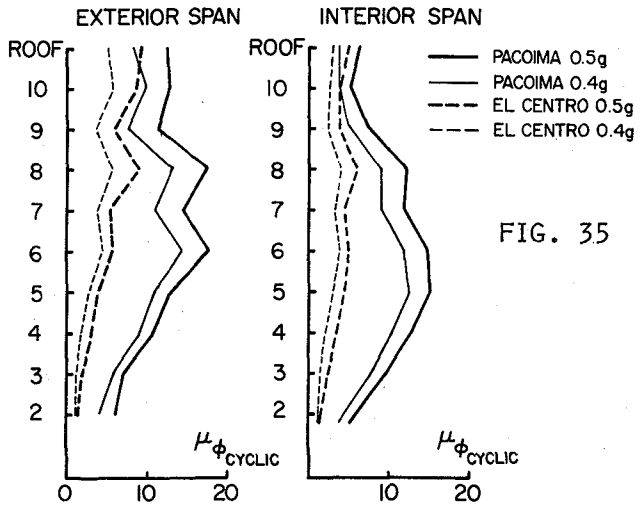

FIG. 35 ENVELOPES OF BEAM CYCLIC CURVATURE DUCTILITY, $\mu_{\phi CYCLIC}$

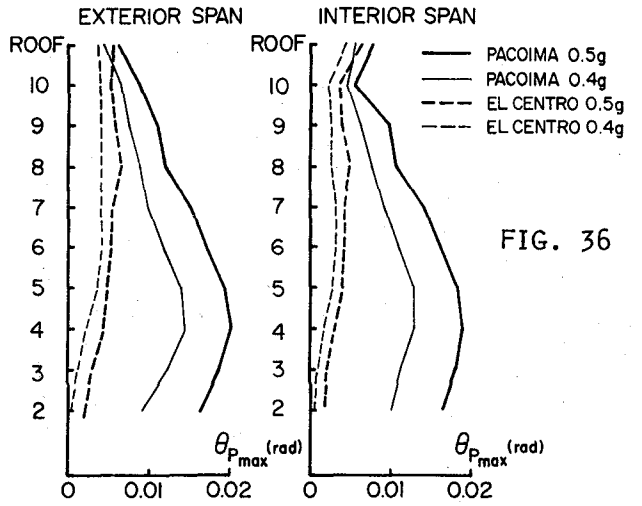

FIG. 36 ENVELOPES OF BEAM PLASTIC ROTATIONS, $\theta_{P_{MAX}}$

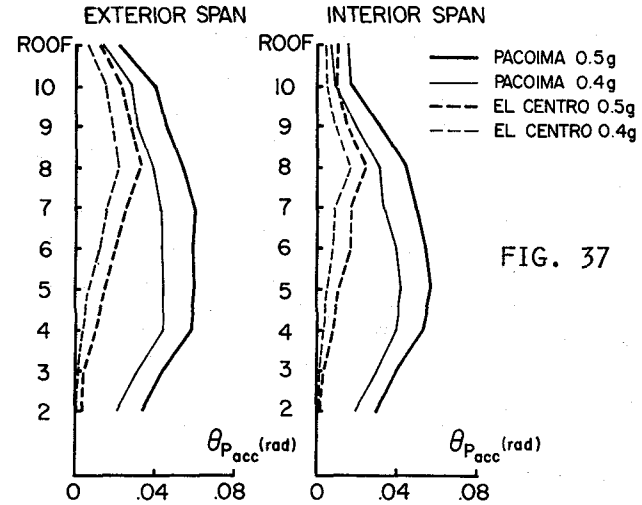

FIG. 37 ACCUMULATED BEAM PLASTIC ROTATIONS, $\theta_{P_{ACC}}$

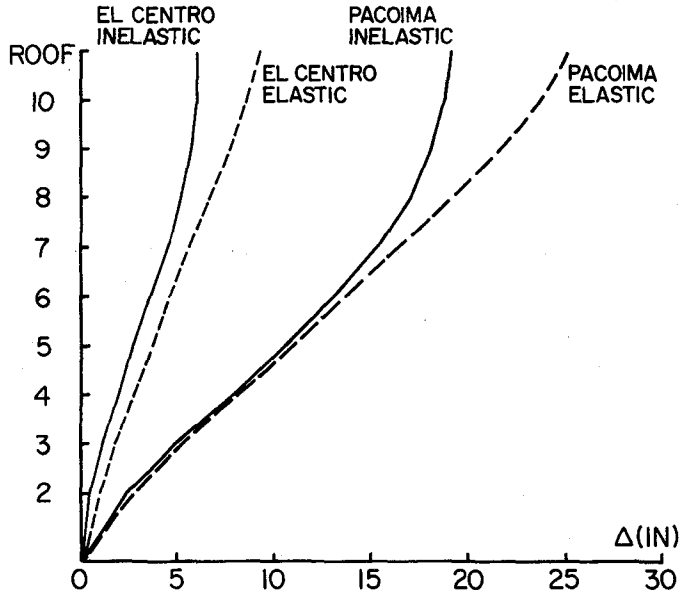

FIG. 38 COMPARISON OF ELASTIC AND INELASTIC STORY DISPLACEMENT ENVELOPES AT 0.5g

1 in. = 25.4 mm
1 kip = 4.448 kN

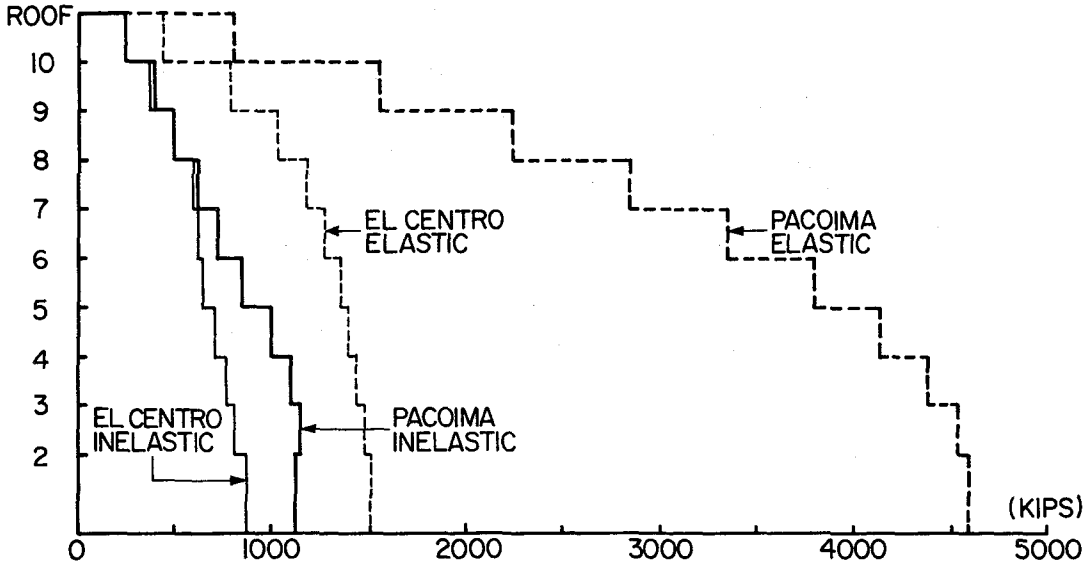

FIG. 39 COMPARISON OF ELASTIC AND INELASTIC STORY SHEAR ENVELOPES

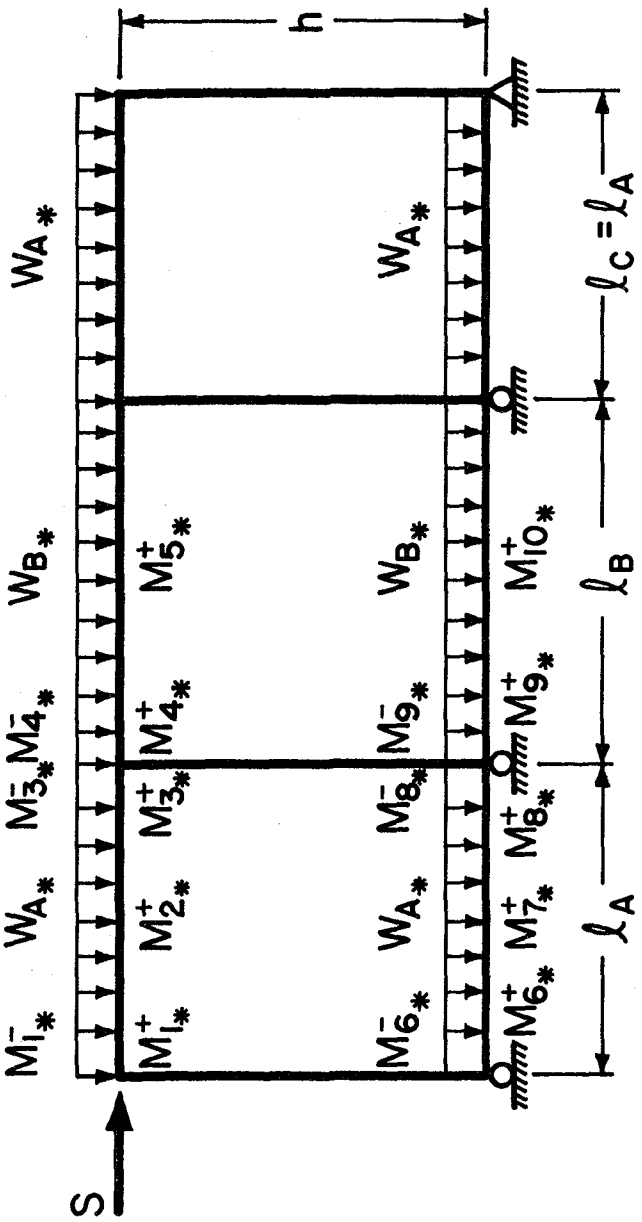

FIG. 40 FINAL DESIGN SUBASSEMBLAGE

1 in. = 25.4 mm
1 ft = 0.3048 m
1 kip = 4.448 kN

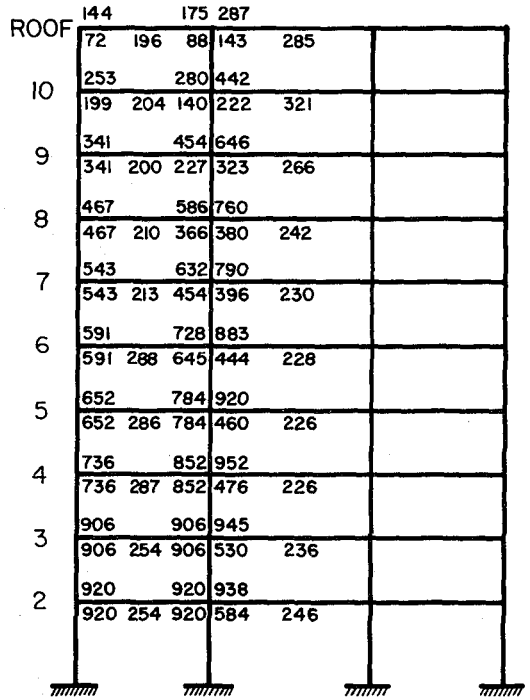

FIG. 41 OPTIMUM BEAM DESIGN MOMENTS FOR FINAL DESIGN (IN K-FT)

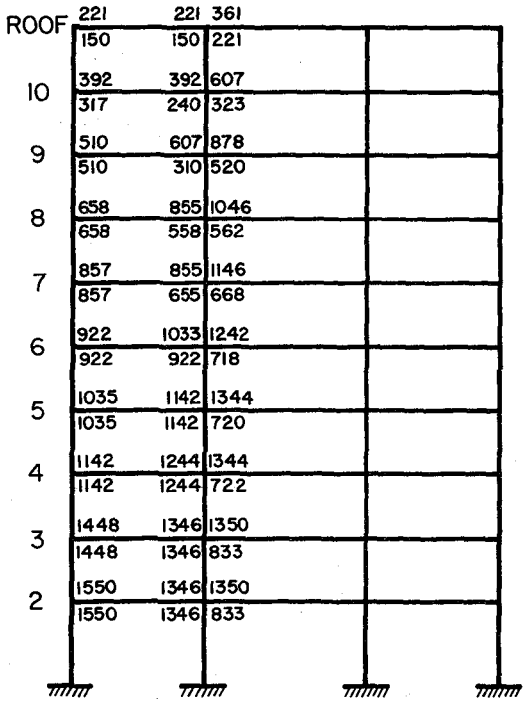

FIG. 42 AS-DESIGNED BEAM MOMENT CAPACITIES FOR FINAL DESIGN (IN K-FT)

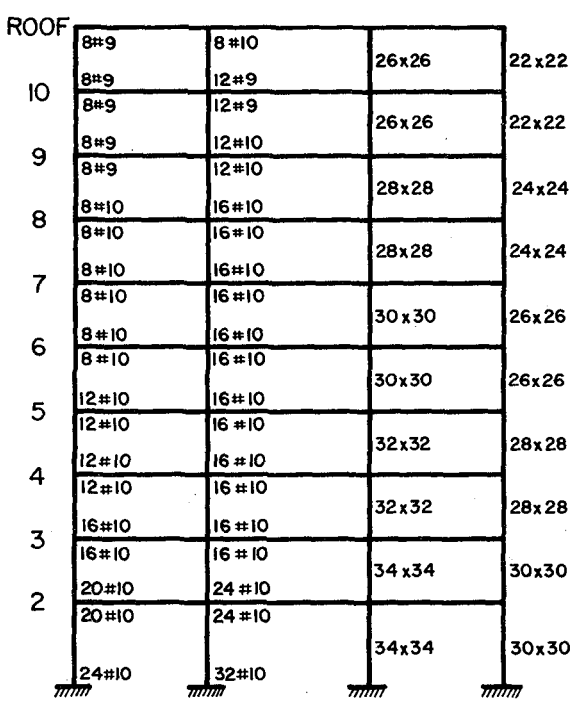

FIG. 43 COLUMN SIZES AND REINFORCEMENT FOR FINAL DESIGN (IN IN.)

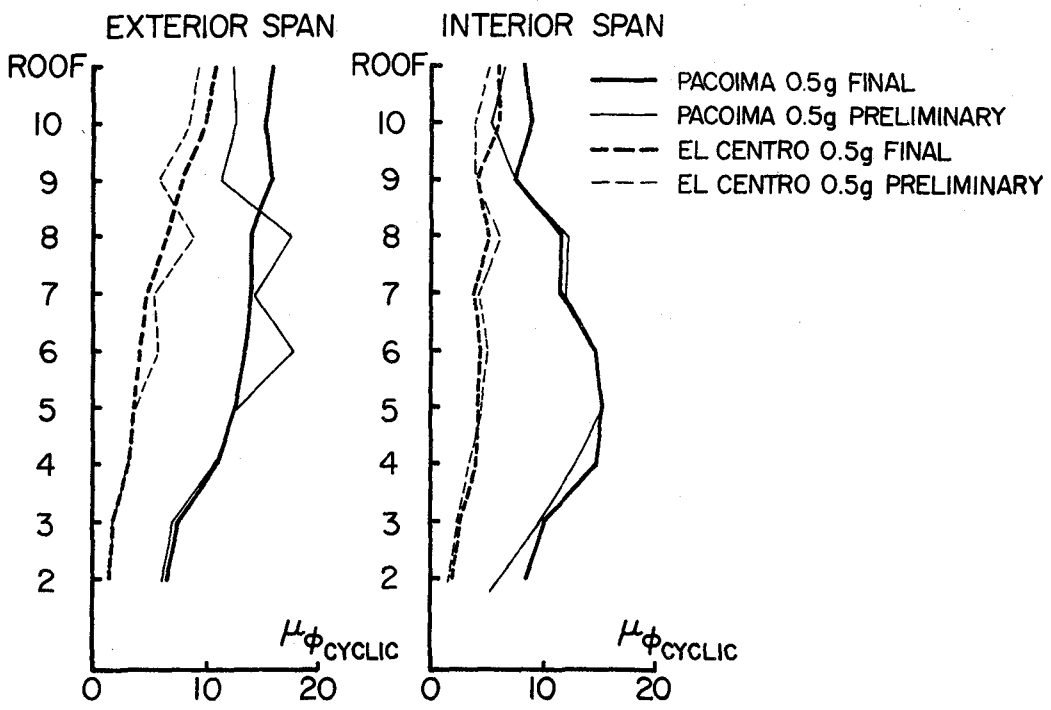

FIG. 44 COMPARISON OF BEAM CYCLIC CURVATURE DUCTILITY ENVELOPES FOR PRELIMINARY AND FINAL DESIGNS

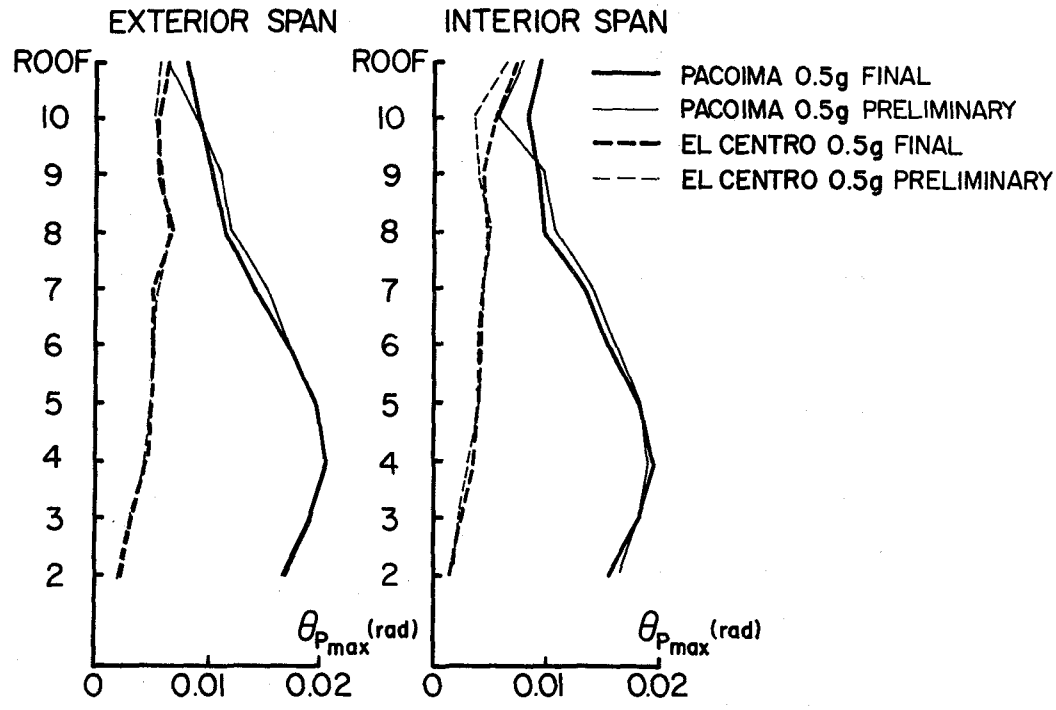

FIG. 45 COMPARISON OF BEAM PLASTIC ROTATION ENVELOPES FOR PRELIMINARY AND FINAL DESIGNS

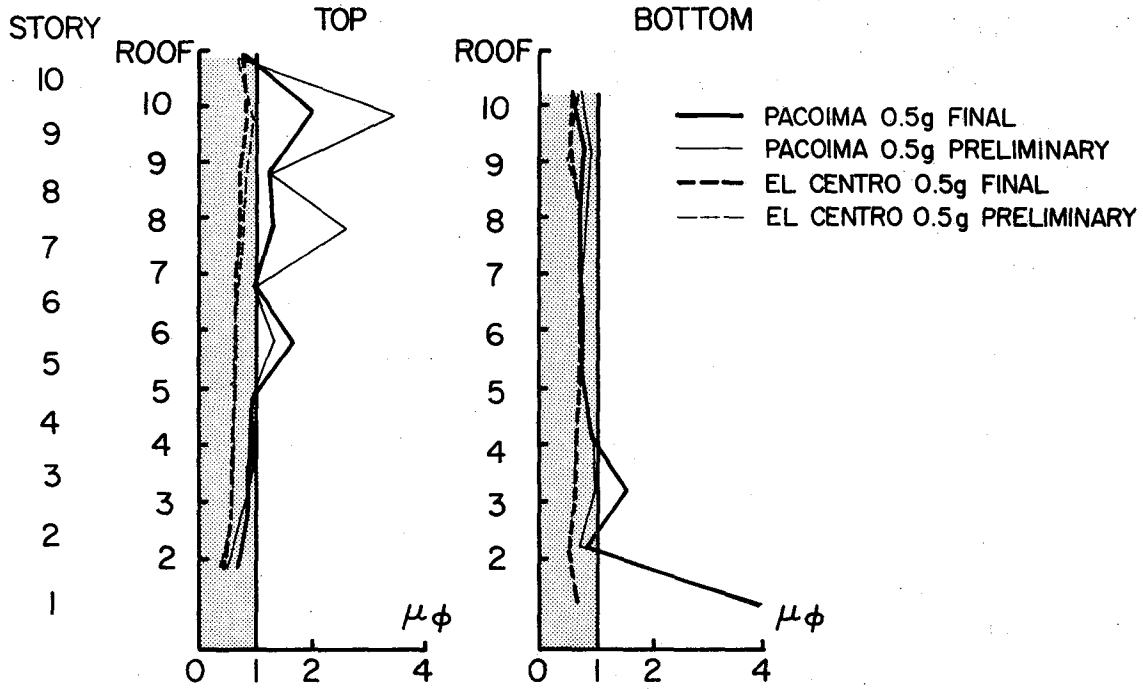

FIG. 46 COMPARISON OF COLUMN CURVATURE DUCTILITY ENVELOPES FOR PRELIMINARY AND FINAL DESIGNS, INTERIOR COLUMN

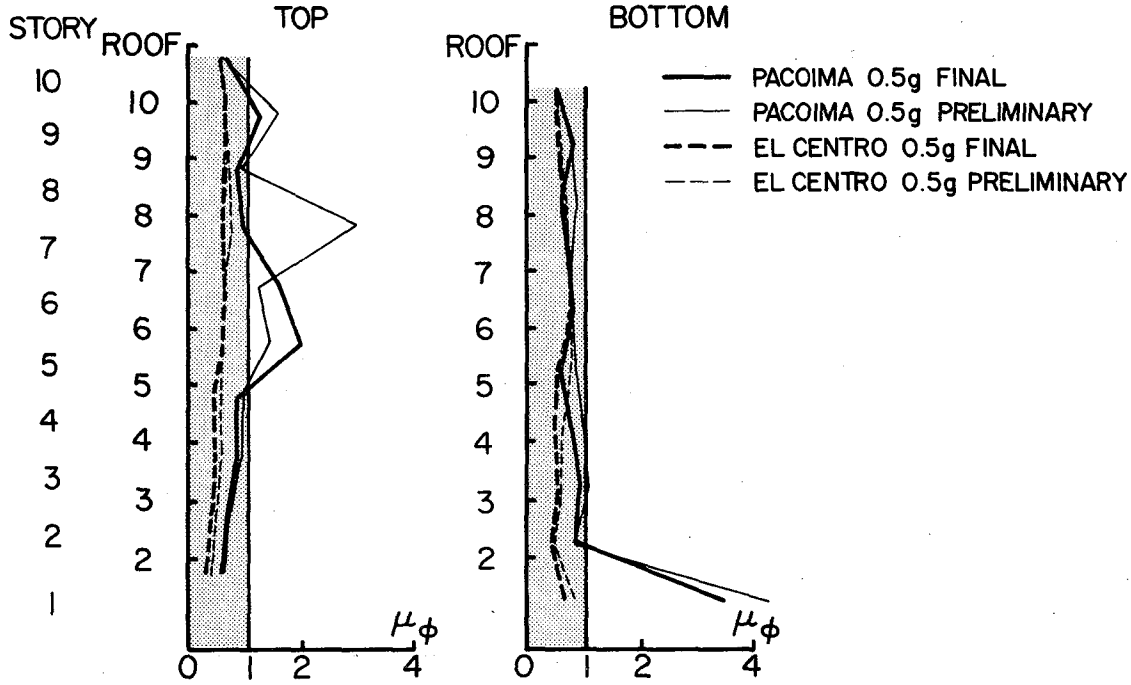

FIG. 47 COMPARISON OF COLUMN CURVATURE DUCTILITY ENVELOPES FOR PRELIMINARY AND FINAL DESIGNS, EXTERIOR COLUMN

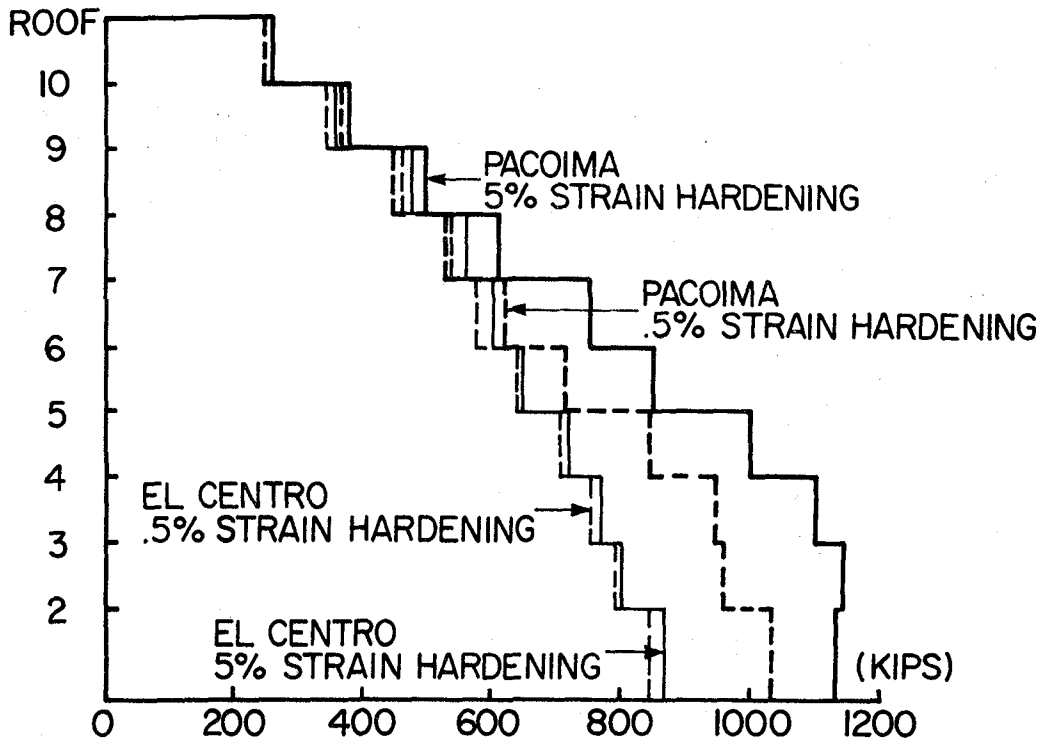

FIG. 48 COMPARISON OF STORY SHEAR ENVELOPES FOR DIFFERENT STRAIN HARDENING RATIOS

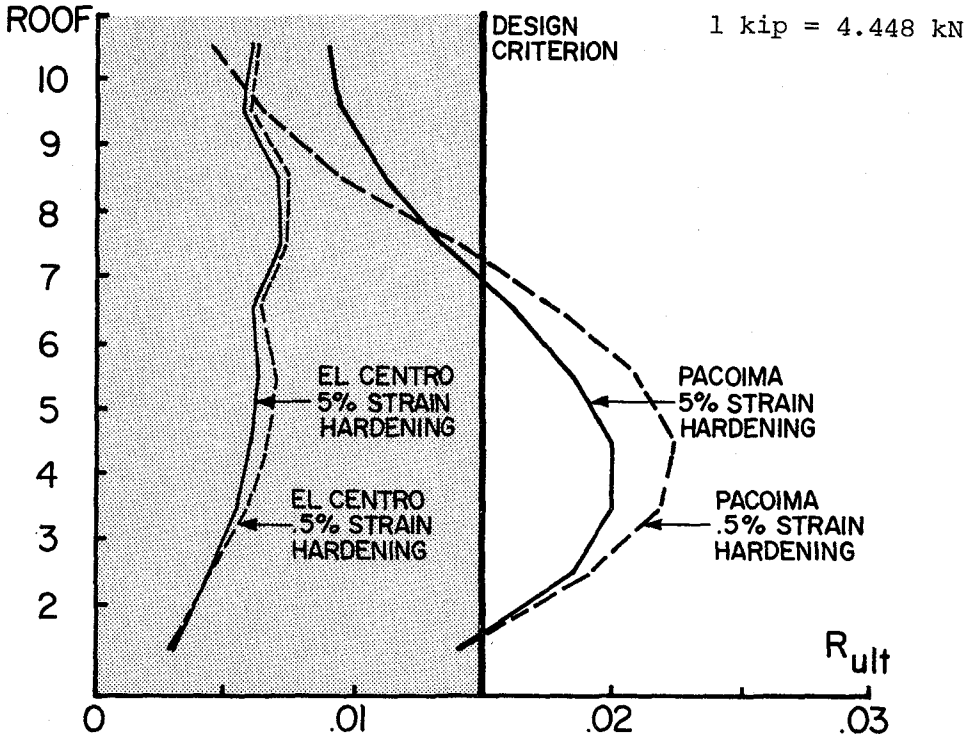

FIG. 49 COMPARISON OF STORY DRIFT INDEX ENVELOPES FOR DIFFERENT STRAIN HARDENING RATIOS

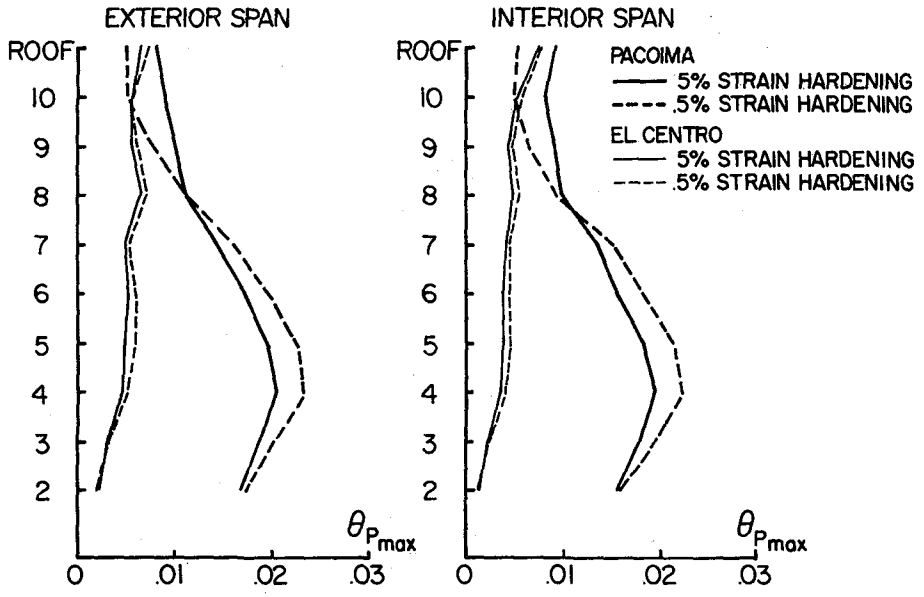

FIG. 50 COMPARISON OF BEAM PLASTIC ROTATION ENVELOPES FOR DIFFERENT STRAIN HARDENING RATIOS

1 in. = 25.4 mm

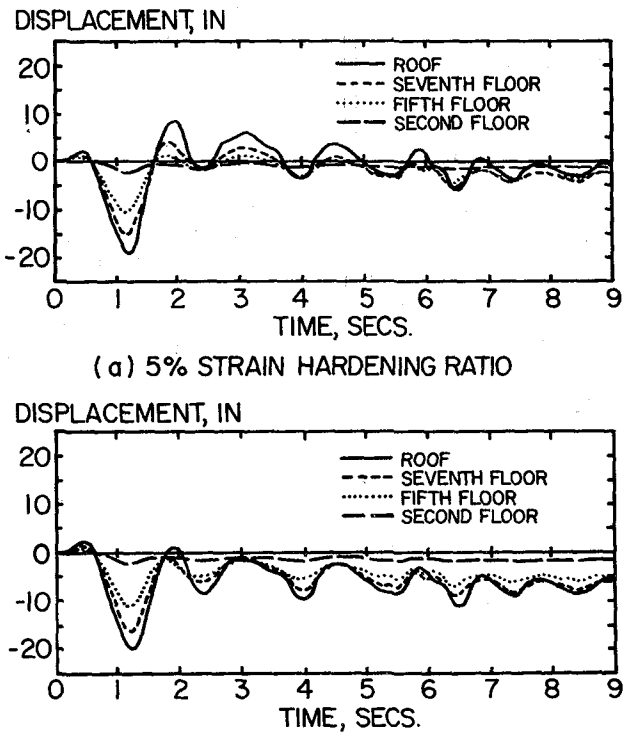

(a) 5% STRAIN HARDENING RATIO

(b) .5% STRAIN HARDENING RATIO

FIG. 51 COMPARISON OF DISPLACEMENT TIME HISTORIES FOR DIFFERENT STRAIN HARDENING RATIOS, PACOIMA GROUND MOTION AT 0.5g

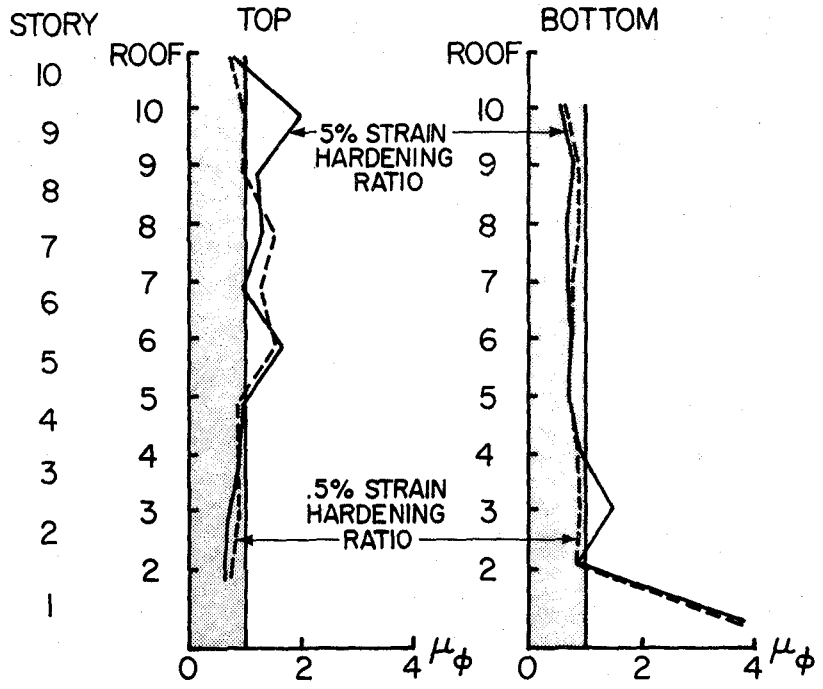

FIG. 52 COMPARISON OF COLUMN CURVATURE DUCTILITY ENVELOPES FOR DIFFERENT STRAIN HARDENING RATIOS, INTERIOR COLUMN DURING RESPONSE TO PACOIMA GROUND MOTION AT 0.5g

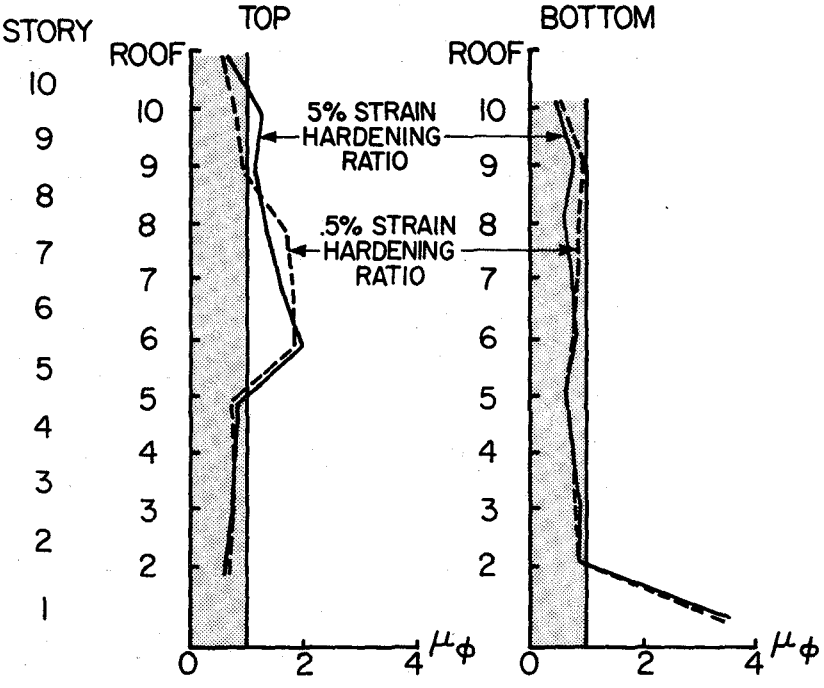

FIG. 53 COMPARISON OF COLUMN CURVATURE DUCTILITY ENVELOPES FOR DIFFERENT STRAIN HARDENING RATIOS, EXTERIOR COLUMN DURING RESPONSE TO PACOIMA GROUND MOTION AT 0.5g

APPENDIX A - DERIVATIONS AND COMPUTATIONS

A.1 Derivation of Equilibrium Constraints

A.1.1 Preliminary Design Subassemblage

For the current design example, 5 independent mechanisms may be identified in the preliminary design subassemblage: 3 beam mechanisms (one for each bay) and 2 sway mechanisms (one for each possible lateral load direction), Fig. A.1. The assumed symmetry of design moments results in 3 independent equilibrium equations:

$$M_1^- + 2M_2^+ + M_3^- \geq \frac{W_{A_G} \ell_A^2}{4} \tag{A.1}$$

and

$$2M_4^- + 2M_5^+ \geq \frac{W_{B_G} \ell_B^2}{4} \tag{A.2}$$

where

$W_G = 1.4\, W_{DL} + 1.7\, W_{LL}$

ℓ_A, ℓ_B = beam clear spans

$$M_1^- + M_1^+ + M_3^- + M_3^+ + M_4^- + M_4^+ \geq F_i \cdot \frac{h_i}{2} + S_{H_{i-1}} \left(\frac{h_{i-1}}{2} + \frac{h_i}{2}\right) = M_H \tag{A.3}$$

The following effective combined mechanisms can be formed.

Double mechanisms:

a-d; b-d; c-d; a-e; b-e; c-e

a-b is not an effective combined mechanism and the combination d-e does not result in a mechanism. Because of the symmetry of design moments, loading, and geometry, only three of these six possible combinations are independent:

a-d

b-d (Fig. A.2)

a-e

The resulting equations are:

$$M_1^- + 2M_2^+ + 2M_3^- + M_3^+ + M_4^+ + M_4^- \geq M_H + \frac{W_{A_L} \ell_A^2}{4} \quad \text{(A.4)}$$

$$2M_1^- + M_1^+ + 2M_2^+ + M_3^- + M_4^- + M_4^+ \geq M_H + \frac{W_{A_L} \ell_A^2}{4} \quad \text{(A.5)}$$

$$M_1^- + M_1^+ + M_3^- + M_3^+ + 2M_4^- + 2M_5^+ \geq M_H + \frac{W_{B_L} \ell_B^2}{4} \quad \text{(A.6)}$$

where

$$W_L = 1.2\, W_{DL} + 1.0\, W_{LL}$$

Triple mechanisms:

a-d-c; a-b-d; a-e-c; a-b-e

Of these four possible combinations, three are independent:

a-d-c

a-b-d (Fig. A.2)

a-b-e

The resulting equilibrium equations are:

$$M_1^- + 2M_2^+ + 2M_3^- + M_3^+ + 2M_4^- + 2M_5^+ \geq M_H + \frac{W_{B_L} \ell_B^2}{4} + \frac{W_{A_L} \ell_A^2}{4} \quad \text{(A.7)}$$

$$2M_1^- + M_1^+ + 2M_2^+ + M_3^- + 2M_4^- + 2M_5^+ \geq M_H + \frac{W_{B_L} \ell_B^2}{4} + \frac{W_{A_L} \ell_A^2}{4} \qquad (A.8)$$

$$2M_1^- + 4M_2^+ + 2M_3^- + M_4^- + M_4^+ \geq M_H + \frac{W_{A_L} \ell_A^2}{2} \qquad (A.9)$$

Quadruple mechanisms:

a-b-c-d; a-b-c-e

Both mechanisms result in the following equilibrium equation:

$$2M_1^- + 4M_2^+ + 2M_3^- + 2M_4^- + 2M_5^+ \geq M_H + \frac{W_{B_L} \ell_B^2}{4} + \frac{W_{A_L} \ell_A^2}{2} \qquad (A.10)$$

A.1.2 Final Design Subassemblage

To find the equilibrium equations for the subassemblage used in the final design, a computer program was written to automate the above process. The program yielded 68 independent equilibrium equations for the final design subassemblage. Because of the significantly larger number of equilibrium constraints associated with the final design subassemblage, the computational effort necessary to solve the resulting optimization problem will be greater than that required to solve the preliminary design problem. In view of this, the design improvements which may be achieved by employing more sophisticated design subassemblages should be weighed against the computational effort required to solve the resulting optimization problem.

A.2 Column Design Moments

The weak girder - strong column design criterion imposes a functional relationship between the column and beam design moments. The relationship, derived from joint equilibrium, is constructed to ensure, to the extent that it is practical, that inelastic behavior is limited to the beams. For the current example, three relationships are required, one for the exterior beam-column joint, and two

for an interior joint. The derivation of these expressions are presented below. In the derivations the notation used assumes that all variables are absolute values.

A.2.1 Exterior Columns

Consider a typical exterior beam-column joint (Fig. A.3). Joint equilibrium requires that:

$$M^T + V^T \frac{h_b}{2} + M^B + V^B \frac{h_b}{2} = M_1^- + V_1 \frac{h_c}{2} \qquad (A.11)$$

If it is assumed that column inflection points are at mid-height:

$$V^T = \frac{2M^T}{\ell_c^T} \quad \text{and} \quad V^B = \frac{2M^B}{\ell_c^B} \qquad (A.12)$$

where

ℓ_c = clear column height

then:

$$M^T \left(1 + \frac{h_b}{\ell_c^T}\right) + M^B \left(1 + \frac{h_b}{\ell_c^B}\right) = M_1^- + V_1 \frac{h_c}{2} \qquad (A.13)$$

Furthermore, if:

$$\ell_c^T = \ell_c^B = \ell_c$$

eq. (A.13) becomes:

$$\frac{\ell_c + h_b}{\ell_c} (M^T + M^B) = M_1^- + V_1 \frac{h_c}{2} \qquad (A.14)$$

From equilibrium of the beam in span A (Fig. A.3b):

$$V_1 = \frac{M_1^- + M_3^+}{\ell_A} + \frac{W_A \ell_A}{2} \qquad (A.15)$$

Incorporating eqs. (A.14) and (A.15) into eq. (A.13):

$$(M^T + M^B) = \frac{\ell_c}{\ell_c + h_b} \left\{ M_1^- + \frac{h_c}{2\ell_A} (M_1^- + M_3^+) + \frac{h_c}{4} W_A \ell_A \right\} \tag{A.16}$$

Since $M_1^+ \leq M_1^-$, eq. (A.16) will control the column design for all possible load conditions.

A.2.2 Interior Column

Two possible load conditions exist. One case is depicted in Fig. A.4. Employing the assumptions made in the derivation of eq. (A.16), the following equilibrium equation is obtained:

$$(M^T + M^B) = \frac{\ell_c}{\ell_c + h_c} \left\{ M_3^- + M_4^+ + V_3 \frac{h_c}{2} + V_4 \frac{h_c}{2} \right\} \tag{A.17}$$

From equilibrium of spans A and B (Fig. A.4b):

$$\begin{aligned} V_3 &= \frac{M_1^+ + M_3^-}{\ell_A} + \frac{W_A \ell_A}{2} \\ V_4 &= \frac{M_4^+ + M_4^-}{\ell_B} - \frac{W_B \ell_B}{2} \end{aligned} \tag{A.18}$$

and eq. (A.17) becomes:

$$\begin{aligned} (M^T + M^B) = \frac{\ell_c}{\ell_c + h_b} \Bigg\{ & M_3^- + M_4^+ + \frac{h_c}{2\ell_A} (M_1^+ + M_3^-) \\ & + \frac{h_c}{2\ell_B} (M_4^+ + M_4^-) + \frac{h_c}{4} (W_A \ell_A - W_B \ell_B) \Bigg\} \end{aligned} \tag{A.19}$$

However, the loading conditions indicated in Fig. A.5 may also control column design and the following expression must also be considered:

$$(M^T + M^B) = \frac{\ell_c}{\ell_c + h_b} \left\{ M_3^+ + M_4^- + \frac{h_c}{2\ell_A} (M_1^- + M_3^+) \right.$$

$$\left. + \frac{h_c}{2\ell_B} (M_4^+ + M_4^-) + \frac{h_c}{4} (W_B \ell_B - W_A \ell_A) \right\} \qquad (A.20)$$

A.2.3 Column Contribution to Merit Function

Equilibrium eqs. (A.16), (A.19), and (A.20) are used to determine the contribution of the column reinforcement to the merit function. At a given beam-column joint, it is assumed that both M^T and M^B contribute a length of reinforcement equal to one-half the column height. However, because the distribution of column reinforcement is assumed to be symmetric about the centroid of the concrete cross section, approximately twice as much reinforcement is required to provide a given moment capacity for a column than for a beam. As a result, the length of column reinforcement is taken as the full, rather than half, column height.

The assumed relationship between moment capacity and steel area:

$$M_i = A_{s_i} f_y \cdot jd \qquad (A.21)$$

is linear in M_i and A_{s_i} and also in M_i and d. To account for the dependency of moment capacity on d, the ratio of the beam and column depths (h_b/h_c) is used as a factor in determining the column contribution to the merit function, $C(M_j)$. In addition, the following factors are considered:

i) F ensures a weak girder - strong column design

ii) PF includes the effect of axial load on the column moment capacity

iii) $1/\phi_c$ accounts for the increase in column design moments attributed to the code required capacity reduction factor. The flexural capacity reduction

factor is excluded because the columns are designed according to unreduced beam capacities.

The fact that the column reinforcement which is distributed through the depth is less effective than the reinforcement in the outside layer in resisting moment has been ignored for simplicity.

The following relationships result:

For an exterior column:

$$C(M_j) = \frac{h_b}{h_c} \ell_c F \frac{1}{\phi_c} \left[M_1^- + \frac{h_c}{2\ell_A} (M_1^- + M_3^+) \right] PF \qquad (A.22)$$

and for an interior column:

$$C(M_j) = \frac{h_b}{h_c} \ell_c F \frac{1}{\phi_c} \left[\frac{1}{2} (M_3^- + M_4^+ + M_4^- + M_3^+) + \frac{h_c}{4\ell_A} (M_1^- + M_1^+ + M_3^+ + M_3^-) + \frac{h_c}{2\ell_B} (M_4^- + M_4^+) \right] PF \qquad (A.23)$$

The gravity load terms have been dropped in both expressions because they are independent of the beam design moments. To prevent any bias in the merit function, eqs. (A.19) and (A.20) were averaged to yield eq. (A.23). Finally, it was assumed that:

$$\ell_c + h_b = \ell$$

and the factor $1/(\ell_c + h_b)$ in eqs. (A.16), (A.19), and (A.20) cancels with the assumed length of column reinforcement.

A.3 Construction of Merit Function

A numerical example of the construction of a typical merit function is presented below. The merit function is given by the expression:

$$Vol = \sum \gamma_i M_i \qquad (A.24)$$

The problem is to determine γ_i for each design moment, M_i. In the current procedure γ_i comprises two parts: γ_i^*, the beam contribution and γ_i^{**}, the column contribution.

A.3.1 Beam Contribution

The beam contribution to the merit function, γ_i^*, is determined on the basis of the ultimate load - elastic moment envelope. Typical envelopes at a lower story are given in Fig. A.6. A typical γ_i^* is the effective length over which the reinforcement necessary to provide moment capacity, M_i, is required. The term γ_i^* includes bar development lengths and also accounts for bar cutoffs.* Thus, it is dependent on the bar size which is assumed in design. For the example, a No. 8 bar is assumed. The development length, ℓ_d^B, for a No. 8 bar is given by the expression:

$$\ell_d^B \geq 0.04\, A_b \frac{f_y}{\sqrt{f'_c}} \qquad \text{(A.25)}$$

For f'_c = 27.58 MPa (4,000 psi) and f_y = 413.7 MPa (60,000 psi), the development length for a bottom bar, ℓ_d, is 762 mm (30 in.) and for a top bar, ℓ_d^T, it is 1.07 m (42 in.).

Based on the constructions in Fig. A.6, the following expressions may be written:

$$\gamma_1^{*-} = 2\left[\ell_{11}^- + \frac{5}{6}\ell_{21}^- + \frac{2}{3}\ell_{31}^- + \frac{1}{2}\ell_{41}^- + \frac{1}{3}\left(\frac{1}{2}\ell_A^-\right) + \ell_d^T\right]$$

$$\gamma_1^{*+} = 2\left[\ell_{11}^+ + \frac{3}{4}\ell_{21}^+ + \ell_d^B\right]$$

$$\gamma_2^{*+} = 2\left[\ell_A^+\right]$$

$$\gamma_3^{*-} = 2\left[\ell_{13}^- + \frac{5}{6}\ell_{23}^- + \frac{2}{3}\ell_{33}^- + \frac{1}{2}\ell_{43}^- + \frac{1}{3}\left(\frac{1}{2}\ell_A^-\right) + \frac{\ell_d^T}{2}\right.$$

*Bar splices have been ignored for simplicity.

$$\gamma_3^{*+} = 2[\ell_{13}^{+} + \frac{3}{4}\ell_{23}^{+} + \frac{\ell_d^B}{2}]$$

$$\gamma_4^{*-} = 2[\ell_{14}^{-} + \frac{5}{6}\ell_{24}^{-} + \frac{2}{3}\ell_{34}^{-} + \frac{1}{2}\ell_{44}^{-} + \frac{1}{3}(\ell_B^{-}) + \frac{\ell_d^T}{2}$$

$$\gamma_4^{*+} = 2[\ell_{14}^{+} + \frac{5}{6}\ell_{24}^{+} + \frac{\ell_d^B}{2}]$$

$$\gamma_5^{*+} = 2[\ell_B^{+}] \qquad \text{(A.26)}$$

The last term in γ_1^{*-}, γ_1^{*+}, γ_3^{*-}, γ_3^{*+}, γ_4^{*-}, and γ_4^{*+} is included to account for bar anchorage. A factor of 2 is included to account for the other half of the frame. The lengths indicated in the above expressions were determined graphically and are summarized below.

ℓ_{11}^{-} = 48 in. $\quad$ ℓ_{13}^{-} = 46 in.

ℓ_{21}^{-} = 18 in. $\quad$ ℓ_{23}^{-} = 20 in.

ℓ_{31}^{-} = 16 in. $\quad$ ℓ_{33}^{-} = 18 in.

ℓ_{41}^{-} = 21 in. $\quad$ ℓ_{43}^{-} = 22 in.

ℓ_A^{-} = 59 in.

ℓ_{11}^{+} = 75 in. $\quad$ ℓ_{13}^{+} = 76 in.

ℓ_{21}^{+} = 46 in. $\quad$ ℓ_{23}^{+} = 44 in.

ℓ_A^{+} = 27 in.

ℓ_{14}^{-} = 54 in. $\quad$ ℓ_{14}^{+} = 90 in.

ℓ_{24}^{-} = 18 in. $\quad$ ℓ_{24}^{+} = 54 in.

ℓ_{34}^{-} = 18 in. $\quad$ ℓ_B^{+} = 19 in.

ℓ_{44}^{-} = 27 in.

ℓ_B^{-} = 46 in.

$$\gamma_1^{*-} = 2[48 + \frac{5}{6}\ 18 + \frac{2}{3}\ 16 + \frac{1}{2}\ 21 + \frac{1}{3}\ (30) + 42]\ \text{in.}$$

$$= 2\ (136\ \text{in.}) = 272\ \text{in.}$$

$$\gamma_1^{*+} = 2[75 + \frac{3}{4}\ (46) + 30]\ \text{in.}$$

$$= 2\ (139.5) = 279\ \text{in.}$$

$$\gamma_2^{*} = 2\ (27)\ \text{in.}$$

$$= 54\ \text{in.}$$

$$\gamma_3^{*-} = 2[46 + \frac{5}{6}\ 20 + \frac{2}{3}\ 18 + \frac{1}{2}\ 22 + \frac{1}{3}\ (30) + 21]\ \text{in.}$$

$$= 2\ (117\ \text{in.}) = 234\ \text{in.}$$

$$\gamma_3^{*+} = 2[76\ \text{in.} + \frac{3}{4}\ 44\ \text{in.} + 15\ \text{in.}]$$

$$= 2[124\ \text{in.}] = 248\ \text{in.}$$

$$\gamma_4^{*-} = 2[54\ \text{in.} + \frac{5}{6}\ 18\ \text{in.} + \frac{2}{3}\ 18\ \text{in.} + \frac{1}{2}\ 27\ \text{in.}$$
$$+ \frac{1}{3}\ (46\ \text{in.}) + 21]$$

$$= 2\ (131\ \text{in.}) = 262\ \text{in.}$$

$$\gamma_4^{*+} = 2[90\ \text{in.} + \frac{5}{6}\ 54\ \text{in.} + 15\ \text{in.}]$$

$$= 2\ (150\ \text{in.}) = 300\ \text{in.}$$

$$\gamma_5^{*+} = 2[19\ \text{in.}]$$

$$= 38\ \text{in.}$$

A.3.2 Column Contribution

The column contribution to the merit function is determined from eqs. (A.22) and (A.23). For the story level under consideration:

$$h_c\ (\text{exterior}) = 30\ \text{in.}$$

$$h_c\ (\text{interior}) = 34\ \text{in.}$$

$$h_b = 34\ \text{in.}$$

$$\ell = 144\ \text{in.}$$

$$\ell_A = 268\ \text{in.}$$

$$\ell_B = 326 \text{ in.}$$

$$\ell_c = \ell - h_b = 110 \text{ in.}$$

$$\phi_c = 0.7$$

The factor PF was determined on the basis of an average axial force - moment (P-M) interaction relationship for the assumed column size. The P-M interaction relationships for steel contents of 1% and 4% were evaluated and approximated by the relationship shown in Fig. A.7, and were then averaged. The minimum design axial force, P_D, was estimated considering both gravity and seismic load effects, and the PF factor was determined by finding the moment capacity at this axial load, M_D, and then dividing it into the moment capacity at zero axial load, M_0:

$$PF = \frac{M_0}{M_D} \tag{A.27}$$

For the story level in this example, PF was 1.01 for the exterior column and 0.895 for the interior column. These values are typical and, in view of the approximations involved in their evaluation, the use of a PF factor may be an unnecessary refinement. Its effect on the optimization solution should be investigated further.

The term F was assumed to be equal to 1.2 (Section 3.3.5).

Substituting the above data into eqs. (A.22) and (A.23) the following expressions are obtained.

For the exterior column:

$$C(M_j) = \frac{34 \text{ in.}}{30 \text{ in.}} (110 \text{ in.})(1.2)\left(\frac{1}{0.7}\right)\left\{M_1^- + \frac{34 \text{ in.}}{2(268 \text{ in.})}(M_1^- + M_3^+)\right\} 1.01$$

$$= 215 \text{ in.} \left\{M_1^- + 0.064\ (M_1^- + M_3^+)\right\} \tag{A.28}$$

and for the interior column:

$$C(M_j) = \frac{34 \text{ in.}}{34 \text{ in.}} (110 \text{ in.})(1.2)\left(\frac{1}{0.7}\right) \left\{\frac{1}{2}\left(M_3^- + M_3^+ + M_4^- + M_4^+\right) + \frac{34 \text{ in.}}{4(268 \text{ in.})}\left(M_1^- + M_1^+ + M_3^+ + M_3^-\right) + \frac{34 \text{ in.}}{2(326 \text{ in.})}\left(M_4^+ + M_4^-\right)\right\} .895$$

$$= 179 \text{ in.} \left\{\frac{1}{2}\left(M_3^- + M_3^+ + M_4^- + M_4^+\right) + 0.032\left(M_1^- + M_1^+ + M_3^+ + M_3^-\right) + 0.052\left(M_4^- + M_4^+\right)\right\} \quad \text{(A.29)}$$

γ_i^{**} is then:

$$\gamma_1^{**-} = 2 (215 \text{ in.} \pm 14 \text{ in.} + 6 \text{ in.})$$

$$= 470 \text{ in.}$$

$$\gamma_1^{**+} = 2 (6 \text{ in.})$$

$$= 12 \text{ in.}$$

$$\gamma_2^{**+} = 0$$

$$\gamma_3^{**-} = 2 (90 \text{ in.} + 6 \text{ in.})$$

$$= 192 \text{ in.}$$

$$\gamma_3^{**+} = 2 (90 \text{ in.} + 6 \text{ in.} + 14 \text{ in.})$$

$$= 220 \text{ in.}$$

$$\gamma_4^{**-} = 2 (90 \text{ in.} + 9 \text{ in.})$$

$$= 198 \text{ in.}$$

$$\gamma_4^{**+} = 2 (99 \text{ in.})$$

$$= 198 \text{ in.}$$

$$\gamma_5^{**} = 0$$

The factor of 2 is used because there are two exterior and interior columns.

A.3.3 Merit Function

γ_i is found by summing the beam and column contributions:

$$\gamma_i = \gamma_i^* + \gamma_i^{**} \tag{A.30}$$

For the example the resulting merit function is:

$$742\ M_1^- + 291\ M_1^+ + 54\ M_2 + 426\ M_3^- + 468\ M_3^+ + 460\ M_4^-$$

$$+ 498\ M_4^+ + 38\ M_5$$

A.4 Slenderness Effects

Moment amplification due to column slenderness effects is included in the proposed design procedure by amplifying the beam design moments. This is in accord with UBC 2610(1)7. The beam moment amplification factor, α_F, is evaluated according to UBC 2610(1)5. The following relationships are employed:

$$\delta = \frac{C_m}{1 - \frac{P_u}{\phi P_c}} \geq 1.0 \tag{A.31}$$

where

$$P_c = \frac{\pi^2 EI}{(k\ell_u)^2} \tag{A.32}$$

$$EI = \frac{\frac{E_c I_g}{5} + E_s I_{se}}{1 + \beta_d} \tag{A.33}$$

β_d = ratio of maximum dead load moment to maximum design load moment

I_g = moment of inertia of gross concrete section about the centroidal axis

I_{s_e} = moment of inertia of reinforcement about the centroidal axis of the cross section

$k\ell_u$ = effective length of column

ϕ = capacity reduction factor

C_m = factor relating the actual moment diagram to an equivalent uniform moment diagram. For the design example, $C_m = 1$

The effective length, $k\ell_u$, depends on the rotational restraint of the joints at the ends of the column. A measure of this restraint is provided by the parameter, ψ, which is defined by the expression:

$$\psi = \frac{\sum(EI_{col}/\ell_c)}{\sum(EI_b/\ell)} \tag{A.34}$$

where

EI_{col} = flexural rigidity of column section

EI_b = flexural rigidity of beam section

The summation is carried out for all members at the joint. In the current procedure, member stiffness (EI) for both beams and columns is based on the gross section properties. The following relationship suggested by Furlong was used to determine the effective length factor k*:

$$k = \frac{20 - \psi_{AV}}{20}\sqrt{1 + \psi_{av}} \qquad \psi_{av} \leq 2$$

$$k = 0.9\sqrt{1 + \psi_{av}} \qquad \psi_{av} > 2 \tag{A.35}$$

where ψ_{AV} is the average value of ψ at the column ends; thus:

$$\psi_{AV} = \frac{\psi_A + \psi_B}{2} \tag{A.36}$$

---

*R. W. Furlong, "Column Slenderness and Charts for Design," Journal of the ACI, Vol. 68, No. 1, January 1971, pp. 9-17.

It should be noted that eq. (A.35) applies to unbraced columns.

The above relationships have been included as a subroutine in the column design program, and the values of δ have been evaluated for each column after it was designed. In the evaluation, δ for the entire story, δ_{ST}, is determined by the expression:

$$\delta_{ST} = \frac{C_m}{1 - \frac{\sum P}{\phi \sum P_c}} \tag{A.37}$$

where the summation is for all the columns in the story. The value of δ_{ST} is compared to δ, which is determined from individual column behavior, and the larger value is used.

The δ values obtained are used in the next iteration of the design process to define the beam moment amplification factor, α_F. At a typical beam-column joint, α_F is obtained by taking the average value of δ at the joint:

$$\alpha = \frac{\delta_{above} + \delta_{below}}{2} \tag{A.38}$$

The term α_F is used to amplify both the positive and negative design moments at the joint. The span design moments are assumed to be unaffected by slenderness effects.

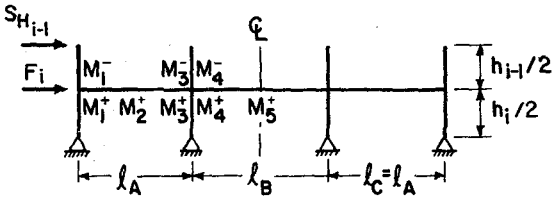

NOTE: ℓ_A AND ℓ_B ARE CLEAR SPANS

(a) DESIGN SUBASSEMBLAGE

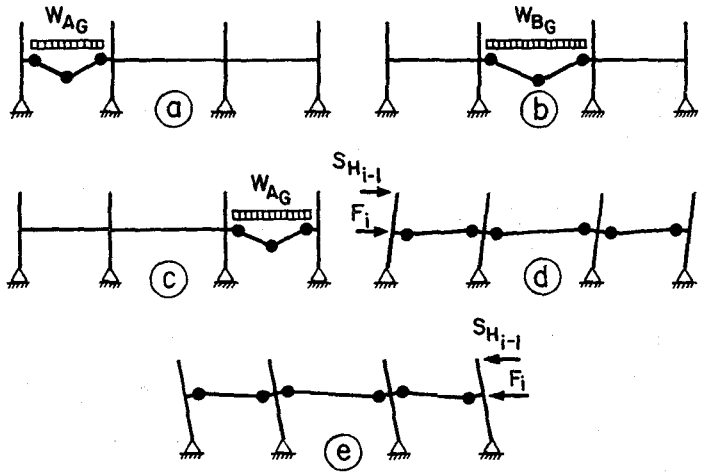

(b) INDEPENDENT MECHANISMS

FIG. A.1 INDEPENDENT MECHANISMS FOR PRELIMINARY DESIGN SUBASSEMBLAGE

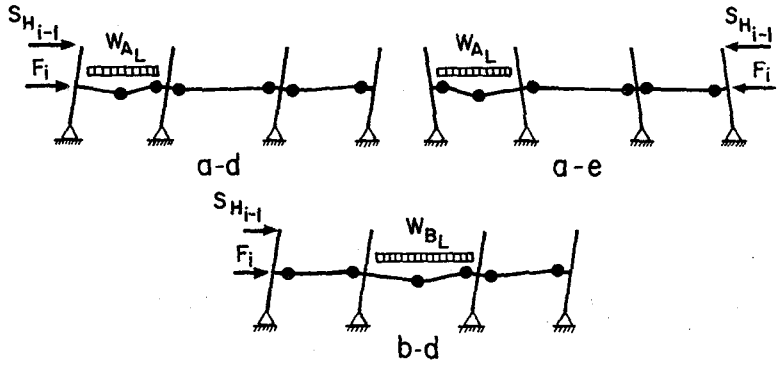

(a) DOUBLE MECHANISMS

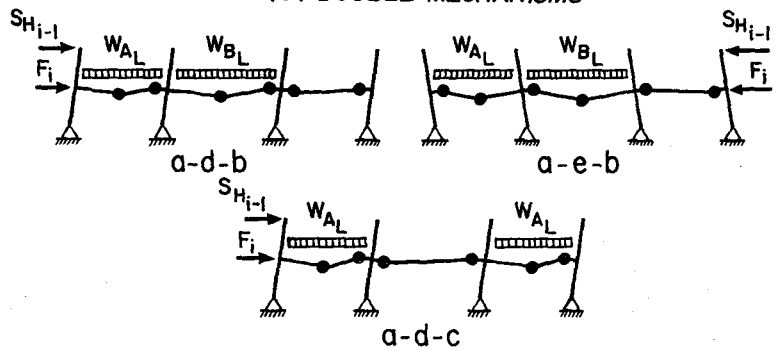

(b) TRIPLE MECHANISMS

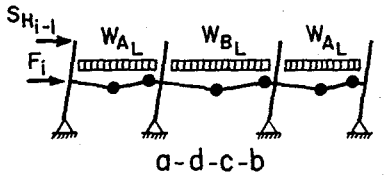

(c) QUADRUPLE MECHANISM

FIG. A.2 COMBINED MECHANISMS FOR PRELIMINARY DESIGN SUBASSEMBLAGE

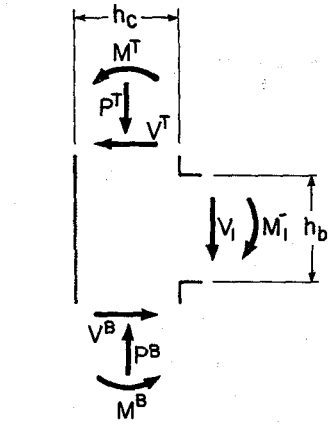

(a) JOINT FORCES

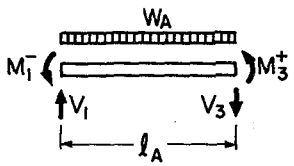

(b) BEAM FORCES

FIG. A.3 EQUILIBRIUM AT A TYPICAL EXTERIOR BEAM-COLUMN JOINT

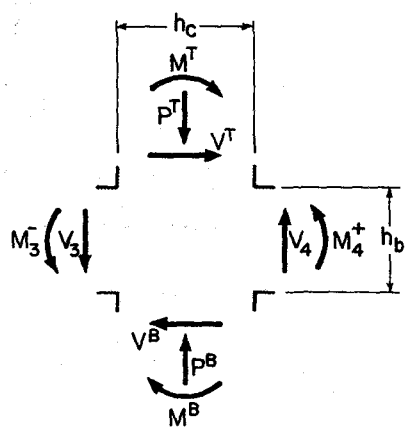

(a) JOINT FORCES

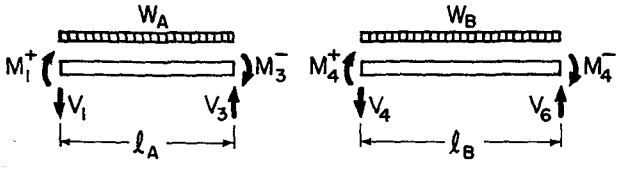

(b) BEAM FORCES

FIG. A.4 EQUILIBRIUM AT A TYPICAL INTERIOR BEAM-COLUMN JOINT (LOAD CASE I)

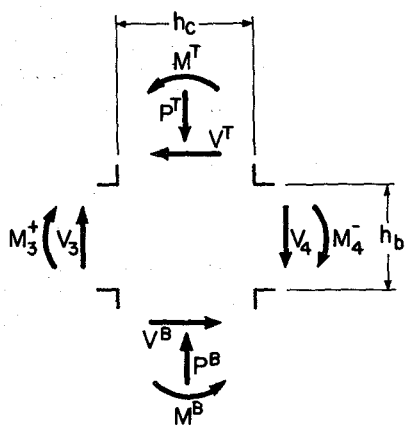

(a) JOINT FORCES

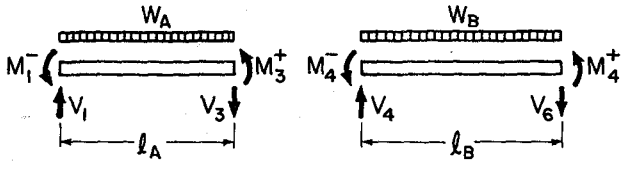

(b) BEAM FORCES

FIG. A.5 EQUILBRIUM AT A TYPICAL INTERIOR BEAM-COLUMN JOINT (LOAD CASE II)

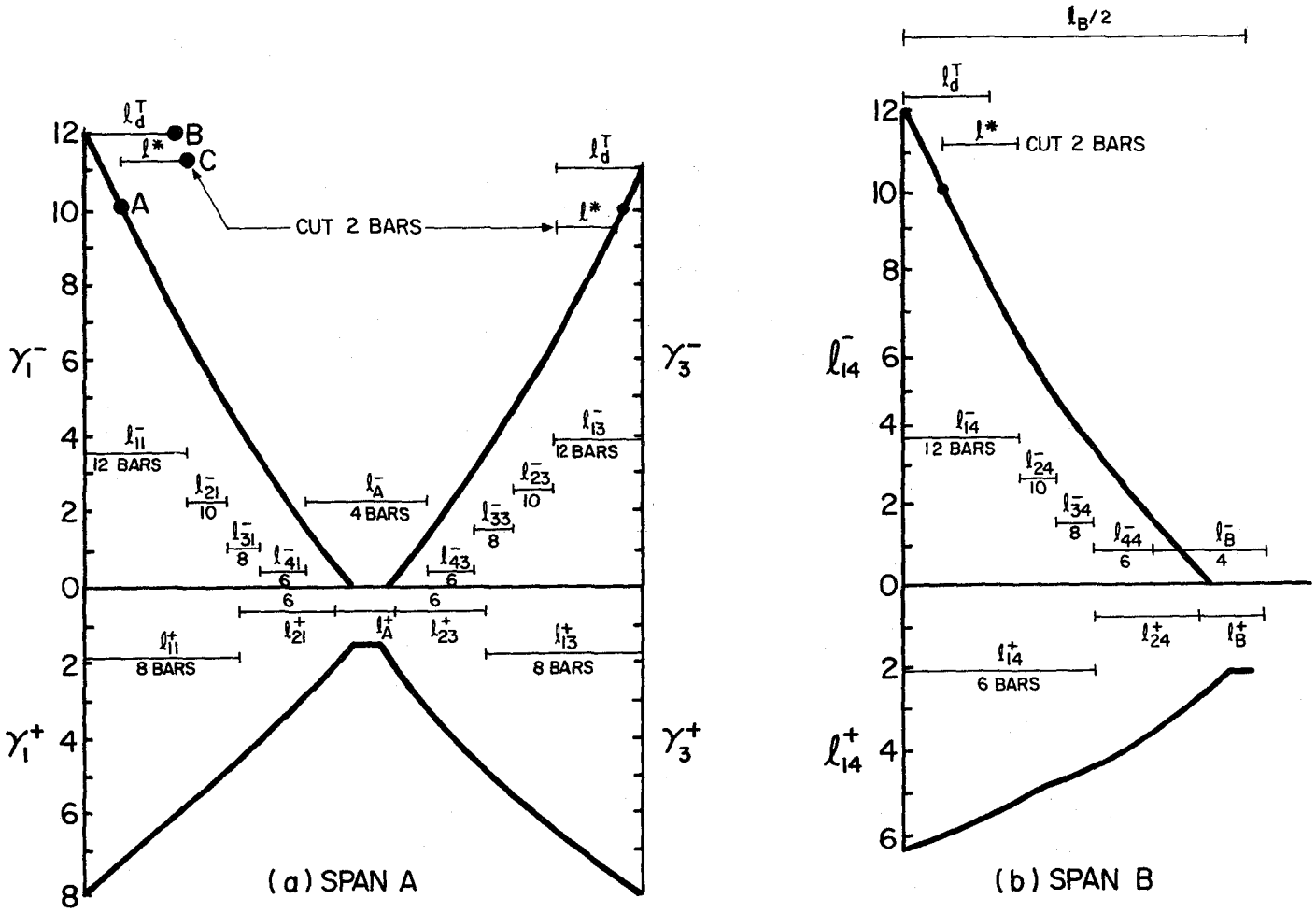

FIG. A.6 TYPICAL ELASTIC MOMENT ENVELOPES AND BAR CURTAILMENT

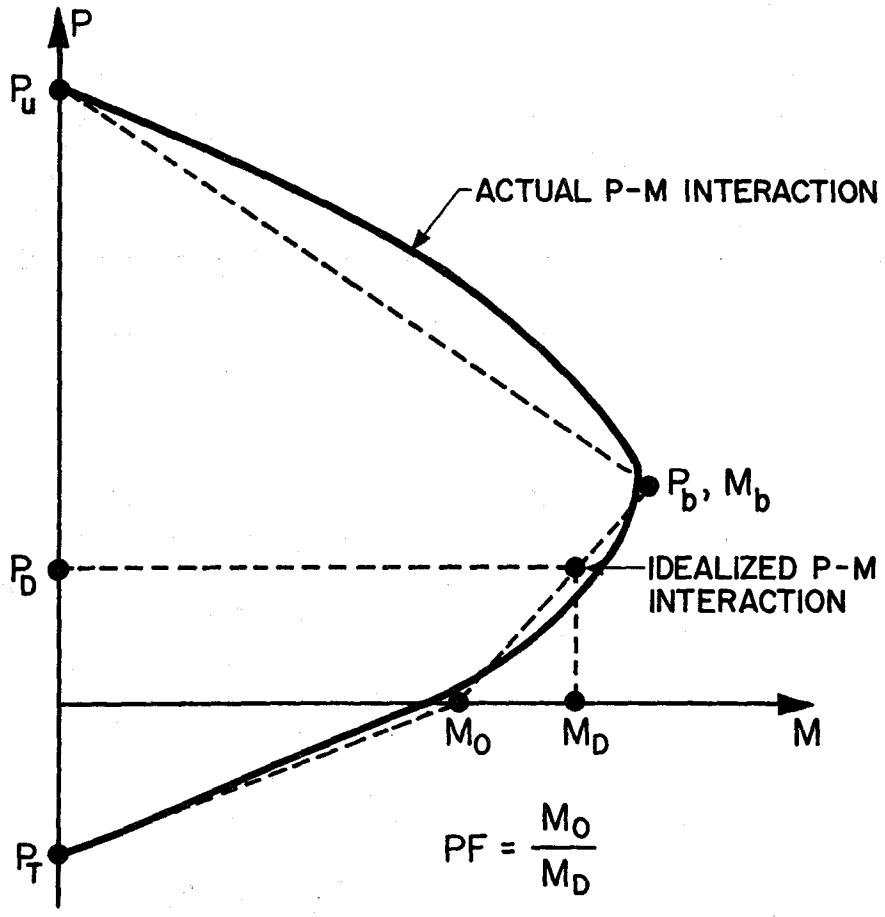

FIG. A.7 DETERMINATION OF PF FACTOR

EARTHQUAKE ENGINEERING RESEARCH CENTER REPORTS

EARTHQUAKE ENGINEERING RESEARCH CENTER REPORTS

NOTE: Numbers in parentheses are Accession Numbers assigned by the National Technical Information Service; these are followed by a price code. Copies of the reports may be ordered from the National Technical Information Service, 5285 Port Royal Road, Springfield, Virginia, 22161. Accession Numbers should be quoted on orders for reports (PB--- ---) and remittance must accompany each order. Reports without this information were not available at time of printing. Upon request, EERC will mail inquirers this information when it becomes available.

EERC 67-1 "Feasibility Study of Large-Scale Earthquake Simulator Facility," by J. Penzien, J. G. Bouwkamp, R. W. Clough, and D. Rea - 1967 (PB 187 905)A07

EERC 68-1 Unassigned

EERC 68-2 "Inelastic Behavior of Beam-to-Column Subassemblages under Repeated Loading," by V. V. Bertero - 1968 (PB 184 888)A05

EERC 68-3 "A Graphical Method for Solving the Wave Reflection-Refraction Problem," by H. D. McNiven and Y. Mengi - 1968 (PB 187 943)A03

EERC 68-4 "Dynamic Properties of McKinley School Buildings," by D. Rea, J. G. Bouwkamp, and R. W. Clough - 1968 (PB 187 902)A07

EERC 68-5 "Characteristics of Rock Motions during Earthquakes," by H. B. Seed, I. M. Idriss, and F. W. Kiefer - 1968 (PB 188 338)A03

EERC 69-1 "Earthquake Engineering Research at Berkeley," - 1969 (PB 187 906)A11

EERC 69-2 "Nonlinear Seismic Response of Earth Structures," by M. Dibaj and J. Penzien - 1969 (PB 187 904)A08

EERC 69-3 "Probabilistic Study of the Behavior of Structures during Earthquakes," by R. Ruiz and J. Penzien - 1969 (PB 187 886)A06

EERC 69-4 "Numerical Solution of Boundary Value Problems in Structural Mechanics by Reduction to an Initial Value Formulation," by N. Distefano and J. Schujman - 1969 (PB 187 942)A02

EERC 69-5 "Dynamic Programming and the Solution of the Biharmonic Equation," by N. Distefano - 1969 (PB 187 941)A03

EERC 69-6 "Stochastic Analysis of Offshore Tower Structures," by A. K. Malhotra and J. Penzien - 1969 (PB 187 903)A09

EERC 69-7 "Rock Motion Accelerograms for High Magnitude Earthquakes," by H. B. Seed and I. M. Idriss - 1969 (PB 187 940)A02

EERC 69-8 "Structural Dynamics Testing Facilities at the University of California, Berkeley," by R. M. Stephen, J. G. Bouwkamp, R. W. Clough and J. Penzien - 1969 (PB 189 111)A04

EERC 69-9 "Seismic Response of Soil Deposits Underlain by Sloping Rock Boundaries," by H. Dezfulian and H. B. Seed - 1969 (PB 189 114)A03

EERC 69-10 "Dynamic Stress Analysis of Axisymmetric Structures under Arbitrary Loading," by S. Ghosh and E. L. Wilson - 1969 (PB 189 026)A10

EERC 69-11 "Seismic Behavior of Multistory Frames Designed by Different Philosophies," by J. C. Anderson and V. V. Bertero - 1969 (PB 190 662)A10

EERC 69-12 "Stiffness Degradation of Reinforcing Concrete Members Subjected to Cyclic Flexural Moments," by V. V. Bertero, B. Bresler, and H. Ming Liao - 1969 (PB 202 942)A07

EERC 69-13 "Response of Non-Uniform Soil Deposits to Travelling Seismic Waves," by H. Dezfulian and H. B. Seed - 1969 (PB 191 023)A03

EERC 69-14 "Damping Capacity of a Model Steel Structure," by D. Rea, R. W. Clough, and J. G. Bouwkamp - 1969 (PB 190 663)A06

EERC 69-15 "Influence of Local Soil Conditions on Building Damage Potential during Earthquakes," by H. B. Seed and I. M. Idriss - 1969 (PB 191 036)A03

EERC 69-16 "The Behavior of Sands under Seismic Loading Conditions," by M. L. Silver and H. B. Seed - 1969 (AD 714 982)A07

EERC 70-1 "Earthquake Response of Gravity Dams," by A. K. Chopra - 1970 (AD 709 640)A03

EERC 70-2 "Relationships between Soil Conditions and Building Damage in the Caracas Earthquake of July 29, 1967," by H. B. Seed, I. M. Idriss, and H. Dezfulian - 1970 (PB 195 762)A05

EERC 70-3 "Cyclic Loading of Full Size Steel Connections," by E. P. Popov and R. M. Stephen - 1970 (PB 213 545)A04

EERC 70-4 "Seismic Analysis of the Charaima Building, Caraballeda, Venezuela," by Subcommittee of the SEAONC Research Committee: V. V. Bertero, P. F. Fratessa, S. A. Mahin, J. H. Sexton, A. C. Scordelis, E. L. Wilson, L. A. Wyllie, H. B. Seed, and J. Penzien, Chairman - 1970 (PB 201 455)A06

EERC 70-5 "A Computer Program for Earthquake Analysis of Dams," by A. K. Chopra and P. Chakrabarti - 1970 (AD 723 994)A05

EERC 70-6 "The Propagation of Love Waves Across Non-Horizontally Layered Structures," by J. Lysmer and L. A. Drake - 1970 (PB 197 896)A03

EERC 70-7 "Influence of Base Rock Characteristics on Ground Response," by J. Lysmer, H. B. Seed, and P. B. Schnabel - 1970 (PB 197 897)A03

EERC 70-8 "Applicability of Laboratory Test Procedures for Measuring Soil Liquefaction Characteristics under Cyclic Loading," by H. B. Seed and W. H. Peacock - 1970 (PB 198 016)A03

EERC 70-9 "A Simplified Procedure for Evaluating Soil Liquefaction Potential," by H. B. Seed and I. M. Idriss - 1970 (PB 198 009)A03

EERC 70-10 "Soil Moduli and Damping Factors for Dynamic Response Analysis," by H. B. Seed and I. M. Idriss - 1970 (PB 197 869)A03

EERC 71-1 "Koyna Earthquake of December 11, 1967 and the Performance of Koyna Dam," by A. K. Chopra and P. Chakrabarti - 1971 (AD 731 496)A06

EERC 71-2 "Preliminary In-Situ Measurements of Anelastic Absorption in Soils using a Prototype Earthquake Simulator," by R. D. Borcherdt and P. W. Rodgers - 1971 (PB 201 454)A03

EERC 71-3 "Static and Dynamic Analysis of Inelastic Frame Structures," by F. L. Porter and G. H. Powell - 1971 (PB 210 135)A06

EERC 71-4 "Research Needs in Limit Design of Reinforced Concrete Structures," by V. V. Bertero - 1971 (PB 202 943)A04

EERC 71-5 "Dynamic Behavior of a High-Rise Diagonally Braced Steel Building," by D. Rea, A. A. Shah, and J. G. Bouwkamp - 1971 (PB 203 584)A06

EERC 71-6 "Dynamic Stress Analysis of Porous Elastic Solids Saturated with Compressible Fluids," by J. Ghaboussi and E. L. Wilson - 1971 (PB 211 396)A06

EERC 71-7 "Inelastic Behavior of Steel Beam-to-Column Subassemblages," by H. Krawinkler, V. V. Bertero, and E. P. Popov - 1971 (PB 211 355)A14

EERC 71-8 "Modification of Seismograph Records for Effects of Local Soil Conditions," by P. Schnabel, H. B. Seed, and J. Lysmer - 1971 (PB 214 450)A03

EERC 72-1 "Static and Earthquake Analysis of Three Dimensional Frame and Shear Wall Buildings," by E. L. Wilson and H. H. Dovey - 1972 (PB 212 904)A05

EERC 72-2 "Accelerations in Rock for Earthquakes in the Western United States," by P. B. Schnabel and H. B. Seed - 1972 (PB 213 100)A03

EERC 72-3 "Elastic-Plastic Earthquake Response of Soil-Building Systems," by T. Minami - 1972 (PB 214 868)A08

EERC 72-4 " Stochastic Inelastic Response of Offshore Towers to Strong Motion Earthquakes," by M. K. Kaul - 1972 (PB 215 713)A05

EERC 72-5 "Cyclic Behavior of Three Reinforced Concrete Flexural Members with High Shear," by E. P. Popov, V. V. Bertero, and H. Krawinkler - 1972 (PB 214 555)A05

EERC 72-6 "Earthquake Response of Gravity Dams Including Reservoir Interaction Effects," by P. Chakrabarti and A. K. Chopra - 1972 (AD 762 330)A08

EERC 72-7 "Dynamic Properties of Pine Flat Dam," by D. Rea, C. Y. Liaw, and A. K. Chopra - 1972 (AD 763 928)A05

EERC 72-8 "Three Dimensional Analysis of Building Systems," by E. L. Wilson and H. H. Dovey - 1972 (PB 222 438)A06

EERC 72-9 "Rate of Loading Effects on Uncracked and Repaired Reinforced Concrete Members," by S. Mahin, V. V. Bertero, D. Rea and M. Atalay - 1972 (PB 224 520)A08

EERC 72-10 "Computer Program for Static and Dynamic Analysis of Linear Structural Systems," by E. L. Wilson, K.-J. Bathe, J. E. Peterson and H. H. Dovey - 1972 (PB 220 437)A04

EERC 72-11 "Literature Survey - Seismic Effects on Highway Bridges," by T. Iwasaki, J. Penzien, and R. W. Clough - 1972 (PB 215 613)A19

EERC 72-12 "SHAKE - A Computer Program for Earthquake Response Analysis of Horizontally Layered Sites," by P. B. Schnabel and J. Lysmer - 1972 (PB 220 207)A06

EERC 73-1 "Optimal Seismic Design of Multistory Frames," by V. V. Bertero and H. Kamil - 1973

EERC 73-2 "Analysis of the Slides in the San Fernando Dams during the Earthquake of February 9, 1971," by H. B. Seed, K. L. Lee, I. M. Idriss, and F. Makdisi - 1973 (PB 223 402)A14

EERC 73-3 "Computer Aided Ultimate Load Design of Unbraced Multistory Steel Frames," by M. B. El-Hafez and G. H. Powell - 1973 (PB 248 315)A09

EERC 73-4 "Experimental Investigation into the Seismic Behavior of Critical Regions of Reinforced Concrete Components as Influenced by Moment and Shear," by M. Celebi and J. Penzien - 1973 (PB 215 884)A09

EERC 73-5 "Hysteretic Behavior of Epoxy-Repaired Reinforced Concrete Beams," by M. Celebi and J. Penzien - 1973 (PB 239 568)A03

EERC 73-6 "General Purpose Computer Program for Inelastic Dynamic Response of Plane Structures," by A. Kanaan and G. H. Powell - 1973 (PB 221 260)A08

EERC 73-7 "A Computer Program for Earthquake Analysis of Gravity Dams Including Reservoir Interaction," by P. Chakrabarti and A. K. Chopra - 1973 (AD 766 271)A04

EERC 73-8 "Behavior of Reinforced Concrete Deep Beam-Column Subassemblages under Cyclic Loads," by O. Küstü and J. G. Bouwkamp - 1973 (PB 246 117)A12

EERC 73-9 "Earthquake Analysis of Structure-Founation Systems," by A. K. Vaish and A. K. Chopra - 1973 (AD 766 272)A07

EERC 73-10 "Deconvolution of Seismic Response for Linear Systems," by R. B. Reimer - 1973 (PB 227 179)A08

EERC 73-11 "SAP IV: A Structural Analysis Program for Static and Dynamic Response of Linear Systems," by K.-J. Bathe, E. L. Wilson, and F. E. Peterson - 1973 (PB 221 967)A09

EERC 73-12 "Analytical Investigations of the Seismic Response of Long, Multiple Span Highway Bridges," by W. S. Tseng and J. Penzien - 1973 (PB 227 816)A10

EERC 73-13 "Earthquake Analysis of Multi-Story Buildings Including Foundation Interaction," by A. K. Chopra and J. A. Gutierrez - 1973 (PB 222 970)A03

EERC 73-14 "ADAP: A Computer Program for Static and Dynamic Analysis of Arch Dams," by R. W. Clough, J. M. Raphael, and S. Mojtahedi - 1973 (PB 223 763)A09

EERC 73-15 "Cyclic Plastic Analysis of Structural Steel Joints," by R. B. Pinkney and R. W. Clough - 1973 (PB 226 843)A08

EERC 73-16 "QUAD-4: A Computer Program for Evaluating the Seismic Response of Soil Structures by Variable Damping Finite Element Procedures," by I. M. Idriss, J. Lysmer, R. Hwang, and H. B. Seed - 1973 (PB 229 424)A05

EERC 73-17 "Dynamic Behavior of a Multi-Story Pyramid Shaped Building," by R. M. Stephen, J. P. Hollings, and J. G. Bouwkamp - 1973 (PB 240 718)A06

EERC 73-18 "Effect of Different Types of Reinforcing on Seismic Behavior of Short Concrete Columns," by V. V. Bertero, J. Hollings, O. Küstü, R. M. Stephen, and J. G. Bouwkamp - 1973

EERC 73-19 "Olive View Medical Center Materials Studies, Phase I," by B. Bresler and V. V. Bertero - 1973 (PB 235 986)A06

EERC 73-20 "Linear and Nonlinear Sesismic Analysis Computer Programs for Long Multiple-Span Highway Bridges," by W. S. Tseng and J. Penzien - 1973

EERC 73-21 "Constitutive Models for Cyclic Plastic Deformation of Engineering Materials," by J. M. Kelly and P. P. Gillis - 1973 (PB 226 024)A03

EERC 73-22 "DRAIN-2D User's Guide," by G. H. Powell - 1973 (PB 227 016)A05

EERC 73-23 "Earthquake Engineering at Berkeley - 1973 " 1973 (PB 226 033)A11

EERC 73-24 Unassigned

EERC 73-25 "Earthquake Response of Axisymmetric Tower Structures Surrounded by Water," by C. Y. Liaw and A. K. Chopra - 1973 (AD 773 052)A09

EERC 73-26 "Investigation of the Failures of the Olive View Stairtowers during the San Fernando Earthquake and Their Implications on Seismic Design," by V. V. Bertero and R. G. Collins - 1973 (PB 235 106)A13

EERC 73-27 "Further Studies on Seismis Behavior of Steel Beam-Column Subassemblages," by V. V. Bertero, H. Krawinkler, and E. P. Popov - 1973 (PB 234 172)A06

EERC 74-1 "Seismic Risk Analysis," by C. S. Oliveira - 1974 (PB 235 920)A06

EERC 74-2 "Settlement and Liquefaction of Sands under Multi-Directional Shaking," by R. Pyke, C. K. Chan, and H. B. Seed - 1974

EERC 74-3 "Optimum Design of Earthquake Resistant Shear Buildings," by D. Ray, K. S. Pister, and A. K. Chopra - 1974 (PB 231 172)A06

EERC 74-4 "LUSH - A Computer Program for Complex Response Analysis of Soil-Structure Systems," by J. Lysmer, T. Udaka, H. B. Seed, and R. Hwang - 1974 (PB 236 796)A05

EERC 74-5 "Sensitivity Analysis for Hysteretic Dynamic Systems: Applications to Earthquake Engineering," by D. Ray - 1974 (PB 233 213)A06

EERC 74-6 "Soil Structure Interaction Analyses for Evaluating Seismic Response," by H. B. Seed, J. Lysmer, and R. Hwang - 1974 (PB 236 519)A04

EERC 74-7 Unassigned

EERC 74-8 "Shaking Table Tests of a Steel Frame - A Progress Report," by R. W. Clough and D. Tang - 1974 (PB 240 869)A03

EERC 74-9 "Hysteretic Behavior of Reinforced Concrete Flexural Members with Special Web Reinforcement," by V. V. Bertero, E. P. Popov, and T. Y. Wang - 1974 (PB 236 797)A07

EERC 74-10 "Applications of Realiability-Based, Global Cost Optimization to Design of Earthquake Resistant Structures," by E. Vitiello and K. S. Pister - 1974 (PB 237 231)A06

EERC 74-11 "Liquefaction of Gravelly Soils under Cyclic Loading Conditions," by R. T. Wong, H. B. Seed, and C. K. Chan - 1974 (PB 242 042)A03

EERC 74-12 "Site-Dependent Spectra for Earthquake-Resistant Design," by H. B. Seed, C. Ugas, and J. Lysmer - 1974 (PB 240 953)A03

EERC 74-13 "Earthquake Simulator Study of a Reinforced Concrete Frame," by P. Hidalgo and R. W. Clough - 1974 (PB 241 944)A13

EERC 74-14 "Nonlinear Earthquake Response of Concrete Gravity Dams," by N. Pal - 1974 (AD/A 006 583)A06

EERC 74-15 "Modeling and Identification in Nonlinear Structural Dynamics - I. One Degree of Freedom Models," by N. Distefano and A. Rath - 1974 (PB 241 548)A06

EERC 75-1 "Determination of Seismic Design Criteria for the Dumbarton Bridge Replacement Structure, Vol. I: Description, Theory and Analytical Modeling of Bridge and Parameters," by F. Baron and S.-H. Pang - 1975 (PB 259 407)A15

EERC 75-2 "Determination of Seismic Design Criteria for the Dumbarton Bridge Replacement Structure, Vol. II: Numerical Studies and Establishment of Seismic Design Criteria," by F. Baron and S.-H. Pang - 1975 (PB 259 408)A11 [For set of EERC 75-1 and 75-2 (PB 241 454)A09]

EERC 75-3 "Seismic Risk Analysis for a Site and a Metropolitan Area," by C. S. Oliveira - 1975 (PB 248 134)A09

EERC 75-4 "Analytical Investigations of Seismic Response of Short, Single or Multiple-Span Highway Bridges," by M.-C. Chen and J. Penzien - 1975 (PB 241 454)A09

EERC 75-5 "An Evaluation of Some Methods for Predicting Seismic Behavior of Reinforced Concrete Buildings," by S. A. Mahin and V. V. Bertero - 1975 (PB 246 306)A16

EERC 75-6 "Earthquake Simulator Story of a Steel Frame Structure, Vol. I: Experimental Results," by R. W. Clough and D. T. Tang - 1975 (PB 243 981)A13

EERC 75-7 "Dynamic Properties of San Bernardino Intake Tower," by D. Rea, C.-Y Liaw and A. K. Chopra - 1975 (AD/A 008 406)A05

EERC 75-8 "Seismic Studies of the Articulation for the Dumbarton Bridge Replacement Structure, Vol. 1: Description, Theory and Analytical Modeling of Bridge Components," by F. Baron and R. E. Hamati - 1975 (PB 251 539)A07

EERC 75-9 "Seismic Studies of the Articulation for the Dumbarton Bridge Replacement Structure, Vol. 2: Numerical Studies of Steel and Concrete Girder Alternates," by F. Baron and R. E. Hamati - 1975 (PB 251 540)A10

EERC 75-10 "Static and Dynamic Analysis of Nonlinear Structures," by D. P. Mondkar and G. H. Powell - 1975 (PB 242 434)A08

EERC 75-11 "Hysteretic Behavior of Steel Columns," by E. P. Popov, V. V. Bertero, and S. Chandramouli - 1975 (PB 252 365)A11

EERC 75-12 "Earthquake Engineering Research Center Library Printed Catalog " - 1975 (PB 243 711)A26

EERC 75-13 "Three Dimensional Analysis of Building Systems (Extended Version)," by E. L. Wilson, J. P. Hollings, and H. H. Dovey - 1975 (PB 243 989)A07

EERC 75-14 "Determination of Soil Liquefaction Characteristics by Large-Scale Laboratory Tests," by P. De Alba, C. K. Chan, and H. B. Seed - 1975 (NUREG 0027)A08

EERC 75-15 "A Literature Survey - Compressive, Tensile, Bond and Shear Strength of Masonry," by R. L. Mayes and R. W. Clough - 1975 (PB 246 292)A10

EERC 75-16 "Hysteretic Behavior of Ductile Moment-Resisting Reinforced Concrete Frame Components," by V. V. Bertero and E. P. Popov - 1975 (PB 246 388)A05

EERC 75-17 "Relationships Between Maximum Acceleration, Maximum Velocity, Distance from Source, Local Site Conditions for Moderately Strong Earthquakes," by H. B. Seed, R. Murarka, J. Lysmer, and I. M. Idriss - 1975 (PB 248 172)A03

EERC 75-18 "The Effects of Method of Sample Preparation on the Cyclic Stress-Strain Behavior of Sands," by J. Mulilis, C. K. Chan, and H. B. Seed - 1975 (Summarized in EERC 75-28)

EERC 75-19 "The Seismic Behavior of Critical Regions of Reinforced Concrete Components as Influenced by Moment, Shear and Axial Force," by M. B. Atalay and J. Penzien - 1975 (PB 258 842)A11

EERC 75-20 "Dynamic Properties of an Eleven Story Masonry Building," by R. M. Stephen, J. P. Hollings, J. G. Bouwkamp, and D. Jurukovski - 1975 (PB 246 945)A04

EERC 75-21 "State-of-the-Art in Seismic Strength of Masonry - An Evaluation and Review," by R. L. Mayes and R. W. Clough - 1975 (PB 249 040)A07

EERC 75-22 "Frequency Dependent Stiffness Matrices for Viscoelastic Half-Plane Foundations," by A. K. Chopra, P. Chakrabarti, and G. Dasgupta - 1975 (PB 248 121)A07

EERC 75-23 "Hysteretic Behavior of Reinforced Concrete Framed Walls," by T. Y. Wang, V. V. Bertero, and E. P. Popov - 1975

EERC 75-24 "Testing Facility for Subassemblages of Frame-Wall Structural Systems," by V. V. Bertero, E. P. Popov, and T. Endo - 1975

EERC 75-25 "Influence of Seismic History on the Liquefaction Characteristics of Sands," by H. B. Seed, K. Mori, and C. K. Chan - 1975 (Summarized in EERC 75-28)

EERC 75-26 "The Generation and Dissipation of Pore Water Pressures during Soil Liquefaction," by H. B. Seed, P. P. Martin, and J. Lysmer - 1975 (PB 252 648)A03

EERC 75-27 "Identification of Research Needs for Improving Aseismic Design of Building Structures," by V. V. Bertero - 1975 (PB 248 136)A05

EERC 75-28 "Evaluation of Soil Liquefaction Potential during Earthquakes," by H. B. Seed, I. Arango, and C. K. Chan - 1975 (NUREG 0026)A13

EERC 75-29 "Representation of Irregular Stress Time Histories by Equivalent Uniform Stress Series in Liquefaction Analyses," by H. B. Seed, I. M. Idriss, F. Makdisi, and N. Banerjee - 1975 (PB 252 635)A03

EERC 75-30 "FLUSH - A Computer Program for Approximate 3-D Analysis of Soil-Structure Interaction Problems," by J. Lysmer, T. Udaka, C.-F. Tsai, and H. B. Seed - 1975 (PB 259 332)A07

EERC 75-31 "ALUSH - A Computer Program for Seismic Response Analysis of Axisymmetric Soil-Structure Systems," by E. Berger, J. Lysmer, and H. B. Seed - 1975

EERC 75-32 "TRIP and TRAVEL - Computer Programs for Soil-Structure Interaction Analysis with Horizontally Travelling Waves," by T. Udaka, J. Lysmer, and H. B. Seed - 1975

EERC 75-33 "Predicting the Performance of Structures in Regions of High Seismicity," by J. Penzien - 1975 (PB 248 130)A03

EERC 75-34 "Efficient Finite Element Analysis of Seismic Structure-Soil-Direction," by J. Lysmer, H. B. Seed, T. Udaka, R. N. Hwang, and C.-F. Tsai - 1975 (PB 253 570)A03

EERC 75-35 "The Dynamic Behavior of a First Story Girder of a Three-Story Steel Frame Subjected to Earthquake Loading," by R. W. Clough and L.-Y. Li - 1975 (PB 248 841)A05

EERC 75-36 "Earthquake Simulator Story of a Steel Frame Structure, Volume II - Analytical Results," by D. T. Tang - 1975 (PB 252 926)A10

EERC 75-37 "ANSR-I General Purpose Computer Program for Analysis of Non-Linear Structural Response," by D. P. Mondkar and G. H. Powell - 1975 (PB 252 386)A08

EERC 75-38 "Nonlinear Response Spectra for Probabilistic Seismic Design and Damage Assessment of Reinforced Concrete Structures," by M. Murakami and J. Penzien - 1975 (PB 259 530)A05

EERC 75-39 "Study of a Method of Feasible Directions for Optimal Elastic Design of Frame Structures Subjected to Earthquake Loading," by N. D. Walker and K. S. Pister - 1975 (PB 247 781)A06

EERC 75-40 "An Alternative Representation of the Elastic-Viscoelastic Analogy," by G. Dasgupta and J. L. Sackman - 1975 (PB 252 173)A03

EERC 75-41 "Effect of Multi-Directional Shaking on Liquefaction of Sands," by H. B. Seed, R. Pyke, and G. R. Martin - 1975 (PB 258 781)A03

EERC 76-1 "Strength and Ductility Evaluation of Existing Low-Rise Reinforced Concrete Buildings - Screening Method," by T. Okada and B. Bresler - 1976 (PB 257 906)A11

EERC 76-2 "Experimental and Analytical Studies on the Hysteretic Behavior of Reinforced Concrete Rectangular and T-Beams," by S.-Y. M. Ma, E. P. Popov, and V. V. Bertero - 1976 (PB 260 843)A12

EERC 76-3 "Dynamic Behavior of a Multistory Triangular-Shaped Building," by J. Petrovski, R. M. Stephen, E. Gartenbaum, and J. G. Bouwkamp - 1976

EERC 76-4 "Earthquake Induced Deformations of Earth Dams," by N. Serff and H. B. Seed - 1976

EERC 76-5 "Analysis and Design of Tube-Type Tall Building Structures," by H. de Clercq and G. H. Powell - 1976 (PB 252 220)A10

EERC 76-6 "Time and Frequency Domain Analysis of Three-Dimensional Ground Motions,San Fernando Earthquake," by T. Kubo and J. Penzien - 1976 (PB 260 556)A11

EERC 76-7 "Expected Performance of Uniform Building Code Design Masonry Structures," by R. L. Mayes, Y. Omote, S. W. Chen, and R. W. Clough - 1976

EERC 76-8 "Cyclic Shear Tests on Concrete Masonry Piers, Part I - Test Results," by R. L. Mayes, Y. Omote, and R. W. Clough - 1976 (PB 264 424)A06

EERC 76-9 "A Substructure Method for Earthquake Analysis of Structure-Soil Interaction," by J. A. Gutierrez and A. K. Chopra - 1976 (PB 247 783)A08

EERC 76-10 "Stabilization of Potentially Liquefiable San Deposits using Gravel Drain Systems," by H. B. Seed and J. R. Booker - 1976 (PB 248 820)A04

EERC 76-11 "Influence of Design and Analysis Assumptions on Computed Inelastic Response of Moderately Tall Frames," by G. H. Powell and D. G. Row - 1976

EERC 76-12 "Sensitivity Analysis for Hysteretic Dynamic Systems: Theory and Applications," by D. Ray, K. S. Pister, and E. Polak - 1976 (PB 262 859)A04

EERC 76-13 "Coupled Lateral Torsional Response of Buildings to Ground Shaking," by C. L. Kan and A. K. Chopra - 1976 (PB 257 907)A09

EERC 76-14 "Seismic Analyses of the Banco de America," by V. V. Bertero, S. A. Mahin, and J. A. Hollings - 1976

EERC 76-15 "Reinforced Concrete Frame 2: Seismic Testing and Analytical Correlation," by R. W. Clough and J. Gidwani - 1976 (PB 261 323)A08

EERC 76-16 "Cyclic Shear Tests on Masonry Piers, Part II - Analysis of Test Results," by R. L. Mayes, Y. Omote, and R. W. Clough - 1976

EERC 76-17 "Structural Steel Bracing Systems: Behavior under Cyclic Loading," by E. P. Popov, K. Takanashi, and C. W. Roeder - 1976 (PB 260 715)A05

EERC 76-18 "Experimental Model Studies on Seismic Response of High Curved Overcrossings," by D. Williams and W. G. Godden - 1976

EERC 76-19 "Effects of Non-Uniform Seismic Disturbances on the Dumbarton Bridge Replacement Structure," by F. Baron and R. E. Hamati - 1976

EERC 76-20 "Investigation of the Inelastic Characteristics of a Single Story Steel Structure using System Identification and Shaking Table Experiments," by V. C. Matzen and H. D. McNiven - 1976 (PB 258 453)A07

EERC 76-21 "Capacity of Columns with Splice Imperfections," by E. P. Popov, R. M. Stephen and R. Philbrick - 1976 (PB 260 378)A04

EERC 76-22 "Response of the Olive View Hospital Main Building during the San Fernando Earthquake," by S. A. Mahin, V. V. Bertero, A. K. Chopra, and R. Collins," - 1976

EERC 76-23 "A Study on the Major Factors Influencing the Strength of Masonry Prisms," by N. M. Mostaghel, R. L. Mayes, R. W. Clough, and S. W. Chen - 1976

EERC 76-24 "GADFLEA - A Computer Program for the Analysis of Pore Pressure Generation and Dissipation during Cyclic or Earthquake Loading," by J. R. Booker, M. S. Rahman, and H. B. Seed - 1976 (PB 263 947)A04

EERC 76-25 "Rehabilitation of an Existing Building: A Case Study," by B. Bresler and J. Axley - 1976

EERC 76-26 "Correlative Investigations on Theoretical and Experimental Dynamic Behavior of a Model Bridge Structure," by K. Kawashima and J. Penzien - 1976 (PB 263 388)A11

EERC 76-27 "Earthquake Response of Coupled Shear Wall Buildings," by T. Srichatrapimuk - 1976 (PB 265 157)A07

EERC 76-28 "Tensile Capacity of Partial Penetration Welds," by E. P. Popov and R. M. Stephen - 1976 (PB 262 899)A03

EERC 76-29 "Analysis and Design of Numerical Integration Methods in Structural Dynamics," by H. M. Hilber - 1976 (PB 264 410)A06

EERC 76-30 "Contribution of a Floor System to the Dynamic Characteristics of Reinforced Concrete Buildings," by L. E. Malik and V. V. Bertero - 1976

EERC 76-31 "The Effects of Seismic Disturbances on the Golden Gate Bridge," by F. Baron, M. Arikan, R. E. Hamati - 1976

EERC 76-32 "Infilled Frames in Earthquake-Resistant Construction," by R. E. Klingner and V. V. Bertero - 1976 (PB 265 892)A13

UCB/EERC-77/01 "PLUSH - A Computer Program for Probabilistic Finite Element Analysis of Seismic Soil-Structure Interaction," by M. P. Romo Organista, J. Lysmer, and H. B. Seed - 1977

UCB/EERC-77/02 "Soil-Structure Interaction Effects at the Humboldt Bay Power Plant in the Ferndale Earthquake of June 7, 1975," by J. E. Valera, H. B. Seed, C.-F. Tsai, and J. Lysmer - 1977 (B 265 795)A04

UCB/EERC-77/03 "Influence of Sample Disturbance on Sand Response to Cyclic Loading," by K. Mori, H. B. Seed, and C. K. Chan - 1977 (PB 267 352)A04

UCB/EERC-77/04 "Seismological Studies of Strong Motion Records," by J. Shoja-Taheri - 1977 (PB 269 655)A10

UCB/EERC-77/05 "Testing Facility for Coupled Shear Walls," by L.-H. Lee, V. V. Bertero, and E. P. Popov - 1977

UCB/EERC-77/06 "Developing Methodologies for Evaluating the Earthquake Safety of Existing Buildings," No. 1 - B. Bresler; No. 2 - B. Bresler, T. Okada, and D. Zisling; No. 3 - T. Okada and B. Bresler; No. 4 - V. V. Bertero and B. Bresler - 1977 (PB 267 354)A08

UCB/EERC-77/07 "A Literature Survey - Transverse Strength of Masonry Walls," by Y. Omote, R. L. Mayes, S. W. Chen, and R. W. Clough - 1977

UCB/EERC-77/08 "DRAIN-TABS: A Computer Program for Inelastic Earthquake Response of Three Dimensional Buildings," by R. Guendelman-Israel and G. H. Powell - 1977

UCB/EERC-77/09 "SUBWALL: A Special Purpose Finite Element Computer Program for Practical Elastic Analysis and Design of Structural Walls with Substructure Option," by D. Q. Le, H. Petersson, and E. P. Popov - 1977

UCB/EERC-77/10 "Experimental Evaluation of Seismic Design Methods for Broad Cylindrical Tanks," by D. P. Clough - 1977

UCB/EERC-77/11 "Earthquake Engineering Research at Berkeley - 1976," - 1977

UCB/EERC-77/12 "Automated Design of Earthquake Resistant Multistory Steel Building Frames," by N. D. Walker, Jr. - 1977

UCB/EERC-77/13 "Concrete Confined by Rectangular Hoops and Subjected to Axial Loads," by J. Vallenas, V. V. Bertero, and E. P. Popov - 1977

UCB/EERC-77/14 "Seismic Strain Induced in the Ground during Earthquakes," by Y. Sugimura - 1977

UCB/EERC-77/15 "Bond Deterioration under Generalized Loading," by V. V. Bertero, E. P. Popov, and S. Viwathanatepa - 1977

UCB/EERC-77/16 "Computer-Aided Optimum Design of Ductile Reinforced Concrete Moment-Resisting Frames," by S. W. Zagajeski and V. V. Bertero - 1977

UCB/EERC-77/17 "Earthquake Simulation Testing of a Stepping Frame with Energy-Absorbing Devices," by J. M. Kelly and D. F. Tsztoo - 1977

UCB/EERC-77/18 "Inelastic Behavior of Eccentrically Braced Steel Frames under Cyclic Loadings," by C. W. Roeder and E. P. Popov - 1977

B3
1

For sale by the National Technical Information Service, U. S. Department of Commerce, Springfield, Virginia 22161.

See back of report for up to date listing of EERC reports.